Further automation in pancreatic islet isolations

R.M. van Rooden

Master thesis submitted in partial fulfillment of the requirements for the degree
MSc in Biomedical Engineering

in the

Faculty of Mechanical, Maritime and Materials Engineering
Delft University of Technology

January 14, 2021

Student number: 1518224
Supervisor: J.B. Doppenberg
Supervisor: dr. M.A. Engelse
Supervisor: dr.ir. E.L. Fratila-Apachitei

Abstract

For patients with severe cases of type 1 diabetes mellitus, the standard treatment of exogenous insulin administration is not sufficient, and, therefore, are eligible for β-cell replacement therapies, such as pancreatic islet transplantations, to regain glycemic control. In order to transplant pancreatic islets, they first need to be separated from the rest of the pancreatic tissue through pancreatic islet isolation procedure. Researchers from the Leiden University medical Center (LUMC) are working on a system, called PancReatic Islet Separation Method (PRISM), that automates large parts of this isolation procedure. During validation studies of the prototype device, PRISM 1.0, two main areas have been identified that can be further improved upon during the development of a version two PRISM device.

One of these areas is the need for the ability to identify pancreatic islets from exocrine tissue in a label free, non-destructive an in- or on-line manner, as an alternative for the use of Dithizone (DTZ), a cytotoxic zinc chelating agent which stains the pancreatic islets red. The other area for improvement is to find a solution for the crowding effects, resulting in a disturbed density gradient, from a large volume of tissue in the limited size Latham bowl.

In an effort to explore alternative options to identify pancreatic islets from exocrine tissue, a research has been conducted in which optical and electrical properties of both tissues were investigated. To this end, experiments have been performed in which the optical absorption and electrical impedance spectra have been investigated. While some differences between pancreatic islets and exocrine tissue have been measured, the results are within the margin of error, and, therefore, no definitive conclusion has been reached on the usability of these methods for pancreatic islet identification.

To overcome the difficulties of a large volume of tissue in the continuous flow centrifuge bowl during the pancreatic islet isolation procedure, research has been done into the optimization of the controllable variables during the creation of sequential and simultaneous density gradients. This research showed that the used tubing could gain more control after applying a treatment protocol and that the developed pump system is linearly progressive and accurate. These findings were then used to re-visit the simultaneous density gradient process, and evaluate the accuracy and repeatability of this process. Ultimately, this process proved to be a robust and reliable method to create simultaneous density gradients, and would, therefore, be able to solve the Latham bowl size limitations.

Contents

Nomenclature

DTZ	Dithizone
FMEA	Failure Mode and Effects Analysis
GLP	Good Laboratory Practice
GMP	Good Manufacturing Practices
HFMEA	Healthcare Failure Mode and Effect Analysis
IEQ	Islet EQuivalent
LUMC	Leiden University Medical Center
PBS	Phosphate-Buffered Saline
PRISM	PancReatic Islet Separation Method
UW	University of Wisconsin

CHAPTER 1

Introduction

Diabetes Mellitus is a disease in which patients are unable to regulate blood glucose levels, and currently affects approximately 463 million people worldwide [1]. In the Netherlands alone, there currently are 1.168 million patients diagnosed with Diabetes Mellitus, out of which approximately 9% are diagnosed with type 1 Diabetes Mellitus ($\sim$0.1 million) [2, 3]. In type 1 diabetes the pancreatic β-cells, which, located in the islets of Langerhans, are responsible for the production of insulin, are destroyed in an autoimmune reaction, which leads to an impaired glycemic control [4, 5]. When a patient fails to maintain normal blood glucose levels (between 60 mg/dL and 140 mg/dL [6]) and is exposed to hyper- or hypoglycemic events, then this can ultimately lead to (severe) complications, such as organ failure or coma [7, 8, 9].

The current treatment for patients with type 1 diabetes is to monitor and balance blood glucose levels manually, by maintaining a well-balanced diet, and exogenous insulin administration [10, 11]. However, for patients with severe complications, it is no longer feasible to only treat the symptoms, but the underlying problem of the destroyed β-cells needs to be treated. One of the treatments to replace pancreatic β-cells is to perform a vascularized pancreas transplantation [12]. These transplantations have shown to improve glycemic control for all recipients, and in 45% of the recipients, long term insulin independence [13], but come at the cost of a severe operation and a lifelong immunosuppression treatment [12, 14, 15, 16]. Unfortunately, there is a declining availability of transplantable donor pancreata, as less postmortem organ donors meet the strict criteria (to minimize the risk of graft failure) for organ donations [17, 18].

To overcome the shortage in available organs, an alternative β-cell replacement therapy has been developed that can make use of an additional pool of organs (deemed unsuitable for vascularized pancreas transplantations), and thus increasing the total amount of available organs for transplantation: Pancreatic islet transplantations [19, 20]. In this treatment, only the pancreatic islets, containing the β-cells, are transplanted through infusion into the patient's liver, where they settle and regain function [21, 22]. This treatment has proven over the years, to improve the quality of life for patients by improving glycemic control and for a portion of the recipients to gain insulin independence ($\sim$44% of recipients are insulin independent after 3 years) [21, 22, 23, 24]. Before pancreatic islets can be transplanted however, they first need to be separated from the exocrine tissue (roughly 99% of the pancreas is exocrine tissue, the remaining 1% are pancreatic islets [25, 26]) through a pancreatic islet isolation procedure. In this lengthy,

manual, multi-step procedure, in a cleanroom facility, the pancreatic islets are isolated from the exocrine tissue with the use of a density gradient [27].

In an effort to make pancreatic islet transplantations more accessible for everyone, researchers from the Leiden University Medical Center (LUMC) have developed a prototype machine, shown in figure C.8, which largely automates the pancreatic islet isolation procedure: PancReatic Islet Separation Method (PRISM) [28]. The aims of the PRISM project are faster pancreatic islet isolation procedures requiring less personnel, while maintaining sterility and pancreatic islet yield and viability, by applying more automation in the process. A validation study of the PRISM prototype, called PRISM 1.0, has proven the concept to work, as the pancreatic islet yield and viability has remained similar to the manual isolation procedure.

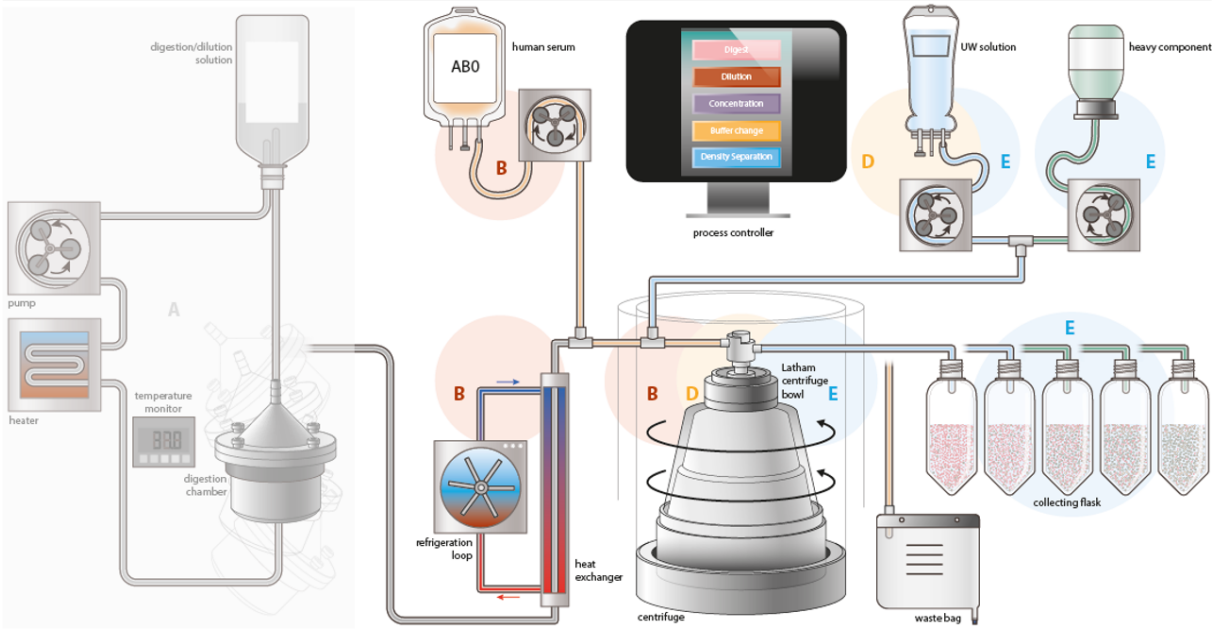

Figure 1.1: Overview of the PRISM isolation process [28]. **A:** Pancreatic tissue is digested using a Ricordi chamber and a mixture of enzymes which break down collagen. **B:** Enzymes are deactivated by cooling and addition of human serum, followed by the tissue then being collected in a continuous flow centrifuge. After which it is washed with ringer acetate. **D:** The fluids are replaced and the tissue is then soaked in University of Wisconsin (UW) preservation solution. **E:** With the creation of a density gradient, the pancreatic islets are isolated from the exocrine tissue and collected in flasks.

The working principles of this automated isolation method, which are best understood with the use of figure 1.3, in which the process is schematically depicted, are as follows:

A) **Digestion phase -** A pancreas (from either allogeneic or autologous origin) is received and infused with a mixture of collagenase and neutral protease enzymes, which, together with the mechanical friction of the steel beads in the Ricordi chamber, break down the tissue to cell clusters. While this is going on, samples are taken and stained with Dithizone (DTZ), to judge the size and morphology of the tissue, to evaluate when to stop the digestion phase. To allow the enzymes to do their work, the digestion fluid mixture is kept at 37° and circulated at 200 ml/min.
B) **Dilution phase -** This phase makes use of a 225ml continuous flow Latham bowl centrifuge, in which the incoming fluids are deposited at the bottom of the bowl and the outgoing fluids leave

at the top, because the centrifuge spins this bowl, the centrifugal forces cause the heavier tissue and fluids to stay in the bowl and the lighter fluids to exit at the top. Once the tissue has been judged to be sufficiently digested, the mixture leaves the digestion loop at 200 ml/min, and flows through a heat exchanger to the continuous flow centrifuge, where it is collected in a Latham bowl. By passing through the heat exchanger, the fluids are cooled to a temperature below 7°C, which, together with the added human serum, reduces the activity of the enzymes and stops the digestion, after which it is washed with ringer acetate.

D) **Soaking phase -** In this phase the fluids in the Latham bowl are replaced with University of Wisconsin (UW) preservation solution which maintains or enhances the specific densities of both exocrine tissue and the pancreatic islets [29, 30]

E) **Density gradient -** After a sufficient period, the separation of the pancreatic islets and the exocrine tissue happens through the use of a density gradient. This can be done because the density of each of the tissues involved is different, dead tissue has a density around 1.045 kg/m^3, pancreatic islets have a density between 1.06 and 1.08 kg/m^3, and exocrine tissue has a density between 1.11 and 1.35 kg/m^3. The density gradient itself is established by mixing UW preservation solution (with a density of 1.045 kg/m^3) with Xenetix 350 (which has a density of 1.409kg/m^3), to create a gradient that rises from 1.045 kg/m^3 to 1.17kg/m^3. As explained before, the working of the Latham bowl causes the lightest fluids to leave the continuous flow centrifuge first, which allows the pancreatic islets to be collected in separate flasks from the exocrine tissue. To evaluate the purity of the tissue in each of the collection flasks, samples are taken which, after being stained with DTZ, are examined with a microscope.

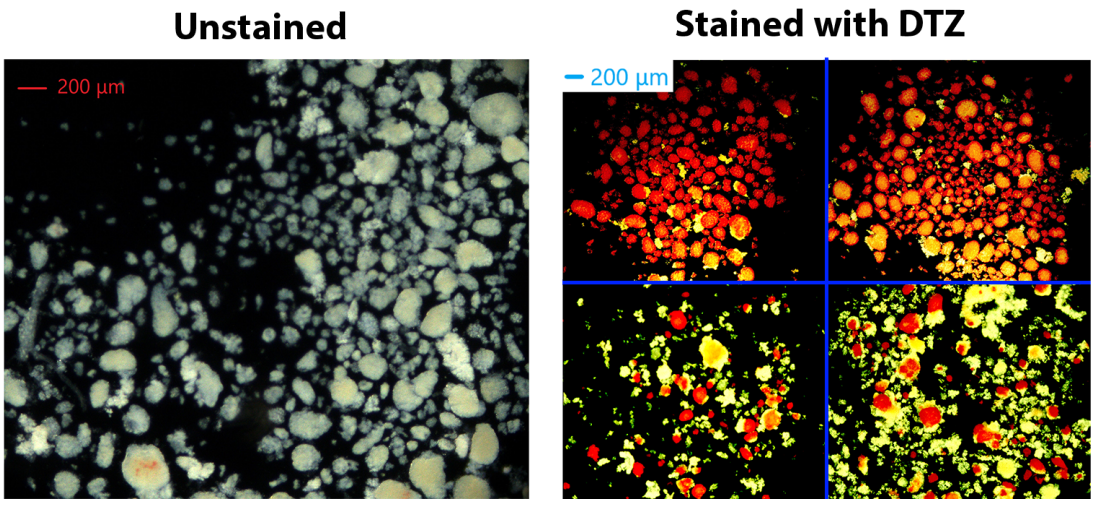

Figure 1.2: Microscopy pictures of tissue samples containing pancreatic islets and exocrine tissue. **Left:** Sample is unstained, difficult to differentiate between pancreatic islets and exocrine tissue. **Right:** Four sample which are stained with Dithizone (DTZ), which stains the pancreatic islets red, leaving the exocrine tissue yellow (due to lighting). This allows for differentiation between tissue types. Pictures are unpublished own data taken using a Carl Zeiss Axiovert 25 microscope.

While PRISM 1.0 has yielded good results, some smaller and larger area's for improvement have been identified. One of these larger area's for improvement, is the lack of the ability to identify pancreatic islets from exocrine tissue without destroying them. Because there visibly is very little difference between pancreatic islets and exocrine tissue, the golden standard is to take samples and stain the tissue with a

zinc chelating agent called Dithizone (DTZ), which interacts with the increased amount of zinc in the insulin producing β-cells [31, 32]. An example of difference between stained and unstained pancreatic islets can be seen in figure 1.2. While this method works well in the identification of pancreatic islets, DTZ is, unfortunately, cytotoxic, which results in this tissue no longer being available for transplantation purposes [33, 34]. Another larger area for improvement has to do with the limited size of the Latham bowl, which unfortunately has a maximum size of 225 ml. During the validation studies of PRISM 1.0, it has been observed that the amount of tissue from large pancreata cause a crowding effect in the Latham bowl. Which leads, during the density gradient, to a disruption of the density gradient and has a detrimental effect on the outcome of the pancreatic islet isolation. A possible solution for this problem, is to split up the tissue and perform two sequential density gradients, this, however, adds more time to the pancreatic islet isolation process. Additionally, the sequential density gradients have shown to have a, yet unexplained, difference in isolation outcomes, making it difficult to fully control this process.

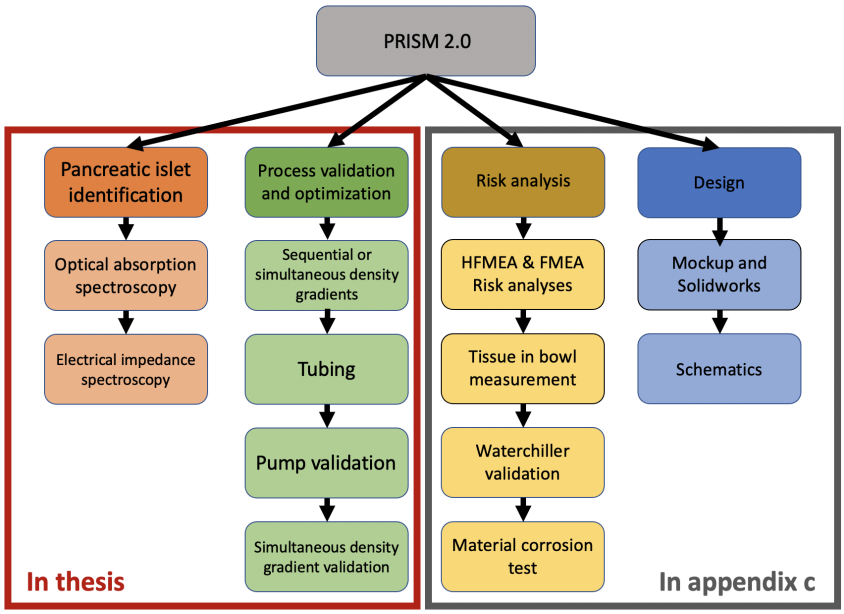

Figure 1.3: Overview of thesis subjects. For the development of PRISM 2.0 various topics and tasks needed to be performed. This overview visualizes the relations between the different topics. The pancreatic islet identification and process validation and optimization topics have been included in the thesis, and the risk analysis and design topics are shown in appendix c.

This ultimately led to the decision to develop a second version of the PRISM machine, which can overcome the shortcomings of the first device. The development of PRISM 2.0 will be the main topic of this thesis, but due to the large number of different subjects which are involved in the development process, choices have been made to include only a limited number of subjects in the thesis. A schematic overview of the subjects, and how they relate to each other, is seen in figure 1.3, and shows four different topics that have been investigated and worked on. From these topics, the pancreatic islet identification and process validation and optimization have been included in the thesis, and the other two subjects which revolve around the risk analysis and the design, are briefly covered in appendix C. Which leads to the topics containing the following content:

Included in thesis:

- **Pancreatic islet identification -** Due to the aforementioned cytotoxic nature of DTZ, all of the tissue samples taken during the pancreatic islet isolation process, cannot be used for transplantation purposes. Therefore, there is a need for the ability to differentiate between pancreatic islets and exocrine tissue in a label free and non-destructive manner, which can be applied in the PRISM environment (in- or on- line). Results from the literature study have shown optical absorption spectroscopy and electrical impedance spectroscopy to be methods that have the potential to be used for this application. This has led to the following research question and hypothesis:

  - ***Research question:*** Are there exploitable optical and/or electrical property differences between pancreatic islets and exocrine tissue?
  - ***Hypothesis:*** A difference in cell composition between pancreatic islets and exocrine tissue, will lead to measurable differences in optical absorption spectroscopy and/or electrical impedance spectroscopy.

  Therefore, novel research will be conducted in which the optical absorption and electrical impedance spectra of pancreatic islets and exocrine tissue will be investigated.

- **Process validation and optimization -** Before the development of PRISM 2.0 can be started, a decision as to be made on how to overcome the limitations by the size of the Latham bowl. To look into this the following research question and hypothesis were created:

  - ***Research question:*** Can optimization of the controllable variables during the density gradient process, lead to a more consistent creation of sequential and/or simultaneous density gradients, in order to solve the Latham bowl size limitations during pancreatic islet isolations?
  - ***Hypothesis:*** By further examining the processes to create sequential and simultaneous density gradients, the expectation is that this will lead to a robust and reliable solution to create said density gradients, aimed at solving the 225 ml Latham bowl size limit.

  Therefore, an initial research will be started to explore both options for development which ultimately should lead to the development of a process that can be used during pancreatic islet isolations.

Included in appendix C:

- **Risk Analysis -** Once the development of PRISM 2.0 starts to take shape and the process is determined, risk analyses will have to be performed to evaluate the design plans. From these risk analyses topics will arise that require further research or validation or possibly redesign. In this section the main findings from this process will be shown.
- **Design -** After the pancreatic isolation process was determined, the new machine needed to be designed, incorporating the lessons learned from PRISM 1.0. An overview of some of the iterative steps that have been taken to come to a final design have been included in this section.

CHAPTER 2

Methodology

Some of the experiments in this thesis have required the use of human cadaveric pancreatic tissue (pancreatic islets and exocrine tissue). The pancreas, from which the tissue is derived, was procured through a multiorgan donor program. This organ was used only if the pancreas could not be used for clinical pancreas or islet transplantation, according to national laws, and if research consent was present. Additionally, care has been taken to minimize amount of needed tissue, allowing for maximum research benefit. The experiments were performed in accordance to the local Good Laboratory Practice (GLP) guidelines.

2.1 Pancreatic islet identification

2.1.1 Optical absorption spectroscopy

Equipment

The experiment was conducted using a SpectraMax i3x device, which is capable of performing an optical absorption spectroscopy procedure between wavelengths of 230nm and 1000nm. The lower end of the spectrum, which is slightly in the ultra violet range, will not be usable, because the Nunc Maxisorp 96 well plates, used in the Leiden University Medical Center (LUMC), absorb the light spectrum below 290nm [35], the absorption spectrum of this plate can be seen in figure A.1. To verify the distribution of the tissue in the wells, a Carl Zeiss Axiovert 25 microscope was used and, to verify the density of the heavy solution the DMA 35 density meter from Anton Paar was used.

Materials

For this experiment, pancreatic islets with an Islet EQuivalent (IEQ) of 20.000 and a purity of 99% were used, which were released after a 24 hour culture period in CMRL1066 culture medium with additives[1]. Additionally, 1 ml of exocrine tissue was available, which was also cultured for 24 hours in CMRL (5% HS)+P/S culture medium. During the experiment, both the pancreatic islets and exocrine tissue were submerged in two different fluids, culture medium CMRL1066[1] and Phosphate-buffered Saline (PBS). An article published by Silva et al. [36], shows, in figure A.2, the transmission spectra of PBS and various culture media, which absorb the light at different wavelengths. To avoid our culture medium (which is not

[1]The list of additives for this culture medium can be seen in appendix B.1.

mentioned in the article) from interfering with the results of the experiment, the pancreatic islets were also submerged in PBS. Furthermore, other fluids, which are used during pancreatic islet isolations using the PancReatic Islet Separation Method (PRISM), were also tested to examine their optical absorption spectrum: University of Wisconsin (UW) preservation solution, Xenetix 350 and Ringer acetate.

Protocol

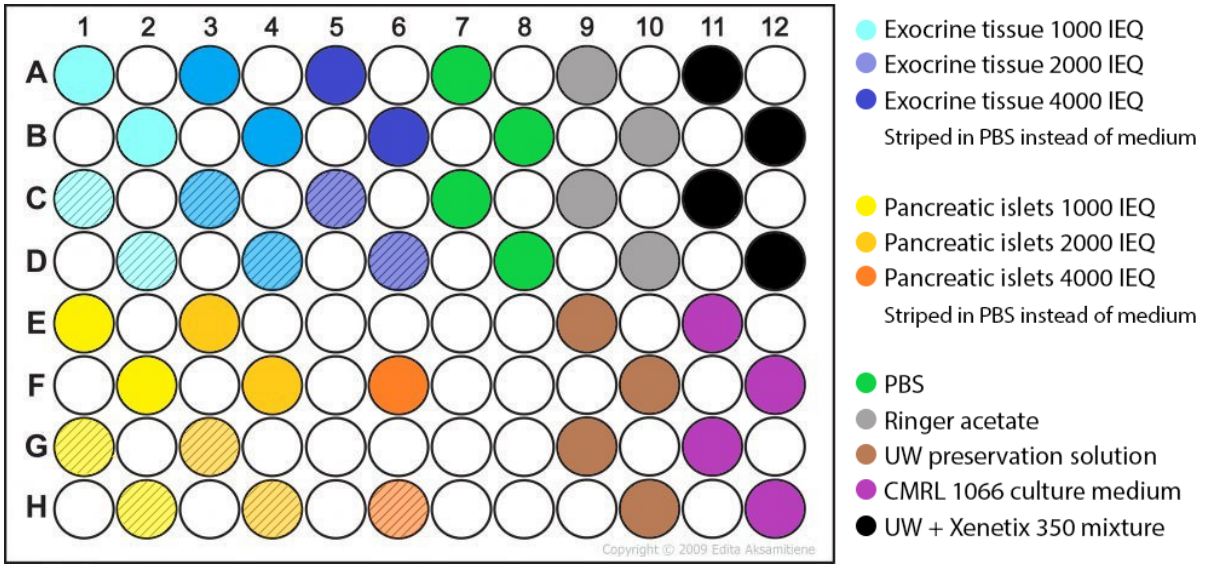

Figure 2.1: The layout of the conditions on a 96 wells plate for the optical spectroscopy absorption protocol.

Preparation

The 96 well plate which was used for this experiment was filled according to the conditions shown in figure 2.1 with a total of 200μl in each well. Before the pancreatic islets and exocrine tissue could be placed in a well, half of the tissue first had to be washed and the fluids replaced by PBS. Once this was finished, the allotted amount of tissue could be deposited in the indicated wells and the fluid levels had to be filled to a total amount of 200μl, with CMRL1066 culture medium and PBS respectively. Once done, the UW and Xenetix 350 mixture had to be prepared by combining them to obtain a density of 1.17kg/m^3, which can be checked with the density meter. Lastly, the remaining wells need to be filled with 200μl of PBS, ringer acetate, UW preservation solution and a mixture of UW and Xenetix 350 respectively.

Measurements

Finally, the measurements are taken by entering the plate into the SpectraMax i3x device. After adjusting the settings to the right 96 well plate, to handle optical differences, the device automatically followed with measurements of the light spectrum between the wavelengths of 230nm and 1000nm.

Data acquisition

The Spectramax i3x automatically collected the data after every measurement in an Excel file. To further analyze the data and create figures, MATLAB was used.

2.1.2 Electrical impedance spectroscopy

Equipment

The experiment was performed with the use of an Applied BioPhysics ECIS model Z Θ, a device capable of performing electrical impedance spectroscopy in the ranges between 250 Hz and 64000 Hz. To run, the ECIS model ZΘ uses 96 well plate with integrated electrodes from Applied BioPhysics (96W20idf). In order to evaluate sufficient coverage of the electrodes with the tissue, a Carl Zeiss Axiovert 25 microscope was used. And lastly, to measure the heavy solution, the DMA 35 density meter from Anton Paar was used.

Materials

Pancreatic islets with an IEQ of 30.000 and a purity of 80% were available for this experiment, which were released after a 24 hour culturing period in CMRL1066 culture medium with additives[2]. A culture bag containing 1 ml of exocrine tissue was also available after an being cultured for 24 hours in CMRL (5% HS)+P/S. The remaining fluids which are needed for this experiment are: CMRL1066[1] culture medium, PBS, UW preservation solution and Xenetix 350.

Protocol

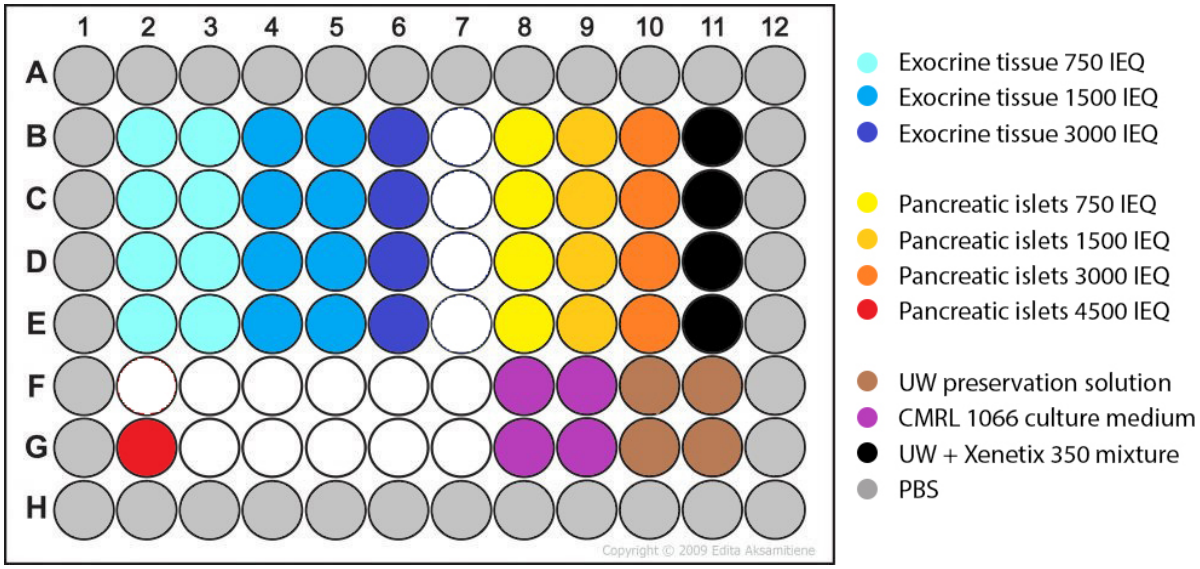

Figure 2.2: The layout of the conditions on a 96 wells plate for the electrical impedance protocol.

Preparation

Before the plate could be filled, it first needed to be cleaned and calibrated. This was done by filling all wells that were going to be used with 200 μl of CMRL 1066 culture medium, and entering the plate in the ECIS model ZΘ machine. The device then followed a 30 minutes stabilization protocol before it reached an equilibrium. The initial values for each well were then used to correct for any possible deviations from what the machine expected.

[2]The list of additives for this culture medium can be seen in appendix B.1.

Once calibrated and cleaned, the plate was extracted from the machine and filled with the conditions as outlined in figure 2.2 to a total amount of 200 μl per well. The pancreatic islets and exocrine tissue were then extracted from the culture bags and deposited in the wells according to the outlined conditions. The wells were then topped off with culture medium to reach the appropriate volume. The wells then had to be checked to make sure the electrodes are properly covered by tissue and are connected to each other, an example of this can be seen in figure 2.3.

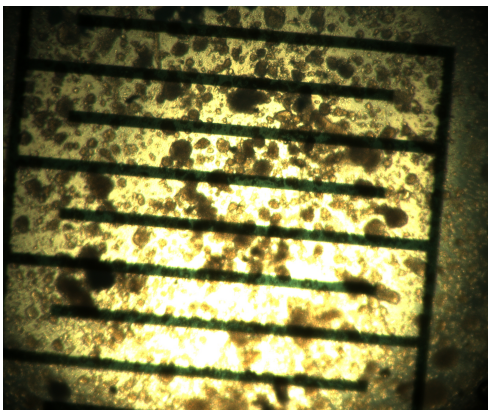

Figure 2.3: Pancreatic islets deposited on electrodes in 96 well plate. Picture is taken using a Carl Zeiss Axiovert 25 using 10x magnification.

Next, the heavy mixture needed to be prepared, by combining UW preservation solution and Xenetix 350 to reach a density of 1.065 kg/m^3, and was added to the culture plate. The remaining empty fluids, CMRL 1066 culture medium, UW preservation solution and Xenetix 350 then needed to be added to culture plate in accordance with the outlined conditions. Due to the ECIS model ZΘ operating at a temperature of 37°C, the plate needed to be outlined by a ring of wells filled with PBS, in order to avoid the other fluids from evaporating. The plate then had to rest for 30 minutes to allow the cells to settle and adhere to the electrodes on the bottom of the culture plate. This is to avoid a potential updraft in the wells, caused by the temperature difference between the ECIS model ZΘ and room temperature fluids, which can deposit the tissue on the outside of the well, away from the electrodes.

Measurements

Once the plate is entered, the ECIS Model ZΘ takes a measurement of each of the calibrated wells and adjusts the values accordingly. After this the device starts the spectrum analysis of the set frequencies, and continues to repeat this for the set amount of time.

Data acquisition

The ECIS Model ZΘ stores the resulting measurements in its own software environment for analysis. There is an option for data exportation using Excel files to other programs, such as MATLAB which was used in the creation of the graphs.

2.2 Process validation and optimization

2.2.1 Exploring sequential and simultaneous density gradients

Equipment

PRISM 1.0 has been used to create a density gradient, due to its capability of programming specific pump and centrifuge speeds at different time intervals. The continuous flow centrifuge, which is used in PRISM is part of the LivaNova Xtra autotransfusion system and uses the 225 ml Xtra Bowl. For the experiments

in which a simultaneous gradient was built, due to the lack of a second LivaNova system, the predecessor of the autotransfusion system, the Dideco Electa, was used. This device is capable of manually setting the rotational speed of the centrifuge to match the setting for PRISM 1.0. This system makes use of a similar 225 ml bowl, which should internally be equal to the LivaNova Xtra bowl. The used pump motors are from Masterflex and made use of the Masterflex Easy-Load 2 peristaltic pump heads. The tubing set for a single gradient consisted of Masterflex Platinum Cured Silicon tubing (in sizes L/S 13, L/S 14 and L/S 16), a BD microlance injection needle 23G was used for the heavy solution injection. For the simultaneous density gradients, it was sufficient to duplicate the tubing set and service both centrifuges. The liquids are collected in 15 ml conical tubes and measured with an Anton Paar DMA 35 density meter.

Materials

The fluids that have been used to build the density gradients are UW preservation solution, with a density of 1.045 kg/m^3, and Xenetix 350, with a density of 1.409 kg/m^3. To avoid the use of tissue in the sequential density gradient experiments, density beads of various colors have been used: green and orange density beads representing dead tissue ($\sim$1.035 kg/m^3), blue and purple beads representing pancreatic islets ($\sim$1.06 - 1.08 kg/m^3), red beads representing exocrine tissue ($\sim$1.11 kg/m^3) and blue beads to visualize the heavy mixture ($\sim$1.14 kg/m^3).

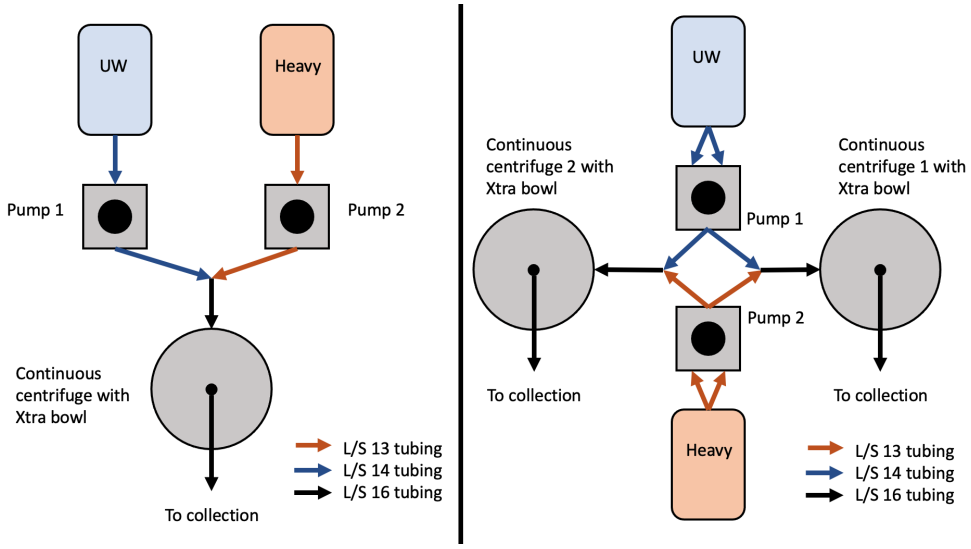

Figure 2.4: Schematic overview of the tubing connections for sequential (left) and simultaneous (right) gradients.

Protocol

Preparation

The tubing set first needed to be autoclaved at 121°C and dried to prevent any residual fluids from remaining in the tubing. Meanwhile, 500 ml of the heavy solution, which consists of UW preservation solution and Xenetix 350 with a combined density of 1.17 kg/m^3, was prepared and transferred to a culture bag. Once this was finished the tubing set was placed in PRISM according to the schematic in figure 2.4, and connected to the two culture bags and the Xtra bowl in the centrifuge.

Measurements

For each of the gradients that had to be created, the PRISM software automatically adjusted the pumping and centrifuge speeds, in accordance to a previously developed protocol, to create a density gradient which rose slowly from 1.045 kg/m^3 to 1.17 kg/m^3. To measure the density, the fluids had to be collected in conical tubes with a sampling size of 13 ml, after reaching a maximum volume of 225 ml in the Xtra centrifuge bowl, after which the simultaneous density gradient experiment is finished. However, during the sequential gradient experiments, the tubing had to be reused to simulate the real situation. Therefore, with use of the pumping system, it was needed to empty the residual fluids of the Xtra centrifuge bowl. When this was finished, a new density gradient protocol was started up and commenced as described before.

Data acquisition

For equal comparison between various conditions, the fluids were allowed to heat up to room temperature before measurements were taken. While this slightly alters the density, it will be the same deviation for each of the measured conditions. To ensure the solution in the conical tubes was properly mixed, it was shaken a few times before the measurements were taken. The resulting values were ultimately taken using the Anton Paar DMA 35 density meter and stored in an Excel file, and finally processed with MATLAB.

2.2.2 Tubing

Equipment

This experiment required a tubing set consisting of either Masterflex L/S 14 platinum cured silicon tubing, or Masterflex L/S 14 Puri-Flex tubing, which were connected with the use of Masterflex luer connections to a culture bag. The pump that was used is a Masterflex Variable-Speed Drive with a maximum RPM of 600, with a Masterflex Easy-Load 2 peristaltic pump head attached. To measure the output volumes, two 500 ml flasks are needed which are weighed by a Sartorius VWR-1502 scale.

Materials

The experiment was conducted using water.

Protocol

Preparation

The tubing was prepared by autoclaving it at 121 °C after which it was allowed to dry. Depending on the treatment protocol that had to be tested, the tubing was connected to either a culture bag with water, or air, and to the pump according to figure 2.5.

In this experiment the baseline needed to be created using platinum cured silicon tubing without any treatment, which is how the tubing was normally used. The remaining protocol tests were performed on the Puri-Flex tubing which received the following treatments: rolled in with water for 15 minutes, rolled in with water for 30 minutes and rolled in with air for 30 minutes. Which can be achieved by circulating either water or air for 15 or 30 minutes through the tubing at a speed of 175 RPM (30% pump rotational

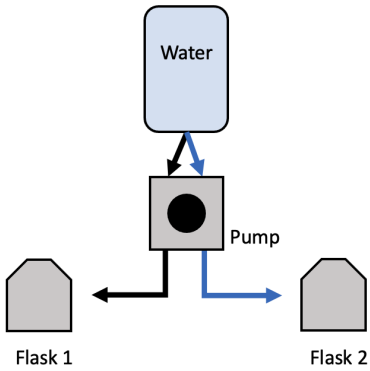

Figure 2.5: Schematic overview of the tubing connections for the validation of the Puri-Flex tubes and the preparation protocol.

speed).

Measurements

The first measurements taken were from the empty flasks, to correct further results for an offset in weight between the two. This was followed by pumping liquid at 40 ml/min (175 rpm) to both flasks. Weight measurements of both flasks were taken when flask 1 reached a volume of 10, 50, 100, 150, 200 and 250 ml. The difference in weight between the two flasks was indicative of the volume difference.

Data acquisition

The data was read from the scale and corrected for the base weight of both flasks. The results have been stored in Excel and processed in MATLAB.

2.2.3 Pump validation

Equipment

The experiments have mainly been performed with the use of newly developed motors from the development department of the LUMC. The Masterflex pump drives from PRISM 1 were also used for comparison. Both the motors made use of the Masterflex Easy-Load 2 peristaltic pump heads for the displacement of liquids. The tubing used in these experiments consisted of Masterflex Puri-Flex tubing with sizes L/S 13 and L/S 14, and Masterflex Platinum cured silicon tubing with size L/S 25, which are capable of achieving a flow of 36 ml/min, 130 ml/min and 1000ml/min at 540 RPM respectively. The displaced water was collected in a flask and measured with a Sartorius VWR-1502 scale. To evaluate the rotational speed of the pump heads, a Testo 465 optical tachometer was used.

Materials

The experiments have been performed with the use of water.

Protocol

Preparation

The tubing needed to be autoclaved at 121 °C and then dried to clear any residual liquids. The tubing was connected according to figure 2.6, and consisted of two equal length tubes of Puri-Flex L/S 13 or L/S 14, or platinum cured silicon L/S 25. The tubing was then rolled in for 30 minutes at 175 RPM, to increase the accuracy of the tubing.

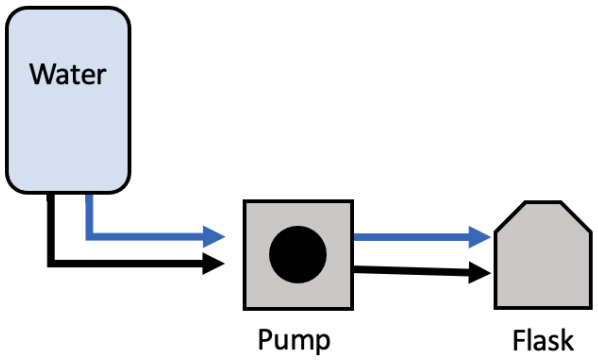

Figure 2.6: Schematic overview of the tubing connections for the validation of the developed pumps.

Measurements The first measurements taken were from the empty collection flask to be able to correct for the empty weight. The rotational speed of the pump was gradually increased from 3% to 100% of the maximum rotational speed of 540 RPM, to evaluate the characteristics of the pump over the full range. For every point the pump was allowed to work for 2 minutes at a time in order to diminish potential effects of the switch on and switch off behavior. After these 2 minutes the displaced volume in the flask was weighed and emptied.

Data acquisition

The data was measured using the Sartorius VWR-1502 scale and collected in Excel, after which MATLAB has been used to process the data.

2.2.4 Simultaneous density gradient validation

Equipment

The pump system that was used is part of the PRISM 1 system, due to its capability of following a programmed protocol, and adjusting the pump speeds accordingly. The pump drives are from Masterflex and made use of Easy-Load 2 peristaltic pump heads which can each fit two tubes. To create simultaneous density gradients, two continuous flow centrifuges had to be used, one was available in PRISM 1, which is from a LivaNova XTRA autotransfusion system, and the other is from the Dideco Electa, which is a predecessor to the LivaNova system. The centrifuges made use of a disposable Latham bowl in which the fluids are contained, which, for the LivaNova system, is the 225 ml Xtra bowl, and for the Dideco system is the BT225 Latham bowl, which is internally equal to the LivaNova bowl. To connect everything, a tubing set made from Masterflex Puri-Flex tubing, containing sizes L/S 13, L/S 14 and L/S 16, was used which was equal in length for both the centrifuges. To ensure the used fluids are mixed, the heavy

component was injected through a 23G BD microlance injection needle. Ultimately, the collected liquids from the density gradients are collected in 15 ml conical tubes and measured with an Anton Paar 35 density meter.

Materials

The fluids that were used to build the density gradients were UW preservation solution, with a density of 1.045 kg/m^3, and Xenetix 350, with a density of 1.409 kg/m^3.

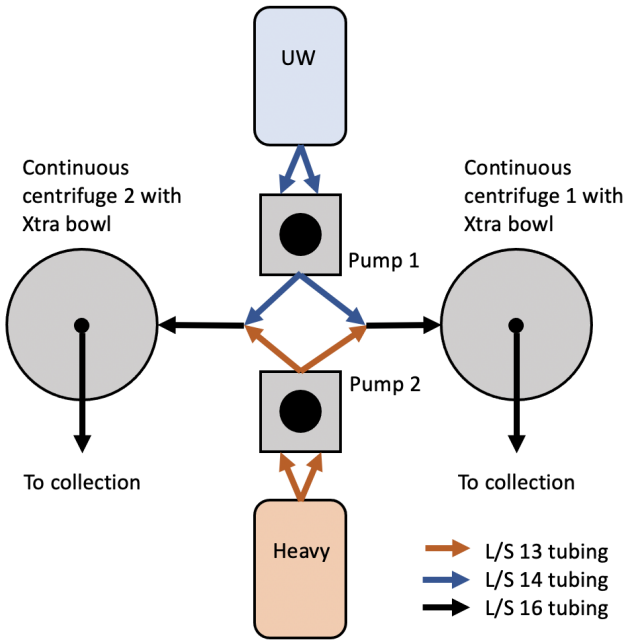

Figure 2.7: Schematic overview of the tubing connections for the validation of the simultaneous density gradients.

Protocol

Preparation

Before the tubing set could be used, it had to be autoclaved at 121°C and then dried to prevent from any fluids from remaining in the tubing. The only liquid that needed to be prepared was the heavy mixture, which needs to be a 1 liter with a density of 1.17 kg/m^3, and consists of UW preservation solution and Xenetix 350. After preparing the fluids, they could then be attached to the tubing set and installed in the machines, as outlined in figure 2.7. This was then followed by a 30 minute rolling in treatment of the tubing set, to increase the accuracy of the tubing.

Measurements

After all the preparations were done, the density gradient protocol was started, in which the PRISM software automatically adjusted the pumping speeds and started the centrifuge at 1500 RPM. As soon as the centrifuge bowl of PRISM started spinning, the centrifuge from the Electa Dideco needed to be started at the same speed as well. The software slowly built up the density gradient from 1.045 kg/m^3 to 1.17

kg/m^3.Once the centrifuge bowls were full, the fluid mixture exited the system and had to be collected in the tubes for measurement.

Data acquisition

The tubes containing the liquids from the density gradient were allowed to heat up to room temperature, in order to have equal conditions across all measurements. The measurements were taken using an Anton Paar DMA 35 density meter after slightly shaking the tube to ensure the mixture within is mixed. The results were then entered in Excel and processed using MATLAB.

CHAPTER 3

Results

3.1 Pancreatic islet identification

3.1.1 Optical absorption spectroscopy

A potential method to use for pancreatic islet identification is optical absorption spectroscopy, by exploring the spectrum of pancreatic islets and exocrine tissue, an estimation can be made on whether or not the differences in composition between the tissues, leads to a difference in optical properties. Two experiments have been performed to investigate the optical absorption spectrum, more were intended, but unfortunately the Spectramax i3x broke down and made further experiments impossible. The two conducted optical absorption spectroscopy experiments are shown separately, due to differences in their resulting values.

Optical absorption spectroscopy experiment 1

To create a baseline against which the tissue can be measured, the first step was to evaluate the culture plate and empty fluids, which are used in the PancReatic Islet Separation Method (PRISM), these results can be seen in figure 3.1. The output from the Spectramax i3x shows the transmittance rather than absorbance, but these values are closely linked to each other. This figure shows that all the light below a wavelength of 290 nm is absorbed by the culture plate in combination with each of the fluids. While most fluids then allow light to pass through, the University of Wisconsin (UW) preservation solution and heavy mixture continues to absorb light until a wavelength of 340 nm. From around 400 nm until 900 nm, each of the conditions has a transmittance of around 93%. Which is followed by a little dip in the transmittance values for each of the conditions.

This was followed by measurements of the pancreatic islets and exocrine tissue in Phosphate Buffered Saline (PBS) and culture medium. However, due to irregularities in the preparation phase, only the results with culture medium have been included in the results section, the results from the PBS measurements can be found in Appendix A.1.1.

Figure 3.2 shows the measurements of pancreatic islets and exocrine tissue submerged in culture medium. Once the culture medium allows the transmittance of light at 290 nm wavelength, the exocrine tissue's transmittance rises quickly. After reaching a wavelength 340 nm, the culture medium levels off and the exocrine tissue shows to have a gradual rise of transmittance up till a wavelength of 900 nm. The

pancreatic islets do not have the initial steep rise of transmittance after reaching a wavelength of 290 nm, but show to have a more gradual rise with increasing wavelengths. This results in a lower transmittance, especially in the region between 290 nm and 600 nm. The measurements of the 2000 Islet EQuivalent (IEQ) condition of the pancreatic islets have a large deviation across the spectrum, but the median is in-between the other two conditions. Additionally, the results show that with an increase in tissue in the well, the amount of transmittance measured decreases.

To allow for easier comparison, the results of the pancreatic islets and exocrine tissue have been combined in figure 3.3. The top graph in this figure shows the mean values of the measurements, and shows the pancreatic islets generally have a lower transmittance than their same IEQ counterpart of exocrine tissue. In the bottom graph the difference in transmittance between equal conditions is depicted, and shows a changing difference over the spectrum. The difference starts out with a maximum around a wavelength of 330 nm and gradually decreases with a rise in wavelength.

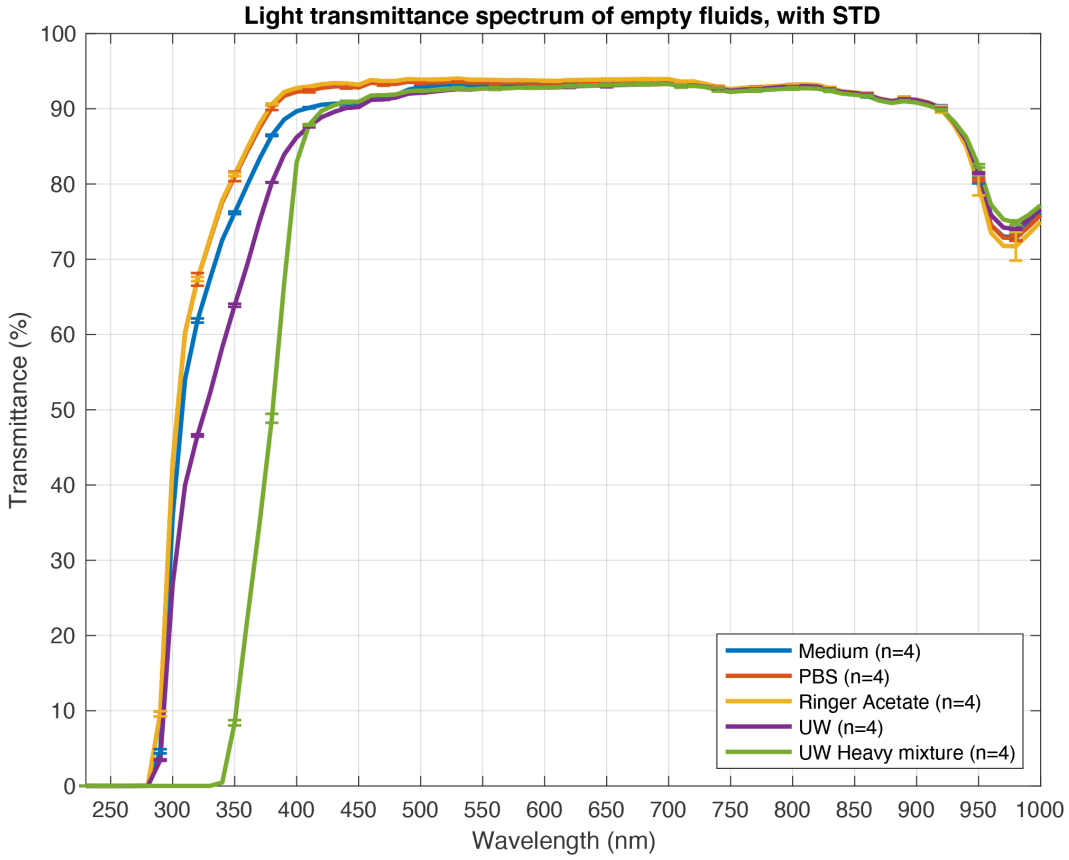

Figure 3.1: Experiment 1: The transmission spectrum of the fluids used in PRISM without any tissue to provide a baseline. The error bars represent the standard deviation of the performed measurements.

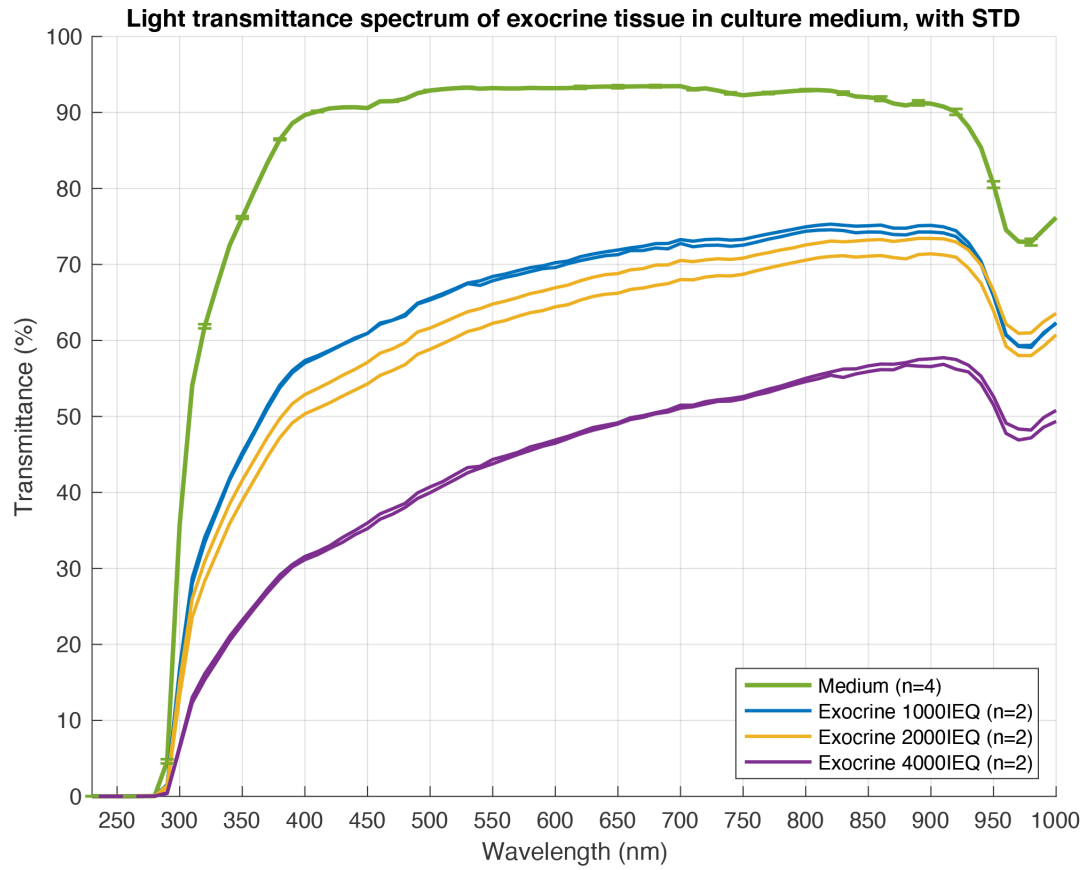

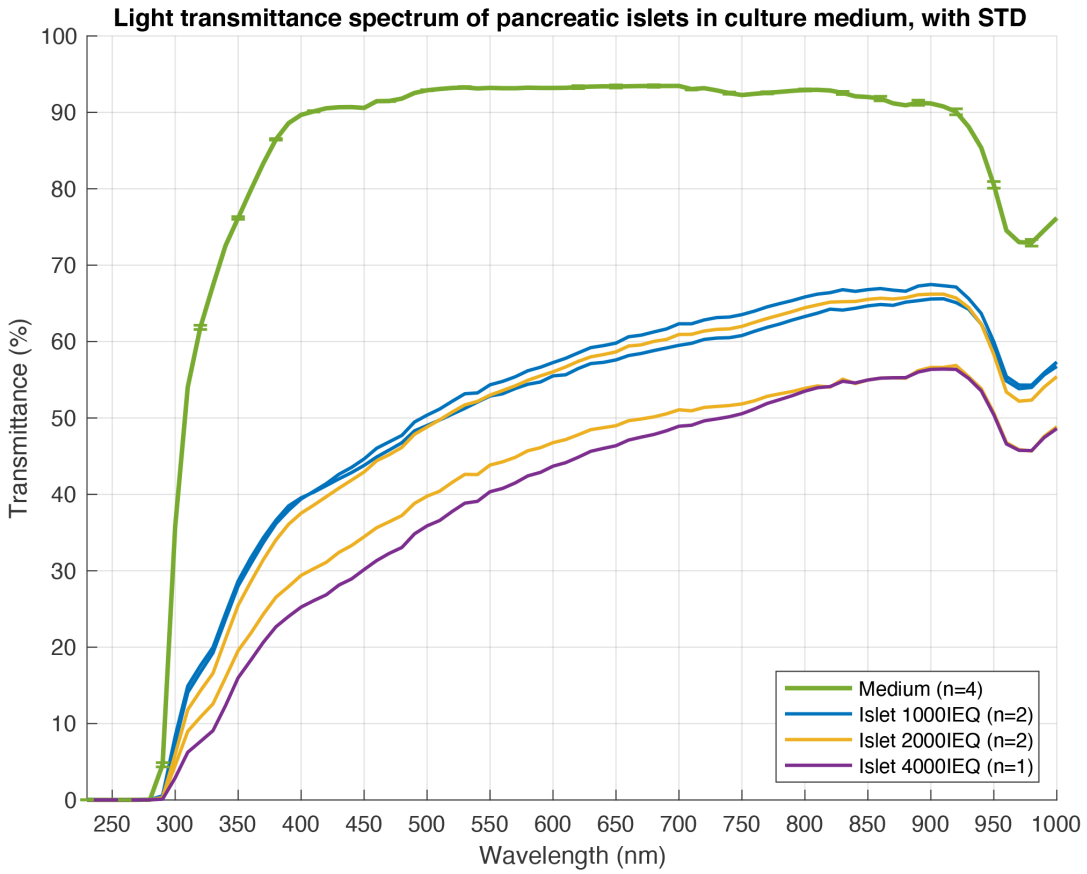

Figure 3.2: Experiment 1: The transmission spectrum of exocrine tissue (top) and pancreatic islets (bottom) suspended in culture medium. The error bars represent the standard deviation of the performed measurements.

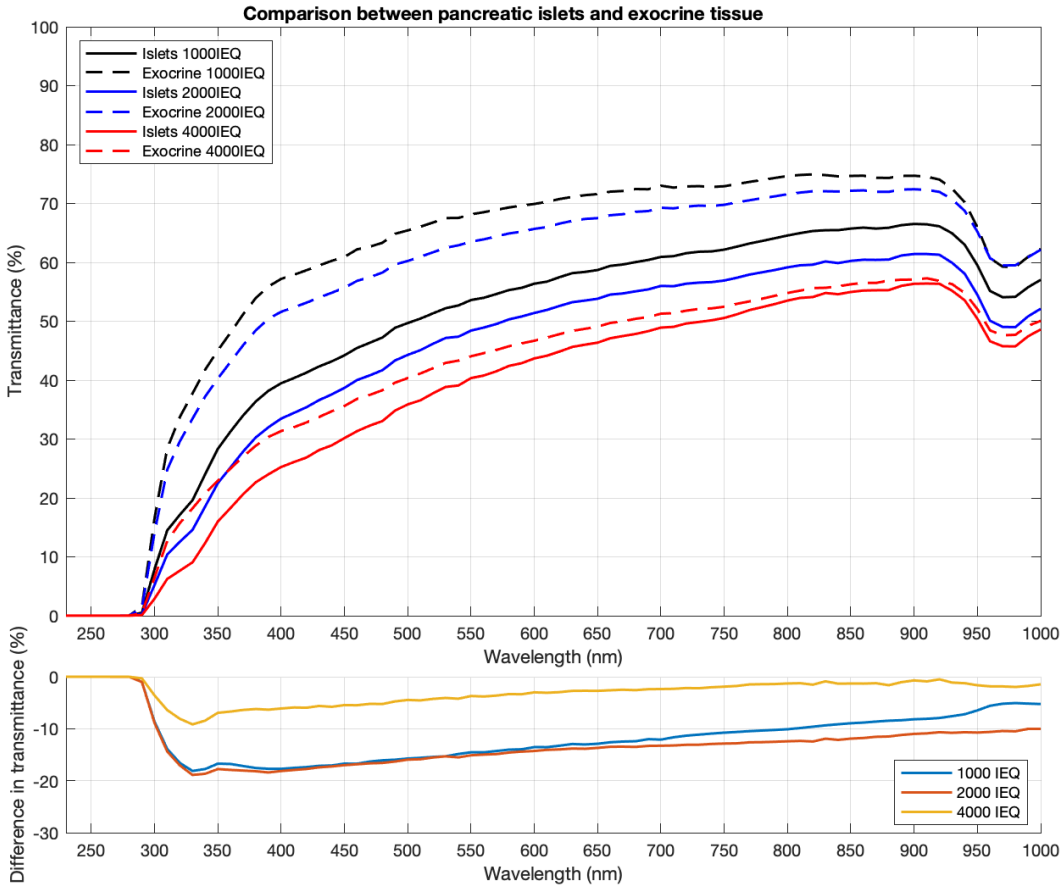

Figure 3.3: Experiment 1: Comparison between pancreatic islets and exocrine tissue suspended in culture medium. Top graph shows the mean transmittance of each condition and the bottom graph shows the difference between conditions (transmittance pancreatic islet - transmittance exocrine tissue).

Optical absorption spectroscopy experiment 2

The second experiment had a similar set up to the first, but was limited to measuring the tissue in culture medium only, in order to facilitate a higher number of measured conditions. To create a frame of reference for further measurements, this experiment started out with a spectrum analysis of the empty fluids, which can be seen in figure 3.4. Similar to experiment 1, the UW and ringer conditions start allowing light to pass through at a wavelength of 290nm, and the heavy mixture at a wavelength of 340 nm. However, the culture medium shows an increased amount of variability between the measurements and has, compared to the previous experiment, a lower overall transmittance value.

The measurements of the exocrine tissue and pancreatic islets can be seen in figure 3.5, and shows that for each of the conditions there was a larger variability between the measurements. In contrast with the first experiment, the resulting transmittance values of the exocrine tissue are lower than those of the pancreatic islets and only show a gradual rise in transmittance with a higher wavelength. The pancreatic islets initially show the steeper rise around a wavelength of 330-350 nm, after which the transmittance gradually rises for the remainder of the spectrum. Similar to the first experiment, a difference in transmittance is observed that is dependent on the amount of tissue present in the well.

Ultimately the mean results of the pancreatic islets and exocrine tissue are plotted in figure 3.6, to allow for easier comparison. The results in the top graph show that the pancreatic islets allow for more transmittance of the light compared with the equal conditions of exocrine tissue. The bottom graph shows the associated difference in transmittance (transmittance value of pancreatic islets minus the value of exocrine tissue) between the conditions. This graph shows a gradual increase of the difference between the two conditions for the 2000 IEQ and 4000 IEQ lines. However, for the 1000 IEQ line this difference shows to be somewhat stationary across the spectrum.

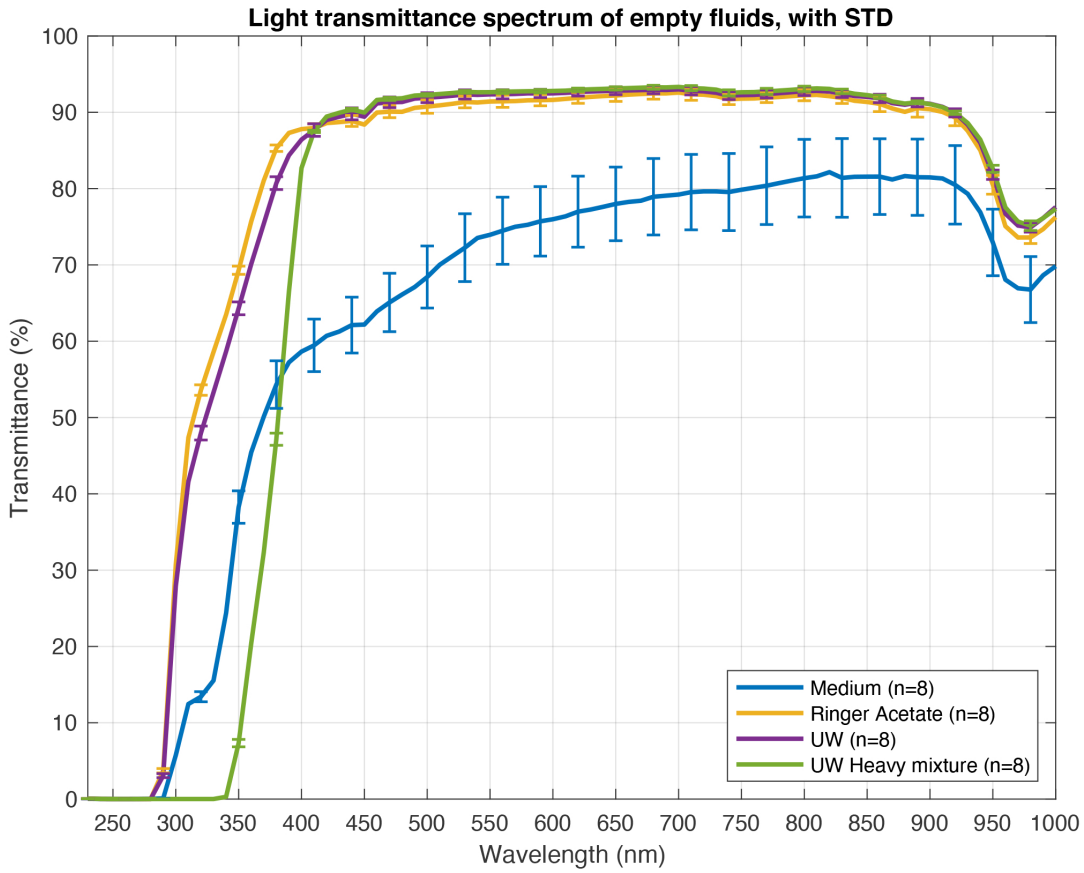

Figure 3.4: Experiment 2: The transmission spectrum of the fluids used in PRISM without any tissue to provide a baseline. The error bars represent the standard deviation of the performed measurements.

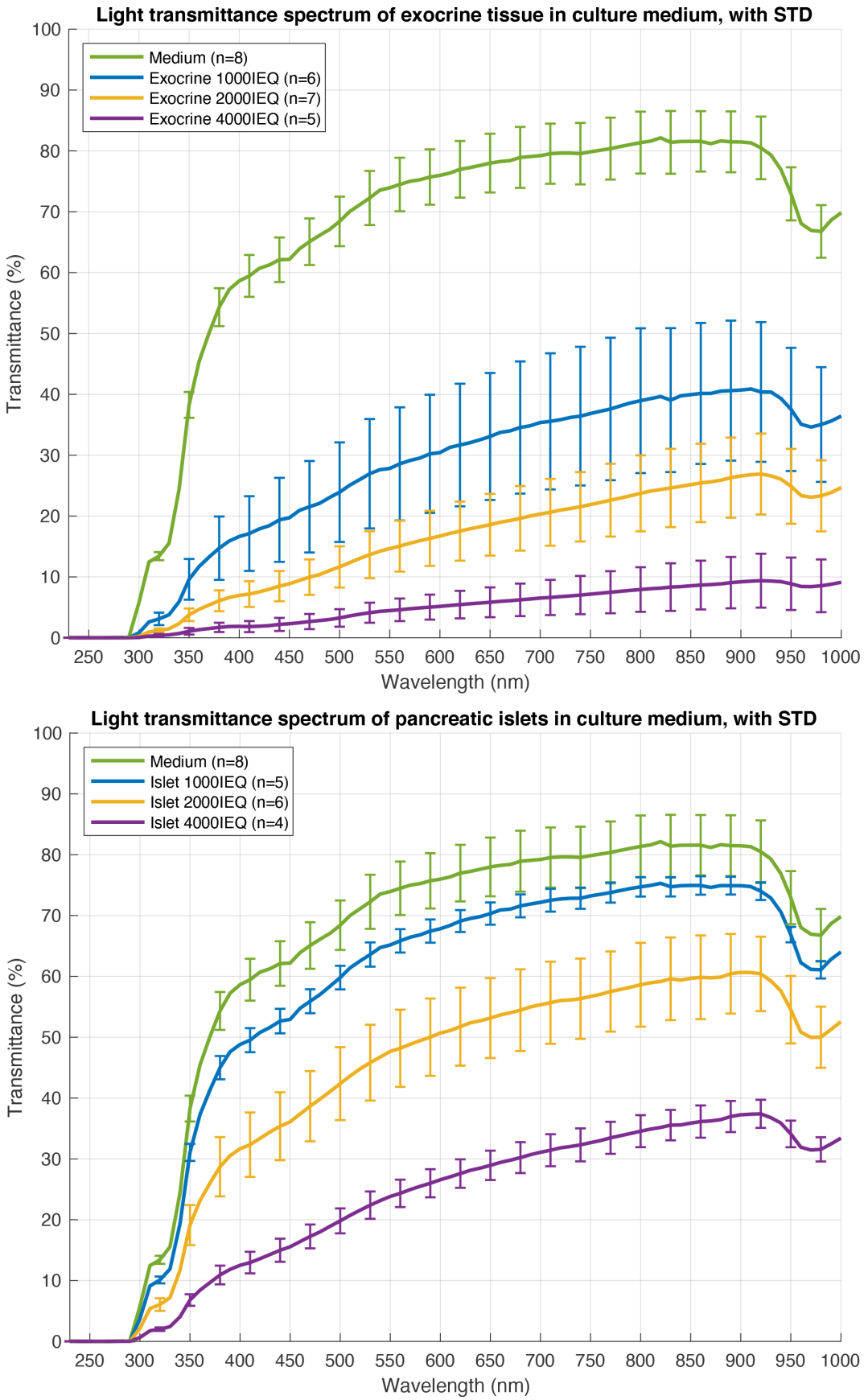

Figure 3.5: Experiment 2: The transmission spectrum of exocrine tissue (top) and pancreatic islets (bottom) suspended in culture medium. The error bars represent the standard deviation of the performed measurements.

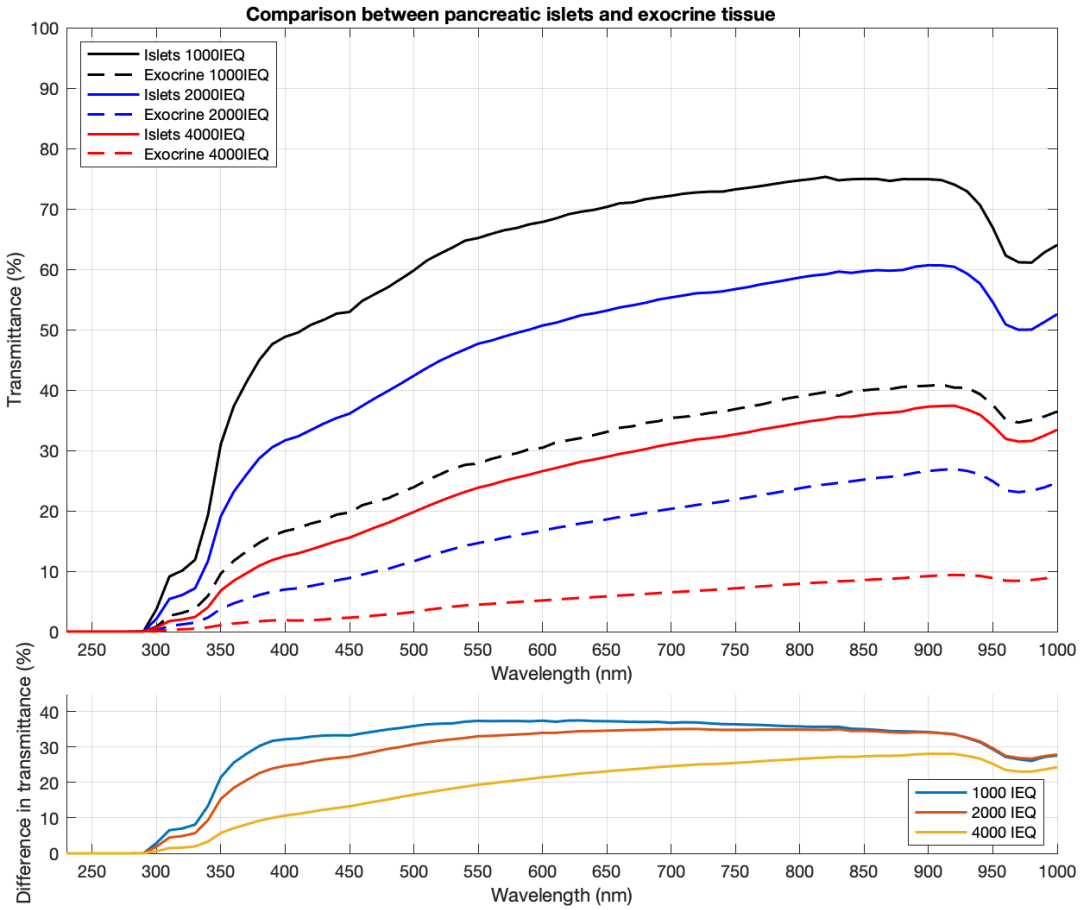

Figure 3.6: Experiment 2: Comparison between pancreatic islets and exocrine tissue suspended in culture medium. Top graph shows the mean transmittance of each condition and the bottom graph shows the difference between conditions (transmittance pancreatic islet - transmittance exocrine tissue).

3.1.2 Electrical impedance spectroscopy

With the exploration of the electrical impedance spectrum of pancreatic islets and exocrine tissue, potential differences in electrical properties of these tissues can be determined, which in turn could be used for identification purposes. In order to create a frame of reference during these measurements, the spectral analysis was first performed on empty fluids, which is shown in figure 3.7. Looking at the top graph of this figure, this graph shows that at lower frequencies all three fluids have similar impedance values, and only begin to diverge from each other at 2000 Hz, and reach a maximum difference at 64000 Hz. The resulting values of each of the conditions has remained fairly stable throughout the measurements, with an average standard deviation 8 Ω. Because the divergence is at its maximum at 64000 Hz, the bottom graph shows the boxplot data of the impedance measurements at this frequency for better comparison.

This was followed with measurements of various conditions of pancreatic islets and exocrine tissue. The results, which can be seen in figure 3.8 and figure 3.9, show, in the top graphs, a similar spectral behavior between both types of tissue. Initially, the impedance values of both types of tissue follow the same slope while decreasing in impedance with an increase of frequency, and do not show to have much difference in-between conditions. However, from a frequency of 8000 and higher, the impedance values start to level off and start to diverge between conditions, with a maximum divergence at 64000 Hz. Therefore, the bottom graph of both figures shows a boxplot of the impedance values at 64000 Hz. The measurements for each of the conditions have been fairly stable but show an increase in of impedance values for an increased amount of tissue in the well.

Finally, to allow for easier comparison, the results at 64000 Hz have been combined in figure 3.10. This graph shows the measured conditions of pancreatic islets to have a lower impedance value than the conditions of exocrine tissue. However, the conditions with a high number of pancreatic islets overlap with the impedance values from exocrine tissue.

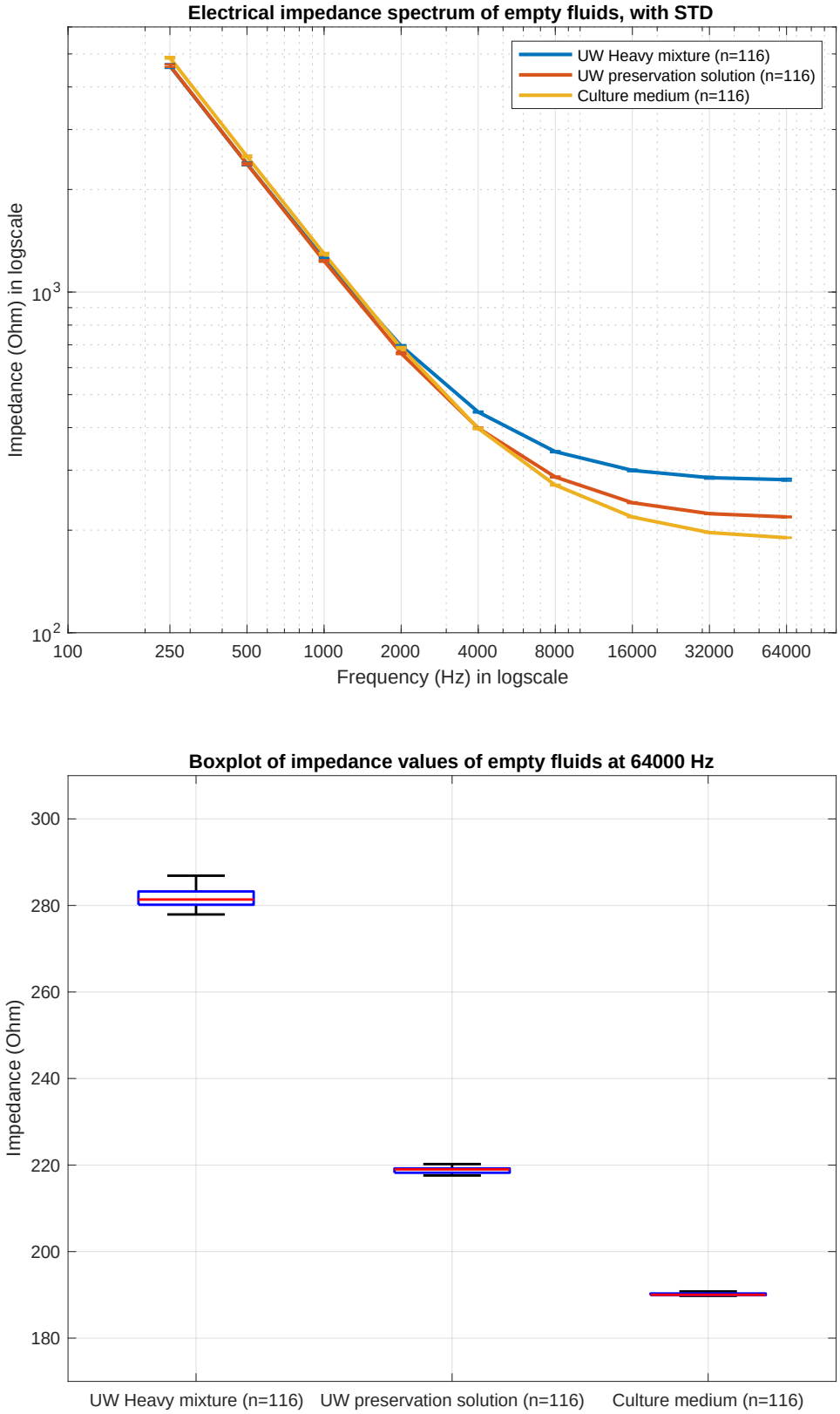

Figure 3.7: Electrical Impedance measurements of empty fluids. Top graph shows the spectrum (in double logarithmic scale) of empty fluids with error bars representing the standard deviation of the performed measurements. The bottom boxplots show the impedance measurements at a frequency of 64000 Hz.

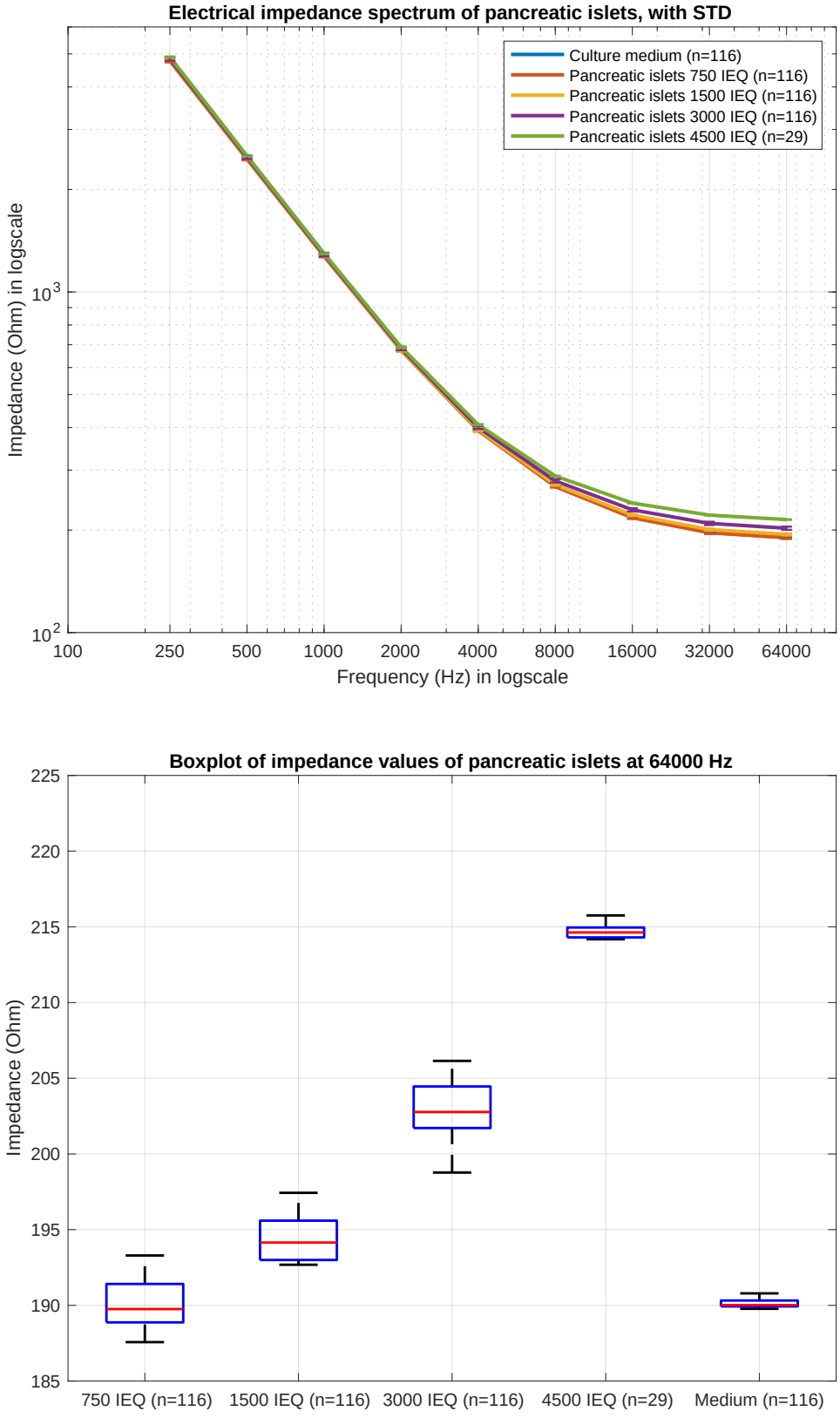

Figure 3.8: Electrical Impedance measurements of pancreatic islets. Top graph shows the spectrum (in double logarithmic scale) of pancreatic islets with error bars representing the standard deviation of the performed measurements. The bottom boxplots show the impedance measurements at a frequency of 64000 Hz.

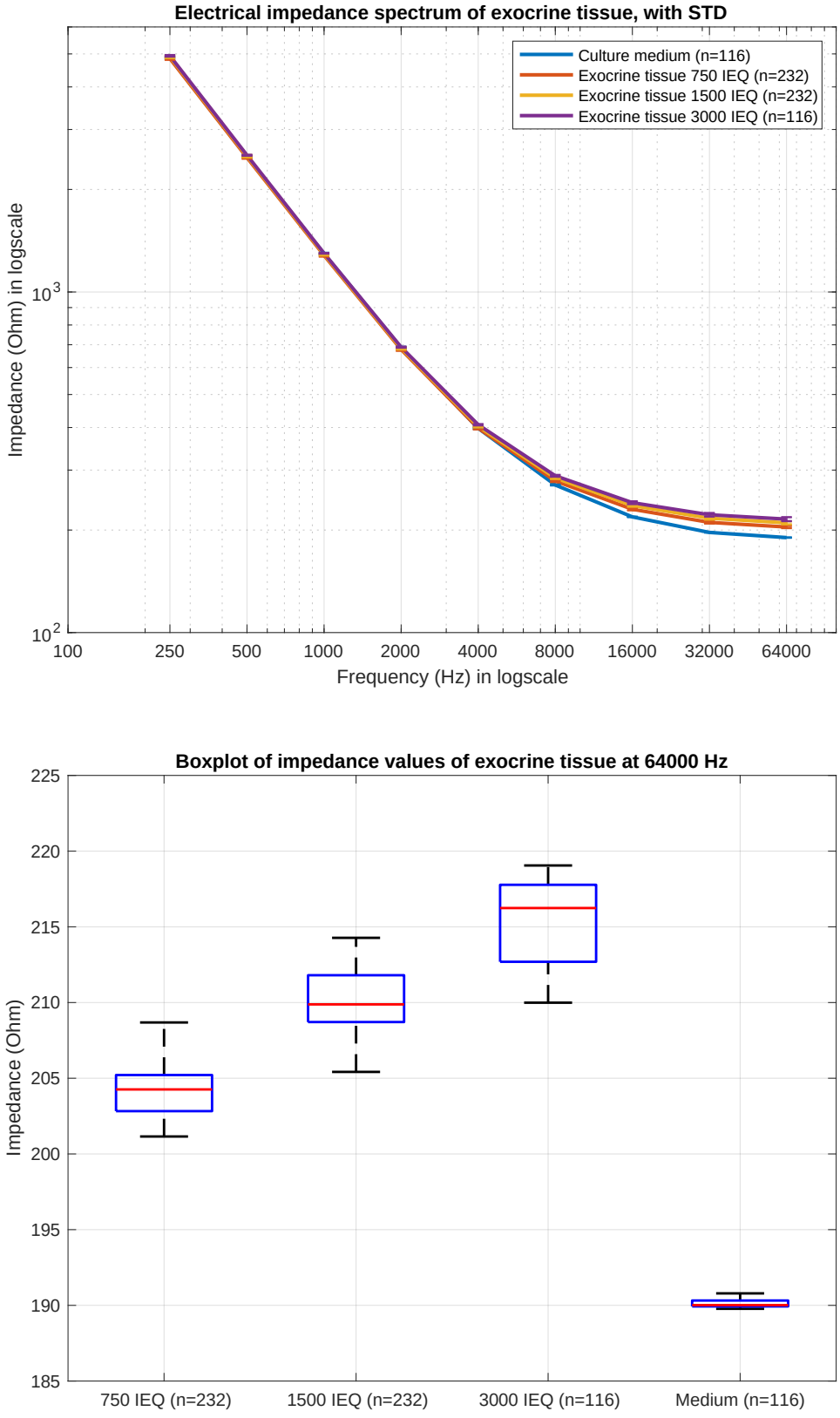

Figure 3.9: Electrical Impedance measurements of exocrine tissue. Top graph shows the spectrum (in double logarithmic scale) of exocrine tissue with error bars representing the standard deviation of the performed measurements. The bottom boxplots show the impedance measurements at a frequency of 64000 Hz.

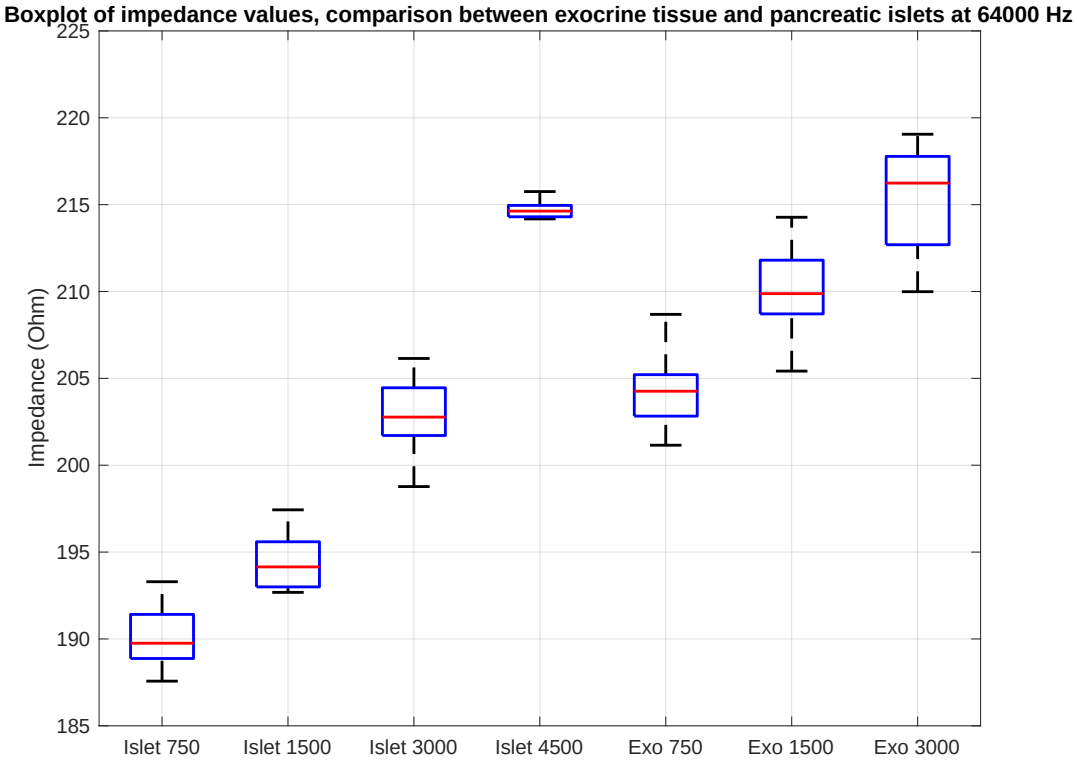

Figure 3.10: Comparison between electrical impedance measurements of pancreatic islets and exocrine tissue at a frequency of 64000 Hz.

3.2 Process validation and optimization

3.2.1 Exploring sequential and simultaneous density gradients

In order to find a possible solution for the limitations introduced by the limited size of the Latham bowls, the following research question and hypothesis were established:

- ***Research question:*** Can optimization of the controllable variables during the density gradient process, lead to a more consistent creation of sequential and/or simultaneous density gradients, in order to solve the Latham bowl size limitations during pancreatic islet isolations?
- ***Hypothesis:*** By further examining the processes to create sequential and simultaneous density gradients, the expectation is that this will lead to a robust and reliable solution to create said density gradients, aimed at solving the 225 ml Latham bowl size limit.

To evaluate the hypothesis, the sequential density gradients were investigated first, the results of these experiments are shown in figure 3.11, and show a different starting position for each of the three density gradients. For the first experiment the density gradient was built in a clean and empty set of tubing, which resulted in a starting density of 1.043 kg/m^3. In contrast, the second gradient is build on the little remaining fluids from the first gradient and shows to have a starting density of 1.067 kg/m^3. In the third gradient the situation of gradient 2 was attempted to be recreated in a clean tubing set and starts with an initial value of 1.055 kg/m^3. The starting point of the density gradients has an effect over the initial phase of the gradient and the results only start to converge at around 390 ml.

To visualize the impact the gradients have on the separation of tissue, density beads have been added to this experiment, figure 3.12 shows the separated density beads in fractions 1 to 10 for each of the gradients, the full image can be seen in figure A.5. One of the main noteworthy observations in this figure is the different composition of the density beads in the initial 4 tubes. Gradient 1, which is the density gradient in the clean set, shows the first tube on the left to contain only orange and green beads (which represent dead tissue) and is followed by two almost empty tubes. In comparison, gradient 2, which is has a different starting density as indicated before, shows a large number of beads in the first container, among which are orange, green, blue and purple (the last two colors represent pancreatic islets). With a starting density in between the first two gradients, gradient 3 again shows to be halfway in-between the other two. The first tube still has orange and green beads visible, but already contains some purple and blue beads, however, not as densely packed as in gradient 2. The tubing that follows the initial one also shows to contain purple and blue beads, which represent pancreatic islets.

The sequential density gradients were followed by two experiments in which two simultaneous density gradients were made, the results of which can be seen in figure 3.13. The goal with simultaneous density gradients is for both of the gradients to follow the exact same gradient and therefore have the same pancreatic islet isolation results. The starting point of both the gradients in each experiment are quite close to each other, but slowly start to diverge as the amount of fluids that pass-through increases with a maximum difference of 0.0047 kg/m^3 for experiment 1 and 0.0062 kg/m^3 for experiment 2. Furthermore, the experiments end with different amounts of liquid that have been pumped through, the differences are: 26 ml in experiment 1 and 39ml in experiment 2. With both methods explored, it is clear that both methods show to have area's for improvement, a decision for further development will have to be made.

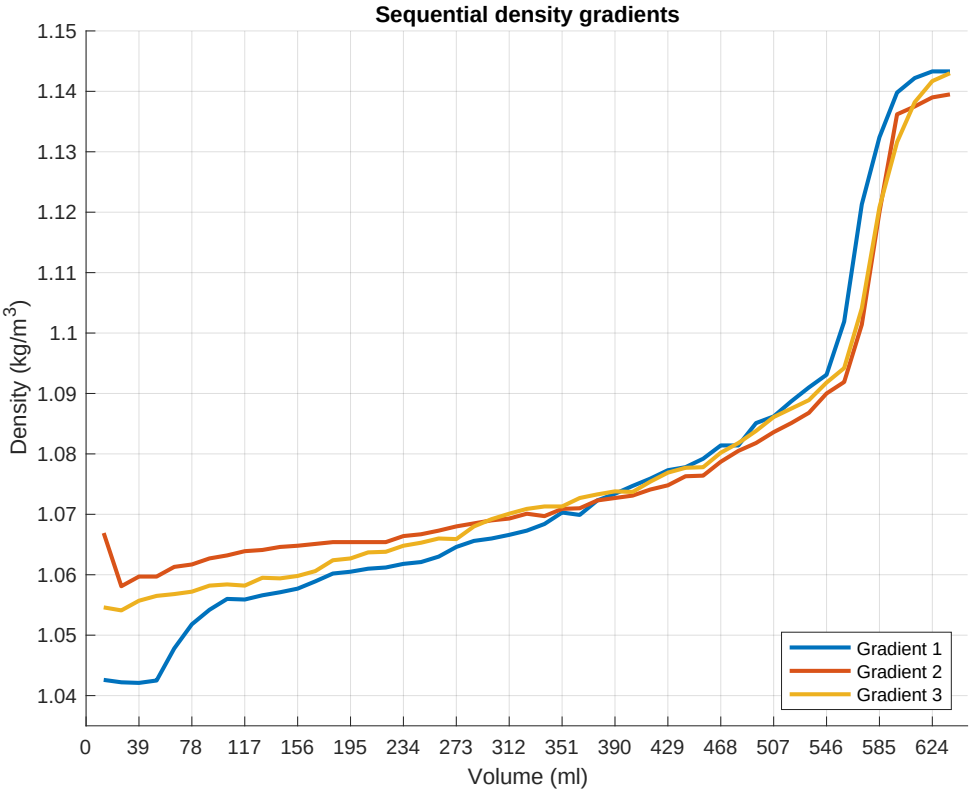

Figure 3.11: Three sequential density gradients in the same Xtra 225ml bowl, measured at 13 ml intervals.

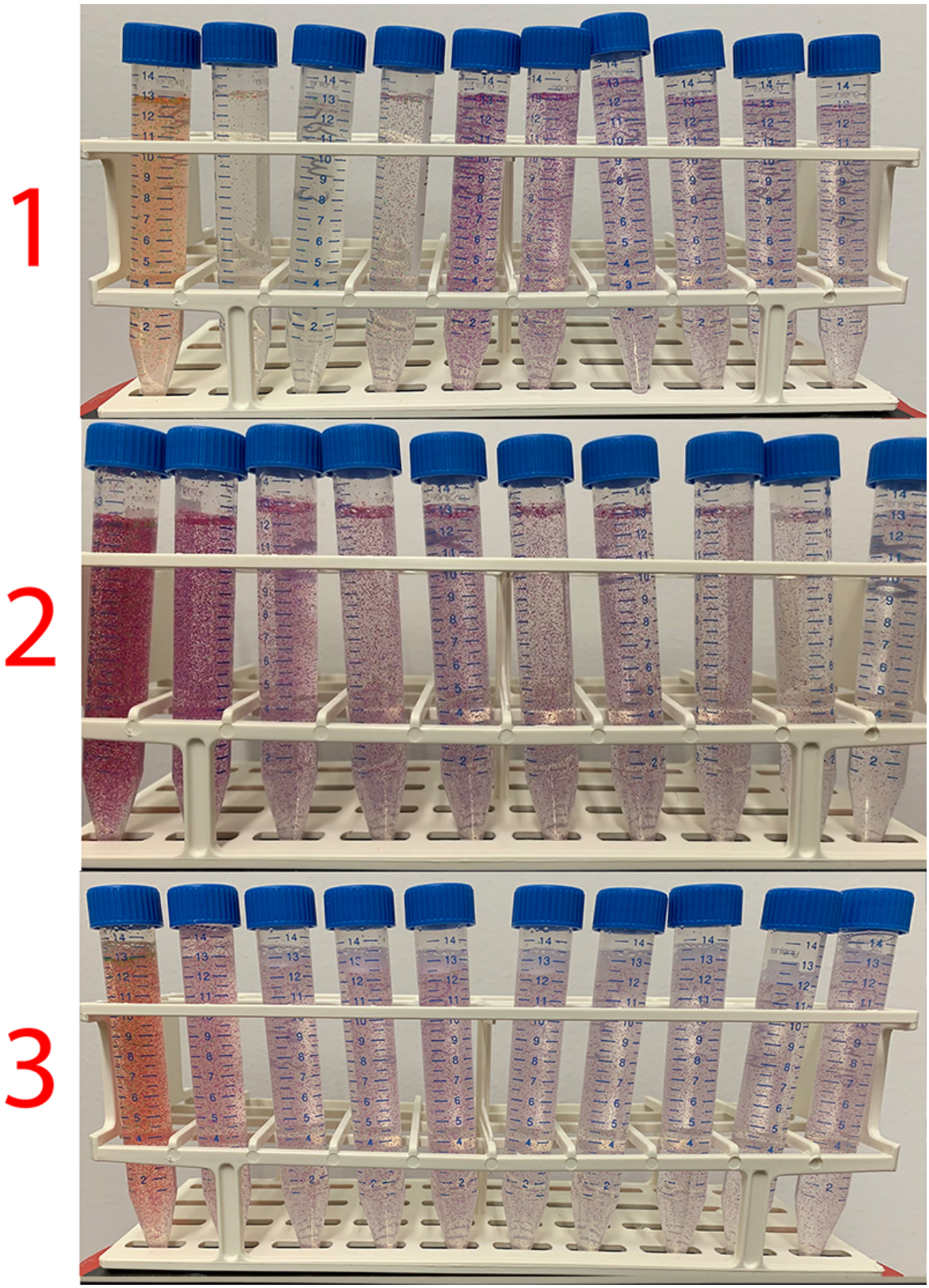

Figure 3.12: The tubes contain the first 10 (with number 1 on the left) fractions of 13 ml from the density gradients as outlined in figure 3.11. The beads each have a specific density and are differently separated in each of the three gradients. The full picture is shown in figure A.5.

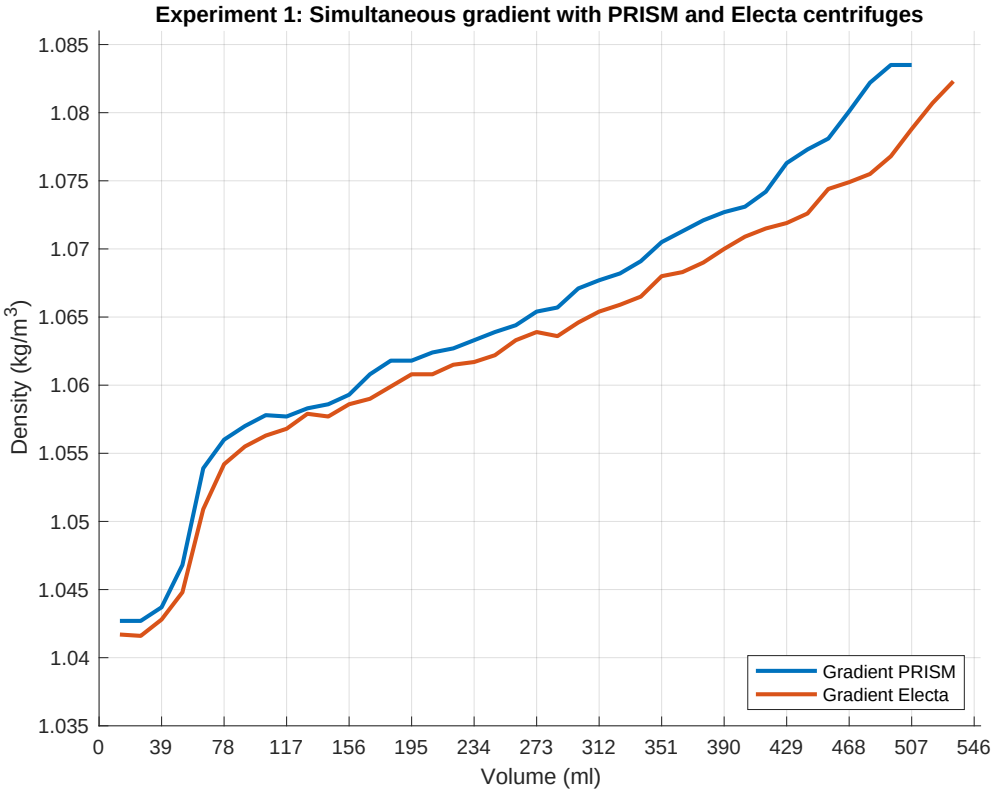

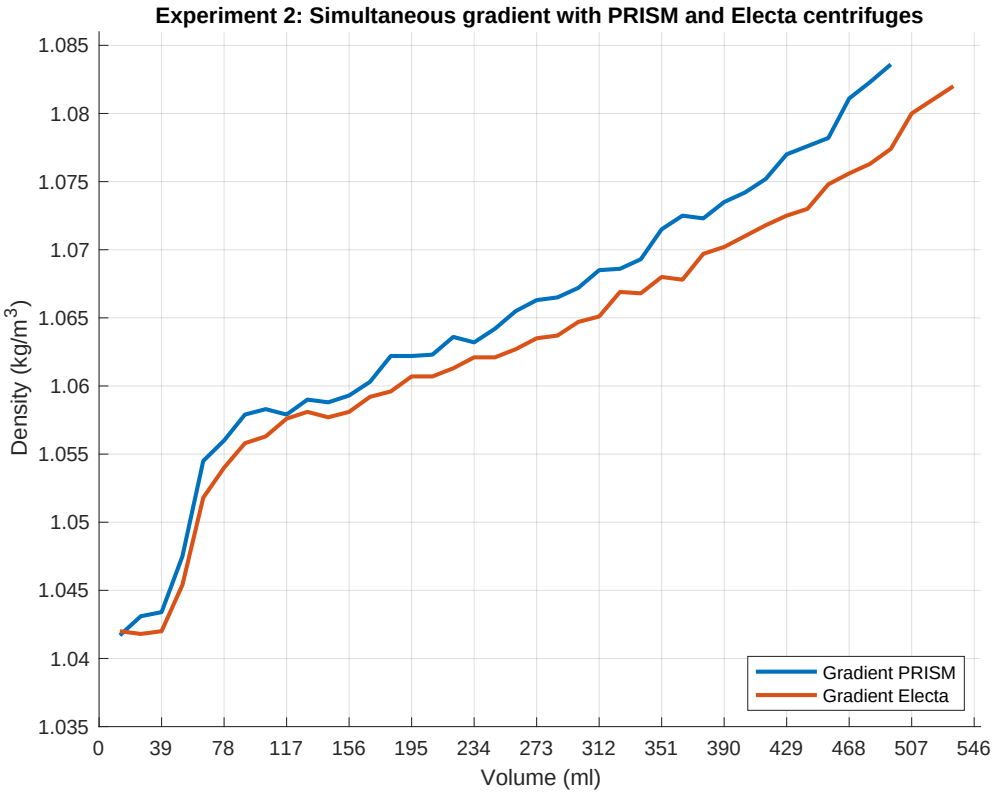

Figure 3.13: First attempts at building simultaneous density gradients by using two continuous centrifuges (one from PRISM and one from Electa). Measurements have been taken at 13 ml intervals.

3.2.2 Tubing

A key factor in performing successful simultaneous density gradients is to have a highly accurate flow through the tubing. Therefore, the following research question was investigated:

- ***Research question:*** Can the standard tubing be used to deliver similar volumes to different containers using a single peristaltic pump head?
- ***Hypothesis:*** A treatment procedure of the tubing before use will lead to more consistent results by making the tubing more malleable.

The results of the experiments to investigate this research question is shown in figure 3.14. A baseline measurement is created with the use of untreated platinum cured silicon tubing, which is the current tubing in PRISM 1.0, and which represents the way the tubing is currently used. The results for this condition show a high variation and reaches a relatively high volume difference between tubes 1 and 2. The Puri-Flex tubing which have been rolled with water perform better, especially when treated for 30 minutes, and show to have a lower variation and low difference between the two tubes. The treatment with air, however, has a higher variation and the highest difference between the two tubes. Ultimately, the tubing with the lowest variation and difference between the two tubes is the Puri-Flex tubing which has been rolled with water for 30 minutes. Upon examination of the tubing after each of the conditions, it was found that the tubing which had a 30 minute treatment with water, had become more pliable where it was in contact with the pump head.

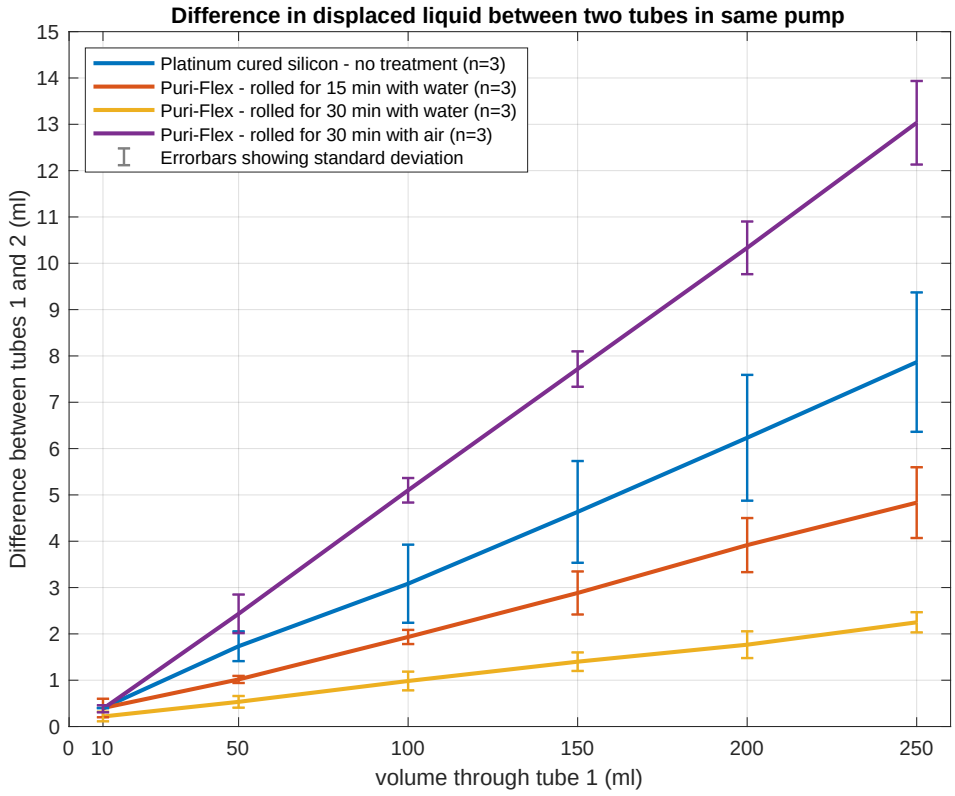

Figure 3.14: Differences in tubing treatment protocols, in which the baseline of platinum cured silicon tubing is compared with Puri-Flex tubing, after receiving a specific treatment. The goal is to achieve a low variation and a low difference between two tubes.

3.2.3 Pump validation

In order to create repeatable simultaneous density gradients, it is important that the characteristics of the developed pumps have a linear progression and accurately match the expected values. Because PRISM 1.0 has previously proven to be capable of creating density gradients, this system has been used as a baseline, and is shown in figure 3.15. The graph shows the percentage of the maximum rotational speed of the pump, which is 540 RPM, on the x-axis, and on the y-axis, it shows the percentage of the maximum flow, which is 36 ml/min for L/S 13 and 130 ml/min for L/S 14. The resulting flow speed initially follows a near linear rise, followed by a slight bump around 60% and eventually reaches a maximum flow of 95% of the tubing capability.

The pump system has been tested with three different control methods, voltage control, pulse width control and a PID controller. The voltage controlled version of the pump has been tested with three types of tubes, L/S 13, L/S 14 and L/S 25, and the results of this are shown in figure 3.16. The flow in the tubes is high compared to the expected line for all three conditions, and reaches the indicated maximum flow rate at around 70% to 80% of the input voltage. At higher pump rotation speeds the flow rates continue to rise but slowly start to level off. While the variability between the measurements is low, the measurements do not represent a linear progression.

The second version of the pump which has been tested includes a pulse width controller and has been tested with the L/S 13 and L/S 14 tubing, the results of which can be seen in figure 3.17. The pulse width controller creates a more linear characteristic for the pump and shows to have a relatively small variance across the measurements. The flow rates in the L/S 14 tubing are closer to the expected values and have a maximum divergence at 70%. The L/S 13 tubing has, however, a higher flow rate than expected at speed settings, and continues to diverge over the entire range. Additionally, the highest measured value of the L/S 13 line, which is higher than the maximum indicated value of the tubing, is at 90% rotation speed. During the experiments, the pump has been observed to show intermittent but steady rotation at lower RPM.

The third version of the pump includes a PID controller, and has been tested with L/S 13 and L/S 14 tubing, as can be seen in figure 3.18. The characteristics of the pump with the PID controller are similar to those of the pulse width controller and show similar divergence from the expected value. The L/S 13 line, again, reaches a higher than indicated maximum flow at around 90% pump speed. At lower speeds the PID controller appears to have difficulty in maintaining a continuous rotation speed, the pump has been observed to handle the lower RPM ranges in a stop and go fashion.

Because there is still a difference between the expected value and the delivered flow by the pump, additional measurements have been taken using a digital tachometer, to see if there is a mismatch between the setpoints and actual values. The results are shown in table 3.1 and show that both methods reach values close to the setpoints. The PID controller ultimately achieves closer values than the pulse width controller.

To find what causes the mismatch between the expected flow and the results so far, another test, using

the PID controller, has been performed in which the pump received a new pump head. In this test only the L/S 14 tubing has been used, and the results show, in figure 3.19, that the flow speeds equal the expected values across the range with a low variance. However, an overshoot at 80% speed has been observed and a slightly lower value for the ultimate flow rate of the L/S 14 line. With the new pump head, the resulting characteristics of the pump with a PID controller are as expected and show little variance between measurements.

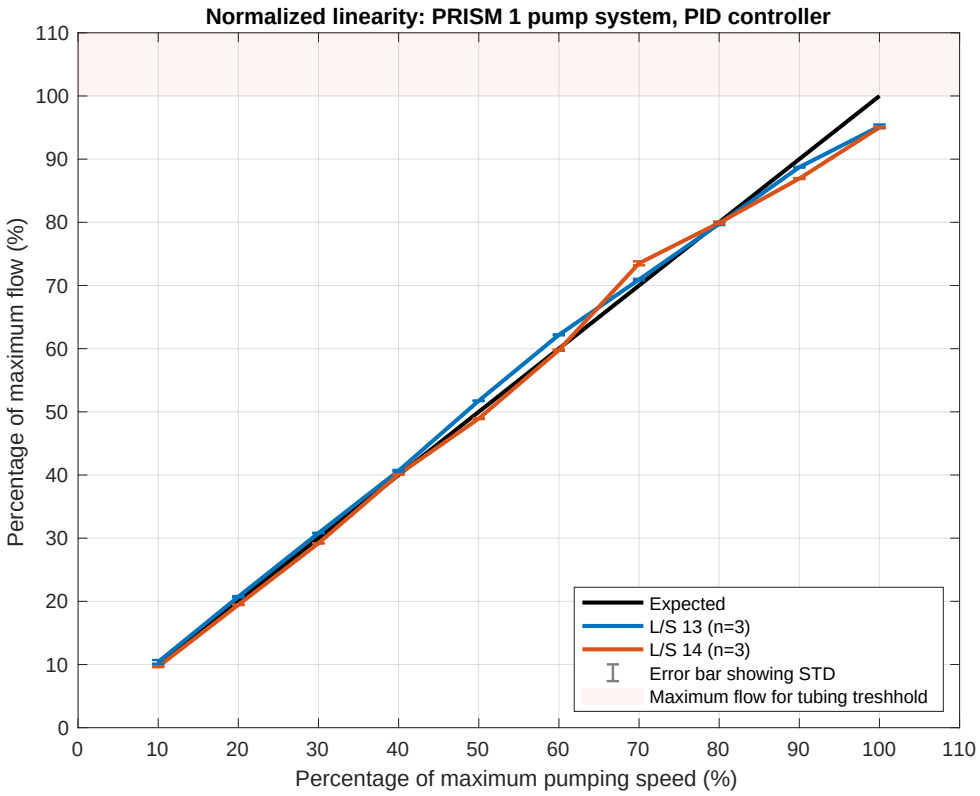

Figure 3.15: Linearity of the PRISM 1 pump using L/S 13 and L/S 14 tubing. Results have been normalized per tubing size to allow for comparison.

RPM measurement		
	Controller mode	
Setpoint RPM	**Pulse width**	**PID**
10	10.2	9.7
15	18.4	14.7
20	21.5	19.9
30	30.6	29.7
50	50.5	49.7
100	99.8	100.2
200	198.2	200.3
300	296.7	299.8
400	397.4	399.7
500	498.8	500.0

Table 3.1: RPM measurement of two different control modes of the developed pump system.

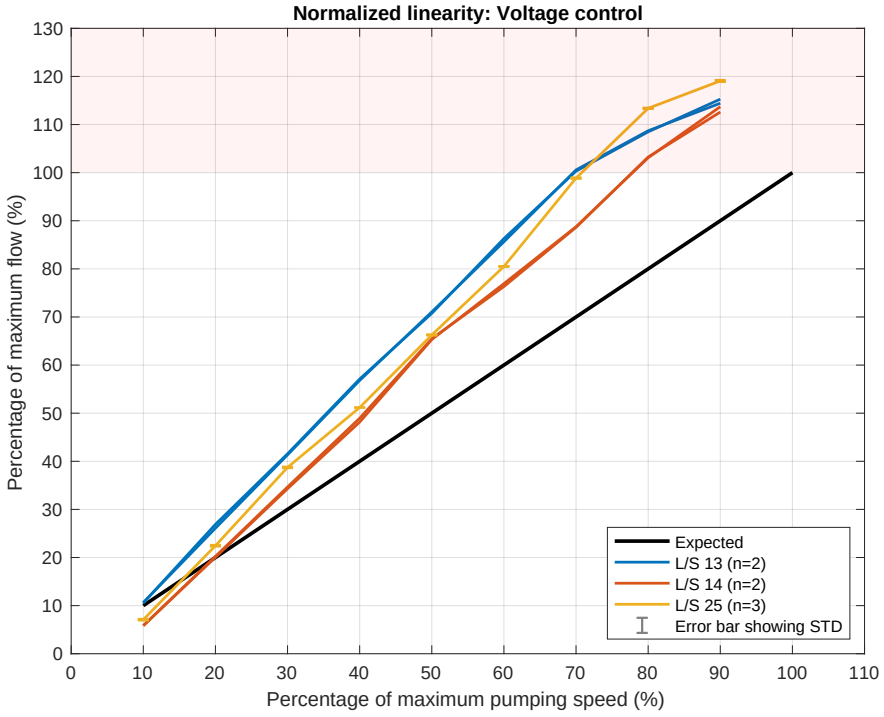

Figure 3.16: Linearity of the voltage controlled pump system using L/S 13, L/S 14 and L/S 25 tubing. Results have been normalized per tubing size to allow for comparison.

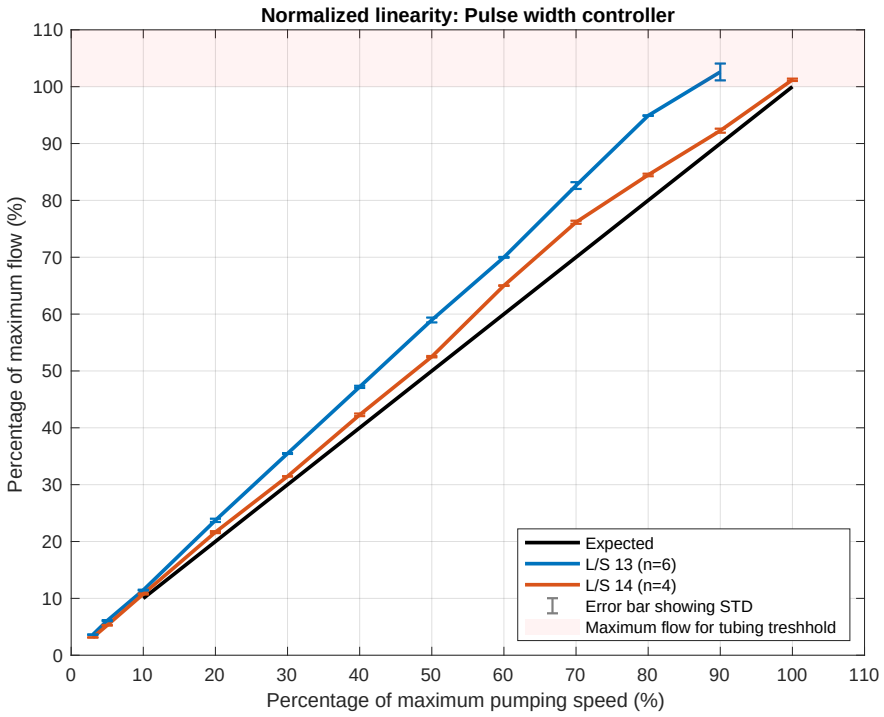

Figure 3.17: Linearity of the pulse width controlled pump system using L/S 13 and L/S 14 tubing. Results have been normalized per tubing size to allow for comparison.

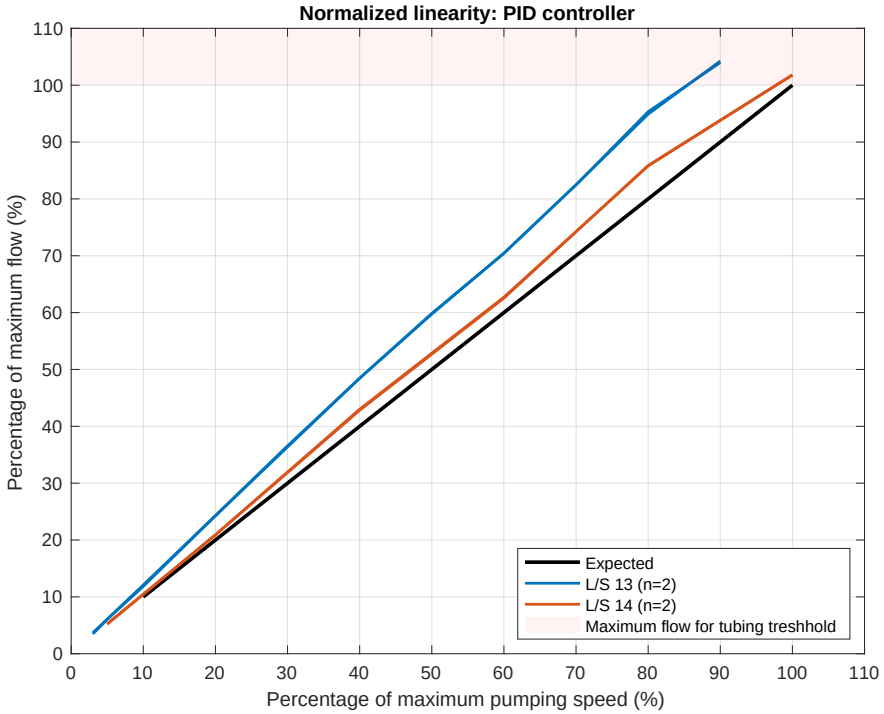

Figure 3.18: Linearity of the PID controlled pump system using L/S 13 and L/S 14 tubing. Results have been normalized per tubing size to allow for comparison.

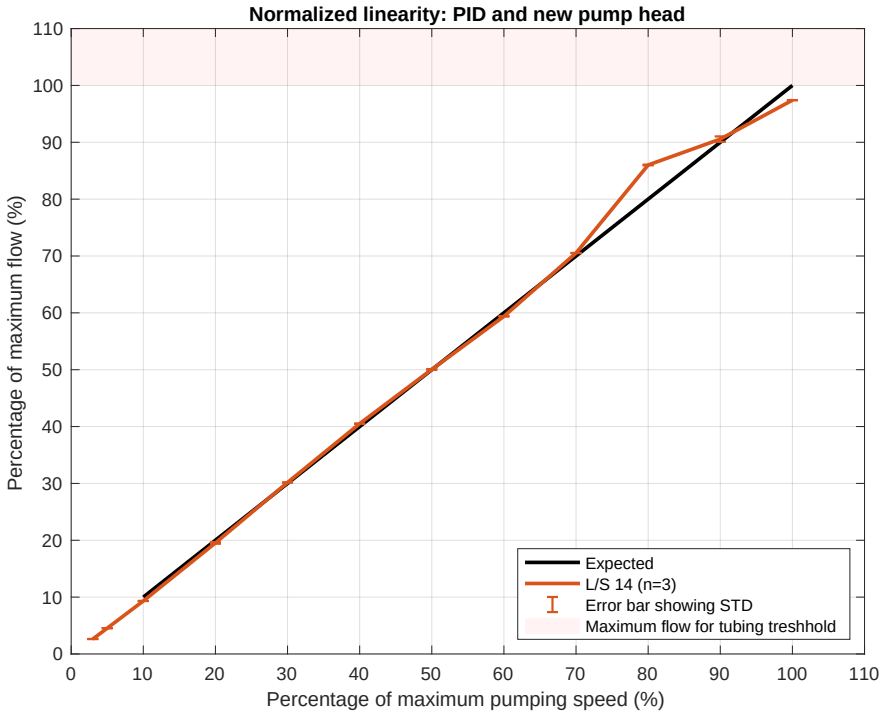

Figure 3.19: To find the cause of the deviating flow measurements, the PID controlled pump has been outfitted with a new pump head. Measurements show the resulting values to be close to the expected values. The linearity plot has been normalized to the tubing to allow for comparison.

3.2.4 Simultaneous density gradient validation

With the tubing and pump system further examined and lessons learned, the original research question and hypothesis can now be revisited:

- ***Research question:*** Can optimization of the controllable variables during the density gradient process, lead to a more consistent creation of sequential and/or simultaneous density gradients, in order to solve the Latham bowl size limitations during pancreatic islet isolations?
- ***Hypothesis:*** By further examining the processes to create simultaneous density gradients, the expectation is that this will lead to a robust and reliable solution to create said density gradients, aimed at solving the 225 ml Latham bowl size limit.

To evaluate the hypothesis, a series of final experiments can be performed in which the lessons, such as the pretreatment of the tubing, can be incorporated to create simultaneous density gradients.

The simultaneous density gradients can be seen in figures 3.20, 3.21 and 3.22, and show in the top graph two density gradients created in the PRISM and Electa continuous flow centrifuges, and in the bottom graph the difference between the two density gradients. To evaluate the performance of the created density gradients, the top graph in the figures contains a theoretical line, which represents the input settings given to PRISM. The results from the first simultaneous density gradient, as shown in figure 3.20, show that both the gradients quite closely follow the same trajectory, with very little difference between the two gradients.

The results from the second gradient, which can be seen in figure 3.21, show that the two gradients initially follow the same gradient, but at 800 seconds, the output from the Electa centrifuge rises in density, and continues to remain at a higher density value (a difference of approximately 0.75%) than the PRISM gradient. At around 1300 seconds, the two gradients converge again and resume following the same trajectory. Around the time of the rise in density (approximately at 800 seconds), the Electra centrifuge was observed to vibrate heavily, and while attempts were made to re-align the arm of the device to stop further vibrations, it took a while for the device to stop vibrating.

The third simultaneous density gradient is shown in figure 3.22, and shows the two gradients to initially follow the same path. But start to slightly diverge around 500 seconds and reaches a maximum divergence of 0.4% at 1150 seconds after which the two gradients start to converge again.

Finally, figure 3.23 shows the mean and standard deviation of all 6 density gradients, in order to evaluate the accuracy with which they can be created from experiment to experiment. This graph shows that the standard deviation lines are close to the mean line across the full gradient. However, there are two periods in which the standard deviation lines are spread out more. At the start of the gradient, up till $\sim$75 seconds, there is some spread which converges quickly. And a slight bump in the deviation lines, starting at 800 seconds, is also observed, which corresponds to the vibrations of the second gradient. In the bottom graph of figure 3.23, the mean difference between the density gradients is plotted and, apart from the aforementioned regions, shows to remain below a difference of 0.3%.

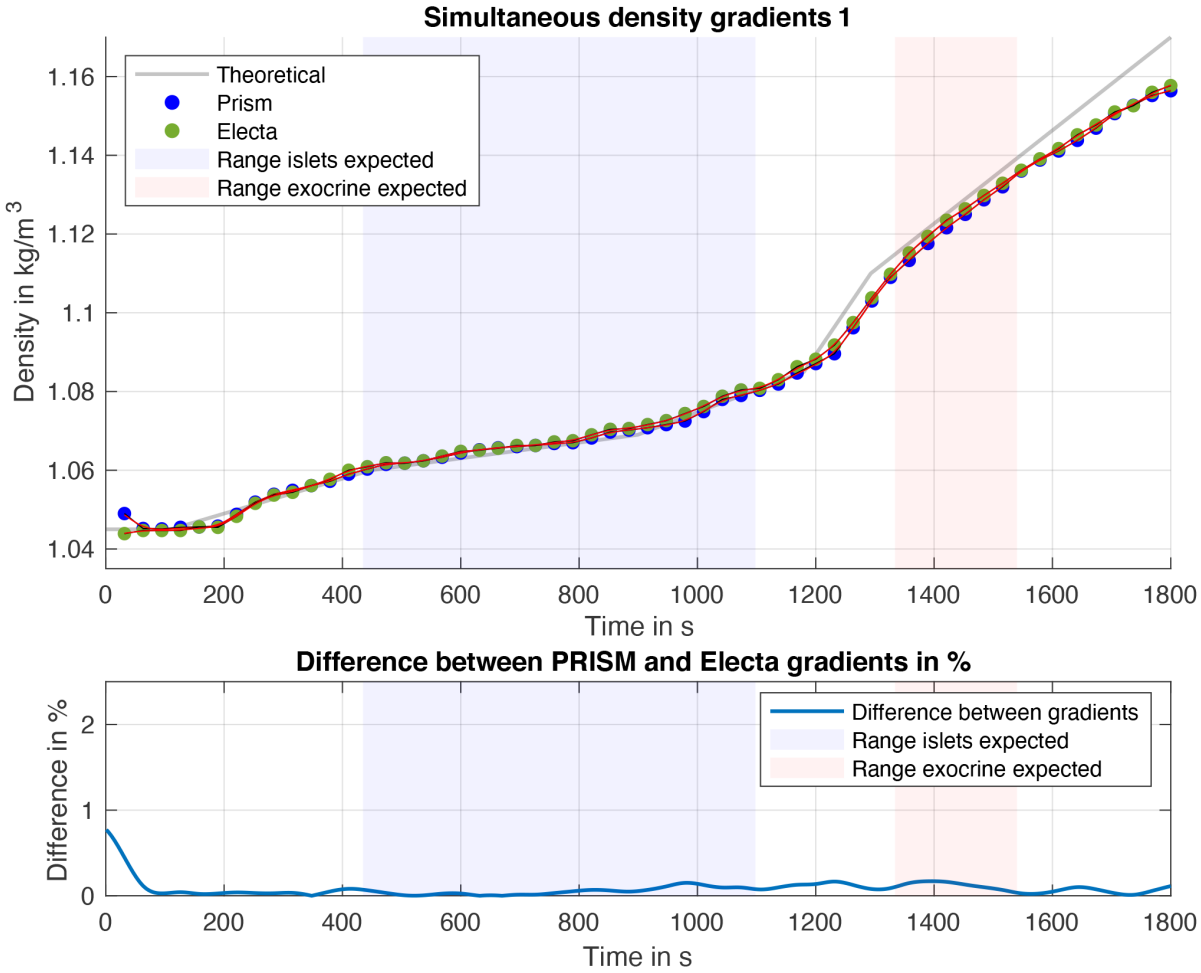

Figure 3.20: Simultaneous density gradients experiment 1, using a PRISM and an Electa continuous flow centrifuge. Top graph shows the density against the time, bottom graph shows the percentual density difference between the two gradients.

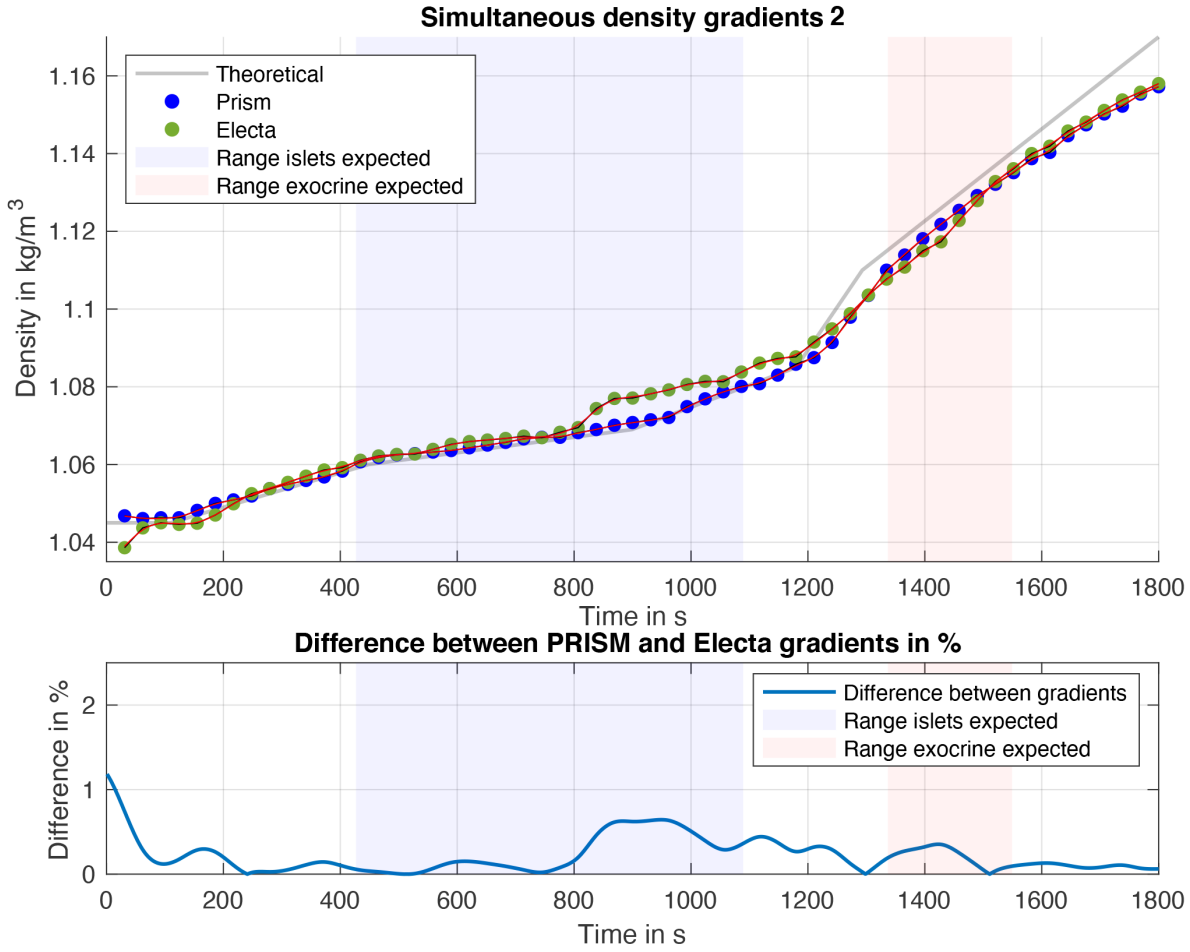

Figure 3.21: Simultaneous density gradients experiment 2, using a PRISM and an Electa continuous flow centrifuge. Top graph shows the density against the time, bottom graph shows the percentual density difference between the two gradients.

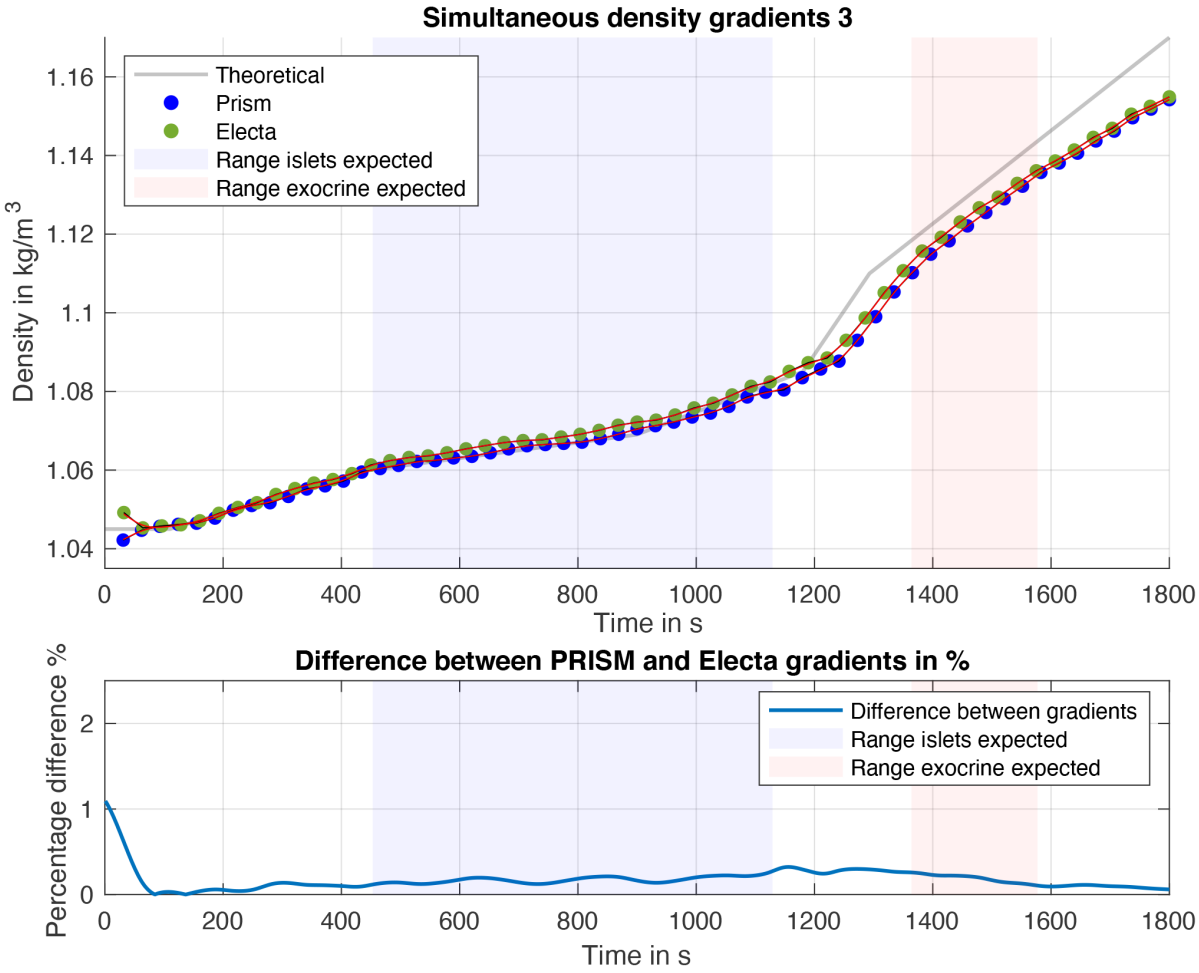

Figure 3.22: Simultaneous density gradients experiment 3, using a PRISM and an Electa continuous flow centrifuge. Top graph shows the density against the time, bottom graph shows the percentual density difference between the two gradients.

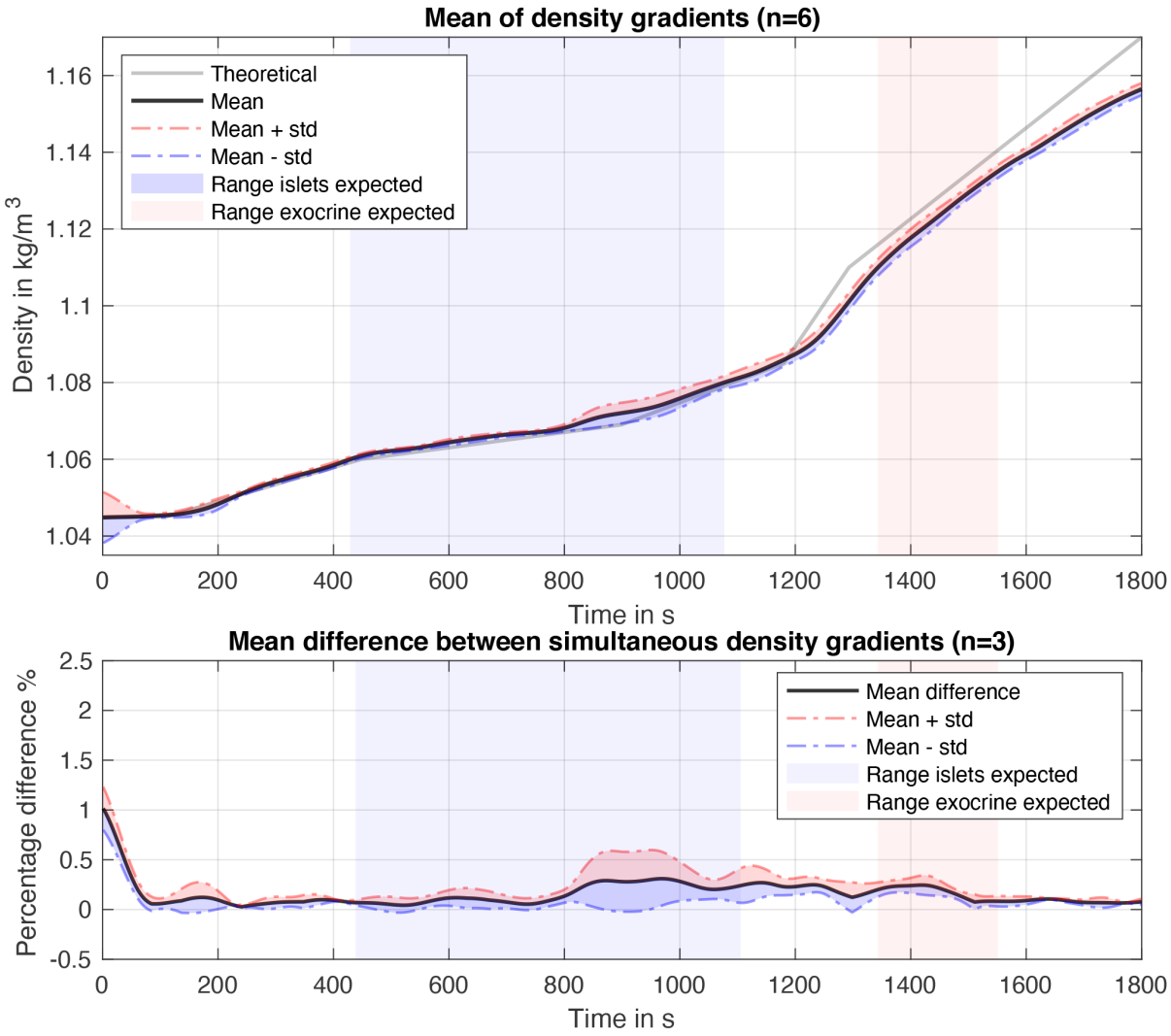

Figure 3.23: Comparison between the simultaneous density gradients. The top graph shows the mean of, and the deviation from, the density gradients with n=6. The bottom graph shows the mean percentual difference between the simultaneous density gradients with n=3.

CHAPTER 4

Discussion

4.1 Pancreatic islet identification

During pancreatic islet isolations there is a need to identify pancreatic islets from exocrine tissue, the common method to this is to stain the tissue with Dithizone (DTZ). This staining method is, however, cytotoxic and results in the destruction of transplantable material. Therefore, there is a need to be able to identify the type of tissue in a non-destructive manner, to this end, the following research question has been examined:

- ***Research question:*** Are there exploitable optical and/or electrical property differences between pancreatic islets and exocrine tissue?
- ***Hypothesis:*** A difference in cell composition between pancreatic islets and exocrine tissue, will lead to measurable differences in optical absorption spectroscopy and/or electrical impedance spectroscopy.

To evaluate the research question and the validity of this hypothesis, experiments have been performed to investigate both the optical absorption and electric impedance spectra.

4.1.1 Optical absorption spectroscopy

To evaluate the performance of the culture plate and the fluids used in PancReatic Islet Separation Method (PRISM), initial measurements were taken with empty fluids, which are shown in figure 3.1 and figure 3.4. These graphs show similar behavior for multiple fluids in which the light below a wavelength of 290 nm is absorbed. conclusion from these measurements is that the absorbance comes from the Nunc Maxisorp 96 well plate that has been used. This is confirmed by a paper from Held et al. [35], in which the transmission spectra of various culture plates are examined, and the Nunc Maxisorp plates have a high absorbance value below 290 nm. Additionally, figures 3.1 and 3.4 show that most of the fluids allow for a high light transmittance across the spectrum with little variability between measurements. There are, however, two exceptions, the University of Wisconsin (UW) and heavy mixture and the culture medium from the second experiment. The UW and heavy mixture consists of UW preservation solution and Xenetix 350, an x-ray contrast agent, which contains a high concentration of iodine molecules. A study by Liu et al. [37], in which the absorption spectrum of iodine in various solutions is measured, shows an absorption peak for iodine at around a wavelength of 320 nm, after which it proceeds to allow light to pass through at around

350 nm, this matches the observed results from the UW heavy mixture. The other fluid with a higher variability between measurements is the culture medium from experiment 2, which is shown in figure 3.4. Not only is the variability between measurements higher, the results of the culture medium measurements are different from experiment 1. One of the additives in the used culture medium (full list in appendix B.1) is human serum, which is a product from blood donations, and can have an impact on the optical response of the culture medium, as shown by Silva et al. [36]. Unfortunately, human serum is not a stable product, as the concentrations and compositions, such as those of fat, can differ between donors and have been shown to have an effect on the optical spectrum [38, 39].

It has proven difficult to deposit the right amount of tissue in a well to match the required amount of Islet EQuivalent (IEQ) for the condition, despite calculating the tissue density in the culture bag during the preparation and checking the results using a microscope. This, unfortunately, lead to differences between the results of "equal" conditions. For example, 2000 IEQ exocrine tissue in culture medium gives a transmittance of 65.69% at a wavelength of 600 nm in experiment 1, and only 16.71% in experiment 2. This could in part be explained by having more or less tissue than expected in the well, resulting in a higher or lower path length of the light through the tissue, and thus absorbing more or less light. Additionally, the donor tissue variability can also play a role in the observed difference in measurements. Tissue from every donor has slight variations in composition, as well as a different reaction to the 24 hour culture period, sometimes resulting in tissue decomposition before this can be used in research. This means more experiments are needed in which more effort is put in matching the correct amount of tissue to the condition.

Another observation in the results, is the high transmittance of exocrine tissue in Phosphate-buffered Saline (PBS) in experiment 1, which is depicted in figure A.4. One of the explanations for this result could be that the amount of exocrine tissue has declined during the preparation phase in which the tissue is washed and centrifuged a few times. It has previously been observed that exocrine tissue starts to decline and die off during the 24 hour culturing period, and the centrifugal forces could have pushed it over the limit. Additionally, due to inexperience, part of the exocrine tissue could have been washed away during these steps, resulting in less tissue to be measured.

Because of the aforementioned complications, it is difficult to make an accurate comparison between exocrine tissue and pancreatic islets. However, in order to get some insights in the behavior of these tissues during the optical absorption spectroscopy, comparison charts have been made and are visible in figure 3.3 and figure 3.6. The bottom graph in both figures shows the difference between the pancreatic islets and exocrine tissue in each of the conditions. When comparing experiment 1 and experiment 2 with each other it becomes clear that they are each other's opposites, with the exocrine tissue allowing more light transmittance than pancreatic islets in experiment 1 and the opposite in experiment 2. This is most likely due to the above explained difficulties in depositing the right amount of material in each well, making it difficult to definitively conclude whether or not the hypothesis is valid or not.

However, one thing that can be observed in both experiments is that the difference lines are sloped, meaning at certain wavelengths the difference in transmittance between the two tissues increases or

decreases. This could potentially be useful for the identification of these tissues. For example, a baseline picture is taken at a wavelength 900 nm and measure the transmittance of each tissue particle in the field of view, which is followed up by a second picture at a wavelength of 400 nm. Then the tissue will show a difference in transmittance, corresponding to being a pancreatic islet of a piece of exocrine tissue, as the difference between the two in- or de-creases.

Unfortunately, due to long term equipment failure, no more than two experiments have been performed, which limits the amount of available data. Before any conclusions can be made on the potential different optical properties between the two types of tissue, and the ability to use this for identification purposes, more experiments are needed. Additionally, the Spectramax i3x is only capable of performing these measurements up to a wavelength of 1000 nm, and as discussed in my literature study, measurements in the near infrared and infrared parts of the spectrum could be a useful addition to the performed measurements in the visible light spectrum. Therefore, it is recommended to both increase the number of experiments, with a refined procedure to achieve equal distributions wells of comparable conditions, as well as extend the measurements into the near infrared and infrared parts of the spectrum using different equipment.

4.1.2 Electrical impedance spectroscopy

The ECIS model ZΘ measures the tissue over a long period of time, in this experiment only the stable measurements have been included, this was in a time frame between 35 minutes and 5 and a half hours. The initial measurements up till 35 minutes have been discarded due to a large deviation from the observed mean of the stable measurements. Which is likely caused by temperature fluctuations and transport movement, resulting in the cells needing to settle and adhere to the electrodes again. The measurements after 5 and a half hours show patterns of unstable measurements and divergent results between wells of the same conditions, which is likely caused by cell death after a relatively long time in a small amount (200μl) of culture medium.

The impedance spectra of all the measured conditions all show an equal behavior compared to each other. The measured impedance values of all the conditions are roughly similar at the lower frequencies and only start to diverge from one another at the higher measured frequencies. This can be attributed to different dielectric dispersions (α,β and γ) playing a dominant role at different frequencies in the impedance spectrum for cells in suspension [40, 41]. The α-dispersion is dominant at frequencies below several kHz and is mainly caused by polarization effects of the used electrodes, which has similar results in the measurements with the used liquids and tissues. This is followed by the β-dispersion with a frequency range between several kHz and 1 GHz, in which the capacitive properties of the cell membrane play a major role, and ultimately followed by the γ-dispersion which occurs when the frequency is higher than 1 GHz and in which the polar orientation of water molecules played a big role. The β-dispersion can, however, be further subdivided in three sub-dispersions in which the following aspects of the submerged cells are the main contributing factor: electric double layer ($<$1MHz), the size of the cell (1 - 10 MHz) and the cell membrane (10 MHz - 1 GHz). Due to limitations by the ECIS model ZΘ, the measurements in the experiment are up till a frequency of 64 kHz, which means the difference in impedance values is caused by the electrical double layer which forms at the surface of the electrodes in contact with either tissue or fluid. Because the differences between measurements are most pronounced at 64 kHz the results show

comparisons between liquids and tissues at this frequency. While this provides a first insight on the electric properties of the pancreatic islets and exocrine tissue, there is more to be explored at higher frequencies.

Looking at the resulting impedance values of pancreatic islets and exocrine tissue at 64 kHz in figure 3.10, it appears that pancreatic islets have a lower impedance when compared with exocrine tissue of similar conditions. This in itself would be an indication that there is potentially a difference in electrical properties between the two tissues, however the same figure shows that the impedance values also rise with the amount of tissue that is present in the well. Which makes the deposited amount of tissue in each of the wells a critical factor for this comparison. While efforts have been taken to deposit similar amounts of tissues for each of the conditions, and to double check that with the use of a microscope, there is still an error margin present. Because of this error margin, the actual impedance values of both of the tissues could be closer to each other than they currently appear. Therefore, it is difficult to definitively confirm or reject the hypothesis without further experiments. To overcome the dependence on the amount of tissue, an alternative, is to limit the amount of tissue to just 1 cell aggregate per well (as long as it covers two electrodes) and repeat these experiments. This would more accurately measure the electrical properties of the two types of tissue, without the disturbances of varying amounts of tissue in the well, and therefore be able to provide a conclusion to the hypothesis.

The resulting impedance values in this experiment (in most conditions with n=116 or higher) show little deviation between measurements from wells with similar conditions and across a longer period of time. However, the experiment has been performed only once with the material from one donor. In order to definitively reach any conclusions from the obtained results, and to eliminate the donor tissue variability, more experiments need to be performed. Additionally, due to equipment limitations only a relatively small part of the impedance spectrum (up to 64 kHz, while normally ranging from 1 Hz to 1 GHz [40]) has been examined. Therefore, additional impedance spectroscopy studies, using equipment that allow for a larger part of the spectrum to be examined, are recommended to be performed.

4.2 Process validation and optimization

4.2.1 Exploring sequential and simultaneous density gradients

To evaluate how to solve the size limitations of the Latham bowls, which are used during pancreatic islet isolations to create the density gradient in, the following research question and hypothesis were looked into:

- ***Research question:*** Can optimization of the controllable variables during the density gradient process, lead to a more consistent creation of sequential and/or simultaneous density gradients, in order to solve the Latham bowl size limitations during pancreatic islet isolations?
- ***Hypothesis:*** By further examining the processes to create sequential and simultaneous density gradients, the expectation is that this will lead to a robust and reliable solution to create said density gradients, aimed at solving the 225 ml Latham bowl size limit.

Should one of these methods prove to be a robust and reliable solution, then this will define the choice for the development path of PRISM 2.0.

One of the behaviors that has been observed with sequential density gradients using PRISM, is a difference in pancreatic islet isolation results between the first and second density gradient, where the bulk of the pancreatic islets exited the bowl in the first few fractions. To explore this further, experiments for the sequential density gradients recreated the conditions at which this happens to try and explain this observed behavior and explore this method for further development. These results are shown in figure 3.11 and show a significant difference between each of the three initial density values: 1.043 kg/m^3, 1.067 kg/m^3 and 1.055 kg/m^3 for gradient 1, 2 and 3 respectively. The initial gradient created by a PRISM isolation is represented by gradient 1, which was followed by a second density gradient, which, after emptying the bowl of the fluids from experiment 1, resulted in gradient 2. The initial high starting density of gradient 2 is likely explained by the system not fully being able to drain itself of all fluids, resulting in a small amount of liquids remaining with a density of 1.14 - 1.17 kg/m^3 (ending density value of gradient 1) mixing with the initial inflow of UW preservation solution and creating a higher density than intended. Because the starting density value of gradient 2 is within the window in which the pancreatic islets are expected (1.06 - 1.08 kg/m^3), it is likely the cause for the observed increase of pancreatic islets that exit the system during PRISM isolations using a sequential gradient. To further visualize the effects of this difference in density gradients, figure 3.12 shows the initial 10 collected fractions of the density gradients which contained various density beads representing different types of tissue. Gradient 1 shows the initial tube to have mainly orange and green beads which represent dead tissue, and starts to gradually show purple and blue beads from fraction 5 and higher. In comparison, gradient 2 shows the first tube to have a high density of beads of various colors: green, orange, blue and purple. Which corresponds with the observed behavior during pancreatic islet isolations.

In an attempt to recreate the starting conditions of gradient 2, a clean bowl and tubing set was rinsed with the heavy solution and then emptied before starting a density gradient. The resulting density gradient (number 3 in the figures), is, however, in between gradient 1 and 2, and just shy of the range in which the pancreatic islets are expected ($<$ 1.06 kg/m^3). Resulting in some purple and blue beads entering tube 1, but not as large an amount as with the second gradient. One of the possible explanations for the different outcomes of gradient 2 and 3 is a reduced soaking time of the bowl during the rinse, resulting in the bowl being differently coated. Or, due to the centrifugal forces, the heavy mixture in the bowl during the density gradient, starts to partially un-mix and deposit some Xenetix 350 (with a density of 1.409 kg/m^3), on the bottom of the bowl which does not get drained.

The density beads, while not a perfect substitute for pancreatic tissue (tissue includes some fatty parts and can cloth together), does give a visualization on the number of pancreatic islets and dead tissue that will exit the Xtra bowl in the initial fractions. This effect is, however, undesirable because the pancreatic islets will be mixed with dead tissue and because a relatively large amount of tissue will come through the exit tubing in a short time frame. This could potentially form a problem for the pancreatic islets, because of the potential shear stresses that arise as they get squeezed to the wall of the tube, which can lead to a decline of surviving pancreatic islets [42]. The differences between the first two density gradients can be controlled, however, to avoid any of the aforementioned risks. By pumping some UW preservation solution into the Xtra bowl, and then thoroughly cleaning it by manually shaking it, the residual content

of the bowl can be cleaned and allowed to be pumped out to the waste bag.

The results of the simultaneous density gradients, shown in figure 3.13, show two experiments in which two gradients have been created using the same pumps. While the gradients show similar behavior, two major observations can be made: The gradients gradually diverge over time and the amount of liquids that pass through each of the bowls is not equal. The divergence of the two measured gradients starts at the beginning of the window in which the pancreatic islets are expected (1.06 - 1.08 kg/m^3), which can potentially lead to a situation in which the outflow for one bowl contains pancreatic islets and the other exocrine tissue, which will then be mixed again, a situation which should be avoided. Both the observations are closely tied to a difference of liquids that pass through the tubing, even though the tubing and equipment is the same. The density gradients which were created using PRISM show a higher density and less liquid needed, which can be the result of a reduced flow through the UW supply tubing as this would normally lower the density. In order to use this method, a high level of process control is needed to accurately supply both bowls with the same amount of liquids to build the density gradient. Which can be achieved by further studies into accurately using the tubing to displace the volume desired, and to evaluate the accuracy of the pumps to build the gradients with. Once under control, this method will have the potential to be successfully used.

The goal of these experiments was to identify which of the methods is a reliable solution to overcome the size limitation of the Latham bowl, and should be opened up for further development to eventually be implemented in PRISM 2.0. While both methods show to have promise, both processes are subject to some difficulties, therefore neither of processes are, in their current form, a reliable and robust method to overcome the Latham bowl size limitations yet. Fortunately, these experiments have shown what will need to be improved in order to become the sought reliable and robust method. With that in mind, and time reduction being one of the original design goals of the PRISM project, the process in which simultaneous density gradients are created is the preferred option for further development. However, to be able to use this process in a reliable and robust manner, further control over this process needs to be gained. To do this, two subjects need to be addressed:

- More control over the displaced volume in the tubing is needed to ensure the right amount of liquids are pumped to each of the bowls. To investigate which steps to take to achieve this the following research question and hypothesis were established:
  - ***Research question:*** Can the standard tubing be used to deliver similar volumes to different containers using a single peristaltic pump head?
  - ***Hypothesis:*** A treatment procedure of the tubing before use will lead to more consistent results by making the tubing more malleable.
- To ensure that the density gradients are reproducible, the newly developed pumping system needs to be validated to have a linear progression and a high accuracy to reach the set point speeds.

Which leads to the following two subjects that need to be investigated: The hypothesis that the application of a treatment protocol will lead to more accurate volume control through the tubing, and that, in order to create accurate density gradients, the newly developed pump system needs to be validated to have a linear progression and has to be highly accurate.

4.2.2 Tubing

To gain more control over the creation of the simultaneous density gradient, steps had to be taken to improve the accuracy of the tubing by minimizing the difference of the displaced volume to two containers using the same peristaltic pump. In order to look into this the following research question and hypothesis were looked into:

- ***Research question:*** Can the standard tubing be used to deliver similar volumes to different containers using a single peristaltic pump head?
- ***Hypothesis:*** A treatment procedure of the tubing before use will lead to more consistent results by making the tubing more malleable.

Unfortunately, due to loss of data, repeats of this experiment and additional conditions have been lost. However, the currently remaining dataset is in line with the expected results based on increasing experience on the topic and provides a fair indication of the behavior of the tubing.

The results shown in figure 3.14 show a comparison between a baseline, represented by the platinum cured silicon tubing without treatment, and the new Puri-Flex tubing with additional treatment protocol as advised, after some deliberations, by Masterflex. The platinum cured silicon tubing shows to have a high variability and difference between the two tubing through the same pump head, which is in line with previous observations during the initial simultaneous density gradients. To combat this, the new Puri-Flex tubing is a much more rigid material which can achieve greater accuracy by treating the tubing before use. The method of "rolling" the tubing, which is basically pumping a liquid at 175 RPM for a certain amount of time, creates a more pliable spot where the steel rollers from the peristaltic pump head come in contact with the tube, and with that increase its accuracy. This phenomenon was best observed after the 30 minute treatment with water. The results of these experiments are shown in figure 3.14 in which the treated tubing shows less variability and a lower difference between the tubes, especially in the case of 30 minutes of rolling. Even though the test has been performed with the use of water, these results should be representative for other liquids such as UW preservation solution and Xenetix 350, as the gains in accuracy come from the pliability of the tubing wall, rather than the difference in liquids.

Unfortunately, pumping liquids for 30 minutes when preparing for an isolation using PRISM is a challenge, due to limited fluids and working in a clean and sterile environment. While some workarounds, such as pumping the fluids back and forth for a few seconds during a time of 30 minutes can be implemented, it opened up an experiment to see if air can be used as a substitute. The results of this, as shown in figure 3.14, are, however, not promising and show the highest difference between the two tubes of the measured conditions. This indicates that the relative incompressibility of water plays a role in preparing the tubing, by creating higher forces that work on the wall of the tube.

The outcome of these experiments ultimately verify the hypothesis, and thus show that the application of proper treatment protocols increases the control over the displaced volume in the tubing, minimizing the volume difference to two separate containers. The application of a 30 minute treatment protocol with liquids shows to minimize the difference between the two tubes to under 1%, which is an acceptable margin of error in the creation of density gradients.

4.2.3 Pump validation

The goal of these experiments is to validate the developed pumping system for PRISM 2.0, by determining the characteristics of the system, to ensure that the density gradients are reproducible. The pump system needs to have a linear progression and a high accuracy to reach the target set points. To this end, different versions of the developed pump have been compared against the baseline created by the PRISM 1.0 pump system. The end goal for the developed system is to have characteristics that are equal to or better than PRISM 1.0, and allow for a reproducible density gradient. The baseline, created by PRISM 1, is shown in figure 3.15, which shows this system is capable of delivering a fairly accurate and stable linear progression of the flow in the tubing, which meets the expected values. The slight slump in flow speed at the upper end of pump speeds is of no consequence, as those speeds do not get used in the PRISM protocol. With a fairly accurate linearity and a proven record of being capable of building density gradients, this is the baseline to compare the pump for PRISM 2.0 against.

To evaluate the raw characteristics of the pump without a microcontroller, one of the versions was regulated by voltage control. The resulting flow speeds for this pump can be seen in figure 3.16, and show that the flow speeds across the range are higher than the expected values, and even pushing the tubing above the indicated maximum flow speed. This shows that the gearing of the pump is too large, as it is capable of reaching speeds that will not be used. By switching to a smaller gearing, a higher torque delivery and accuracy can be achieved. Another conclusion from this experiment is that there is a definite need for a control system, which is capable of creating a more linear buildup of the flow rates which are closer to the expected values.

A second version of the pump was developed with a pulse width controller, that looks at the size of signals from the encoder to regulate the rotational speed. The results of the experiment are shown in figure 3.17, and show that the flow rates are closer to the expected values. However, the flow rate of the L/S 13 tubing is too high compared with the expected values across the entire range. It reaches the maximum indicated flow rate at 90% of the pumping capabilities, which causes the measurements to be somewhat less stable. Looking at the L/S 14 tubing, this shows results which are closer to the expected values, but still encounters a bump in the resulting values around 70% pump rotational speed.

Because the pulse width controller did not yet reach the expected values, a PID controlled version was developed, the resulting measurements of this system are shown in figure 3.18. The overall characteristics of this system are however quite similar to the system with the pulse width controller. The L/S 13 line is again high across the whole range and the L/S 14 line is closer to the expected values but shows again to have a bump with too much flow.

Because both systems were expected to be able to reach the expected values, a cause for this deviation had to be found. With the use of an optical tachometer, the rotational speed of both the pulse width and PID controlled pump systems was measured. The results, which are shown in table 3.1, show that both control modes are, in fact, very close to the setpoint RPM values, with the PID controller being able to more accurately produce the setpoint values. This meant the rotational speeds of the pump were not at fault for causing the deviation of the flow speeds.

Eventually, the cause was found in a faulty Masterflex Easyload 2 pump head which was used in the measurements. After outfitting the PID controlled pump with a new pump head the experiment was repeated, the results of which are shown in figure 3.19. The flow rates produced by this pump show to have a linear increase which is very close to the expected values. The observed increase of flow speed at 80% pump speed can be corrected for if need be, but during the PRISM protocols the pump seldom reaches this speed. Unfortunately, at the time the L/S 13 tubing was not available, resulting in this experiment needing to be repeated with that particular tubing.

Some observations that have been made during the experiments are the behavior of both controllers at low speeds. The PID controller showed to behave in a stop and go fashion, likely due to a low sampling frequency at these speeds, and the pulse width controller showed to continue rotating, albeit intermittently with a high frequency. While both controllers show to have similar fluid flows, this different behavior does cause a slight problem. Due to coming to a complete standstill, caused by the roller encountering the tubing, the PID controlled pump needs to increase the amperage a lot to continue rotating. The increase in amperage causes the controller to become increasingly hot, which might cause problems in the long run. Therefore, a system which combines the pulse width control at low frequencies and PID control at higher frequencies will be developed.

The experiments so far show the developed pump with a PID controller to have a linear progression and is capable of accurately reaching the setpoint values. This means that the developed pumping system is able to create repeatable density gradients, and is on the right development path for PRISM 2.0. However, some area's for improvement have been identified, such as, smaller gearing and combining the controllers, which still need to be implemented in a final version of the pump system. Therefore, a definitive conclusion can only be provided when that system is ready for a validation study.

4.2.4 Simultaneous density gradient validation

After closer examination of some controllable variables in the previous sections, the lessons learned can now be used to re-evaluate the research question aimed at solving the limitations of the Latham bowls:

- ***Research question:*** Can optimization of the controllable variables during the density gradient process, lead to a more consistent creation of sequential and/or simultaneous density gradients, in order to solve the Latham bowl size limitations during pancreatic islet isolations?
- ***Hypothesis:*** By further examining the processes to create simultaneous density gradients, the expectation is that this will lead to a robust and reliable solution to create said density gradients, aimed at solving the 225 ml Latham bowl size limit.

Now a better understanding of the overall process and controllable variables has been gained, the hypothesis can now be evaluated by conducting further experiments in which simultaneous density gradients are created. Should these lessons indeed lead to a robust and reliable solution to create these density gradients, then this process can ultimately be used in PRISM 2.0.

The results from the simultaneous density gradient experiments 1 and 3, as shown in figures 3.20 and 3.22, show that overall, the simultaneous density gradients can accurately be created and follow almost the same gradient. The gradient lines start off at approximately 1.045 kg/m^3 and gradually rise during the phase in which the pancreatic islets are expected (1.06 kg/m^3 to 1.08 kg/m^3 [43, 30]). This would translate in the pancreatic islets slowly leaving the continuous flow centrifuges, without an increased risk of crowding and potential detrimental shear stresses from being pushed against the wall [42]. The second range of interest is when the exocrine tissue is expected (1.11 kg/m^3 to 1.35kg/m^3 [43, 30]), and this again shows there is little deviation between the two gradient lines. In gradient 3, the results from the PRISM gradient are lagging behind a little bit, but with a maximum error of 0.3% in this range, this is of no consequence for the results of the isolation.

During the second experiment, shown in figure 3.21, the Dideco Electa centrifuge was observed to vibrate heavily, which is seen in gradient line. At approximately 800 seconds the density of the Electa rises and then levels off, which indicates the vibrations have mixed the internal fluids. Even though it took some time to stop the vibrations, the resulting increase in density remained below 1.08 kg/m^3, which means that during this disturbance still only the pancreatic islets are expected to leave the device. With the disturbed gradient, a higher amount of the heavy solution has left the centrifuge than planned for, which results in the Electa density gradient being a little bit lower than the PRISM gradient during the phase where the exocrine tissue is expected. Despite these difficulties, the difference between the gradients remained below 0.75% and would not have caused the gradients to fail. However, this does indicate a need for a robust and solid holder for the continuous flow centrifuge, with a good alignment for the rotational axis, to avoid any vibrations from happening.

Another observation which was made during all three experiments, is that the starting density for each of the gradients is different. While this results in a large difference between the two gradients, in all cases the maximum density at this initial value was below 1.05 kg/m^3. Meaning that this would not cause the pancreatic islets to rise ahead of time. Additionally, the difference between the two gradients quickly diminished after which each of the gradients started to follow the same trajectory again. Because this odd behavior does not lead to any complications, this can be accepted as it is.

To evaluate the repeatability of the simultaneous density gradients, the mean results and deviations have been plotted in the top graph of figure 3.23. This graph shows that, even with the vibrating Electa centrifuge, the gradient lines are very close to each other and can be repeated multiple times across the experiments. The bottom graph of this figure shows the mean difference and deviations, and shows that overall (with the exception of the starting values) the mean difference does not rise above 0.3%, indicating that there is accurate control over the simultaneous density gradients.

Because the accuracy and repeatability of the experiments is sufficient, the conclusion is that this method is a reliable and robust way to create simultaneous density gradients. Therefore, the hypothesis that closer examination of the process to create simultaneous density gradients, will lead to a robust and reliable solution to create simultaneous density gradient, is accepted. Which means that this process is a good solution to overcome the Latham bowl size limitation, and can be further developed for PRISM 2.0.

CHAPTER 5

Conclusion

Researchers from the Leiden University Medical Center (LUMC) are working on automating the pancreatic islet isolation procedure, in an effort to make pancreatic islet transplantations more accessible for patients with severe symptoms of type 1 diabetes mellitus. A prototype device, which is called PancReatic Islet Separation Method (PRISM) 1.0, had undergone rigorous validation studies in which this method proved to be a good method to use in pancreatic islet isolation procedures. However, two major areas for improvement have been identified, one of which is the need for a label free, non-destructive and in- or on-line applicable method to identify pancreatic islets from exocrine tissue. The other area for improvement is to solve the crowding effect in the Latham bowl during the density gradient creation, resulting from too much tissue for the bowl size. Therefore, it has been decided to develop a version 2.0 PRISM device which can overcome these problems. This has led to the two main research questions for this thesis:

1. Are there exploitable optical and/or electrical property differences between pancreatic islets and exocrine tissue?
2. Can optimization of the controllable variables during the density gradient process, lead to a more consistent creation of sequential and/or simultaneous density gradients, in order to solve the Latham bowl size limitations during pancreatic islet isolations?

During the investigation of the first research question, the hypothesis was that a difference in cell composition between pancreatic islets and exocrine tissue, will lead to measurable differences in optical absorption spectroscopy and/or electrical impedance spectroscopy. To verify or reject this hypothesis, optical absorption spectroscopy and electrical impedance spectroscopy experiments have been conducted. The results from the optical absorption spectroscopy experiments, shown in figures 3.3 and 3.6, show differences in the absorption spectrum between pancreatic islets and exocrine tissue, but, unfortunately, vary to such a degree that the results have opposite outcomes. This is most likely caused by the amount of tissue deposited in the wells, rather than the optical properties of the tissue types. The results from the electrical impedance spectroscopy, shown in figure 3.10, show a slight difference in impedance values between pancreatic islets and exocrine tissue. However, because the impedance values rise with an increased amount of tissue in the wells, the results are likely influenced by tissue variations in the well due to deposition errors. This means an accurate comparison between the two types of tissues is very difficult. Because of the aforementioned difficulties, based on the current results it is therefore impossible to definitively accept or reject the hypothesis, and answer the research question definitively, therefore,

more experiments are needed.

For the second research question, which is aimed at solving the imposed limitations by the limited size of the Latham bowls, the hypothesis was that by further examining the processes to create sequential and simultaneous density gradients, this will lead to a robust and reliable solution to create these density gradients, and is ultimately aimed at solving the 225 ml Latham bowl size limit. Initial exploration of both these methods showed that the method to create simultaneous density gradients has promise, but needed further improvement before the hypothesis could be verified. To that end, experimental studies have been conducted in which more control over the displaced volume in the tubing was gained after an initial treatment protocol, and a validation study performed to evaluate the linear progression and accuracy of the pump system. The lessons learned from these experiments have been used to re-evaluate the second research question and hypothesis. This study, the results of which are shown in figure 3.23, in which these simultaneous density gradients were created, shows that the taken measures lead to an accurate and repeatable process. It can, therefore, be concluded that this optimization step, has led to a reliable and robust process to create simultaneous density gradients, which can overcome the limitations from the limited size of the Latham bowls. Ultimately, this opens up this method as the development path for PRISM 2.0.

CHAPTER 6

Recommendations

While the initial exploration of the optical absorption and electrical impedance spectra gives an insight in how pancreatic islets and exocrine tissue perform in these measurements, a solid conclusion cannot yet be provided. Therefore, it is recommended to increase the number of repeats for these experiments, in which greater care is taken on the amount of tissue deposited in each of the wells that are to be measured. Additionally, due to limitations of the available equipment, only parts of the spectra have been analyzed. Literature has shown that the near infrared range has the potential to be used for pancreatic islet identification purposes, it is, therefore, recommended to expand these experiments to include the near infrared spectrum. Similarly, the device used for the electrical impedance spectroscopy was only capable of examining the spectrum up till a frequency of 64 kHz, whereas literature shows impedance measurements ranging up to the GHz range. This additional range would allow for more electrical properties of the tissues to be examined, and, therefore, it is recommended to expand the experiments for electrical impedance measurements to include the higher frequencies.

With the development of PancReatic Islet Separation Method (PRISM) 2.0 well underway, and different components nearing finishing stages, more validation studies can be performed to explore if these components meet the design criteria. Furthermore, larger validation studies that include combinations of various components can be performed, such as the combined evaluation of the systems that are needed to create two simultaneous density gradients. Therefore, it is recommended to build a test set up in which various processes of the pancreatic islet isolation processes using PRISM can be simulated and validated, before the final creation of the complete device.

List of Figures

List of Tables

Bibliography

[1] Internation Diabetes Federation, *IDF Diabetes Atlas Ninth*. 2019.

[2] Ministerie van Volksgezondheid Welzijn en Sport, "Diabetes mellitus: aantal patiënten bekend bij de huisarts." https://www.staatvenz.nl/kerncijfers/diabetes-mellitus-aantal-patiënten-bekend-bij-de-huisarts, 2018.

[3] Rijksinstituut voor Volksgezondheid en Milieu, "Diabetes mellitus | Cijfers & Context | Huidige situatie | Volksgezondheidenzorg.info." https://www.volksgezondheidenzorg.info/onderwerp/diabetes-mellitus/cijfers-context/huidige-situatie#node-aandeel-diabetes-type-1-totaal-naar-leeftijd-en-geslacht, 2015.

[4] M. S. Islam, *The islets of Langerhans. Preface.*, vol. 654. 2010.

[5] D. W. Cooke and L. Plotnick, "Type 1 Diabetes Mellitus in Pediatrics," *bcm.edu*, 2008.

[6] L. Jovanovic, C. M. Peterson, B. B. Saxena, M. Y. Dawood, and C. D. Saudek, "Feasibility of maintaining normal glucose profiles in insulin-dependent pregnant diabetic women," *The American Journal of Medicine*, vol. 68, pp. 105–112, 1 1980.

[7] S. R. Heller, P. Choudhary, C. Davies, C. Emery, M. J. Campbell, J. Freeman, S. A. Amiel, R. Malik, B. M. Frier, K. V. Allen, N. N. Zammitt, K. MacLeod, K. F. Lonnen, D. Kerr, T. Richardson, S. Hunter, and D. McLaughlin, "Risk of hypoglycaemia in types 1 and 2 diabetes: Effects of treatment modalities and their duration," *Diabetologia*, vol. 50, pp. 1140–1147, 6 2007.

[8] Diabetes Control and Complications Trial Research Group, "Progression of Retinopathy with Intensive versus Conventional Treatment in the Diabetes Control and Complications Trial," *Ophthalmology*, vol. 102, no. 4, pp. 647–661, 1995.

[9] Diabetes Control and Complications Trial Research Group, "Effect of intensive diabetes treatment on the development and progression of long-term complications in adolescents with insulin-dependent diabetes mellitus: Diabetes Control and Complications Trial," *Sciences-New York*, vol. 99, no. 3, pp. 341–349, 1981.

[10] M. V. Hansen, U. Pedersen-Bjergaard, S. R. Heller, T. M. Wallace, K. Rasmussen, H. V. Jørgensen, S. Pramming, and B. Thorsteinsson, "Frequency and motives of blood glucose self-monitoring in type 1 diabetes," *Diabetes Research and Clinical Practice*, vol. 85, pp. 183–188, 8 2009.

[11] J. Pickup and H. Keen, "Continuous subcutaneous insulin infusion at 25 years: evidence base for the expanding use of insulin pump therapy in type 1 diabetes.," 3 2002.

[12] S. A. White, J. A. Shaw, and D. E. Sutherland, "Pancreas transplantation," 5 2009.

[13] A. C. Gruessner, D. E. Sutherland, and R. W. Gruessner, "Long-term outcome after pancreas transplantation," 2 2016.

[14] G. Tydén, F. P. Reinholt, G. Sundkvist, and J. Bolinder, "Recurrence of Autoimmune Diabetes Mellitus in Recipients of Cadaveric Pancreatic Grafts," *New England Journal of Medicine*, vol. 335, pp. 860–863, 9 1996.

[15] A. Humar, R. Kandaswamy, D. Granger, R. W. Gruessner, A. C. Gruessner, and D. E. Sutherland, "Decreased surgical risks of pancreas transplantation in the modern era," *Annals of Surgery*, vol. 231, no. 2, pp. 269–275, 2000.

[16] R. W. Gruessner, D. E. Sutherland, C. Troppmann, E. Benedetti, N. Hakim, D. L. Dunn, and A. C. Gruessner, "The surgical risk of pancreas transplantation in the cyclosporine era: An overview," *Journal of the American College of Surgeons*, vol. 185, pp. 128–144, 8 1997.

[17] A. Proneth, A. A. Schnitzbauer, F. Zeman, J. R. Foerster, I. Holub, H. Arbogast, W. O. Bechstein, T. Becker, C. Dietz, M. Guba, M. Heise, S. Jonas, S. Kersting, J. Klempnauer, S. Manekeller, V. Müller, S. Nadalin, B. Nashan, A. Pascher, F. Rauchfuss, M. A. Ströhlein, P. Schemmer, P. Schenker, S. Thorban, T. Vogel, A. O. Rahmel, R. Viebahn, B. Banas, E. K. Geissler, H. J. Schlitt, and S. A. Farkas, "Extended pancreas donor program - the EXPAND study rationale and study protocol," *Transplantation Research*, vol. 2, p. 12, 7 2013.

[18] Eurotransplant, "Yearly Statistics: Deceased donors used for transplant in 2019, by donor country," 2019.

[19] H. A. Clayton, S. M. Swift, J. M. Turner, R. F. James, and P. R. Bell, "Non-heart-beating organ donors: A potential source of islets for transplantation," *Transplantation*, vol. 69, pp. 2094–2098, 5 2000.

[20] F. Ris, C. Toso, F. U. Veith, P. Majno, P. Morel, and J. Oberholzer, "Are Criteria for Islet and Pancreas Donors Sufficiently Different to Minimize Competition?," *American Journal of Transplantation*, vol. 4, pp. 763–766, 5 2004.

[21] P. Maffi and A. Secchi, "Clinical results of islet transplantation," *Pharmacological Research*, vol. 98, pp. 86–91, 6 2015.

[22] M. F. Nijhoff, M. A. Engelse, J. Dubbeld, A. E. Braat, J. Ringers, D. L. Roelen, A. R. Van Erkel, H. S. Spijker, H. Bouwsma, P. J. Van Der Boog, J. W. De Fijter, T. J. Rabelink, and E. J. De Koning, "Glycemic stability through islet-after-kidney transplantation using an alemtuzumab-based induction regimen and long-term triple-maintenance immunosuppression," *American Journal of Transplantation*, vol. 16, no. 1, pp. 246–253, 2016.

[23] B. Ludwig, S. Ludwig, A. Steffen, H. D. Saeger, and S. R. Bornstein, "Islet versus pancreas transplantation in type 1 diabetes: Competitive or complementary?," 12 2010.

[24] F. B. Barton, M. R. Rickels, R. Alejandro, B. J. Hering, S. Wease, B. Naziruddin, J. Oberholzer, J. S. Odorico, M. R. Garfinkel, M. Levy, F. Pattou, T. Berney, A. Secchi, S. Messinger, P. A. Senior, P. Maffi, A. Posselt, P. G. Stock, D. B. Kaufman, X. Luo, F. Kandeel, E. Cagliero, N. A. Turgeon, P. Witkowski, A. Naji, P. J. O'Connell, C. Greenbaum, Y. C. Kudva, K. L. Brayman, M. J. Aull, C. Larsen, T. W. Kay, L. A. Fernandez, M. C. Vantyghem, M. Bellin, and A. M. Shapiro, "Improvement in outcomes of clinical islet transplantation: 1999-2010," *Diabetes Care*, vol. 35, pp. 1436–1445, 7 2012.

[25] E. N. Marieb and K. Hoehn, *Human Anatomy & Physiology*. Pearson, 10th ed., 2016.

[26] G. J. Tortora and B. Derrickson, *Principles of Anatomy & Physiology*. Wiley, 13th ed., 2011.

[27] M. F. Nijhoff, V. A. L. Huurman, J. Dubbeld, A. R. van Erkel, T. A. Rabelink, M. A. Engelse, and E. J. P. de Koning, "Transplantatie van eilandjes van Langerhans. De procedure, indicaties en uitdagingen.," *Nederlands Tijdschrift voor Geneeskunde*, vol. 133, no. 12, pp. 633–634, 2018.

[28] J. B. Doppenberg, M. A. Engelse, and E. J. P. de Koning, "PRISM: A Fast, Compact, In-line, High Yield, Human Pancreatic Islet Isolation Method," in *IPITA 2017 - 16th International Congress of the International Pancreas and Islet transplant Association*, (Oxford, United Kingdom), 2017.

[29] M. Ramamirez-Dominguez, *Pancreatic Islet Isolation*, vol. 938. 2016.

[30] G. S. Robertson, D. R. Chadwick, J. Davies, S. Rose, H. Contractor, R. F. James, P. R. Bell, and N. J. London, "The effectiveness of components of university of wisconsin solution in improving human pancreatic islet purification," *Transplantation*, vol. 57, no. 3, pp. 346–354, 1994.

[31] F. Chimienti, "Zinc, pancreatic islet cell function and diabetes: New insights into an old story," *Nutrition Research Reviews*, vol. 26, no. 1, pp. 1–11, 2013.

[32] W. Maret, "Zinc in pancreatic islet biology, insulin sensitivity, and diabetes," *Preventive Nutrition and Food Science*, vol. 22, no. 1, pp. 1–8, 2017.

[33] W. A. Hansen, M. R. Christie, R. Kahn, and A. Lernmark, "Supravital dithizone staining in the isolation of human and rat pancreatic islets | Request PDF," 1989.

[34] S. A. Clark, K. M. Borland, S. D. Sherman, T. C. Rusack, and W. L. Chick, "Staining and in vitro toxicity of dithizone with canine, porcine, and bovine islets.," *Cell transplantation*, vol. 3, pp. 299–306, 7 1994.

[35] P. Held, "The Importance of Using the Appropriate Microplate for Absorbance Measurements in the Ultraviolet Region of the Spectrum," *BioTek Tech Note*, 2009.

[36] D. F. T. Silva, R. A. Mesquita-Ferrari, K. P. S. Fernandes, M. P. Raele, N. U. Wetter, and A. M. Deana, "Effective Transmission of Light for Media Culture, Plates and Tubes," *Photochemistry and Photobiology*, vol. 88, pp. 1211–1216, 9 2012.

[37] Z.-B. Liu, J.-G. Tian, W.-P. Zang, W.-Y. Zhou, F. Song, C.-P. Zhang, J.-Y. Zheng, and H. Xu, "Flexible alteration of optical nonlinearities of iodine charge-transfer complexes in solutions," *Optics Letters*, vol. 29, no. 10, p. 1099, 2004.

[38] S. L. Jacques, “Optical properties of biological tissues: A review,” 6 2013.

[39] W. E. Connor, D. B. Stone, and R. E. Hodges, “the Interrelated Effects of Dietary Cholesterol and Fat Upon Human Serum Lipid Levels.,” *The Journal of clinical investigation*, vol. 43, no. 8, pp. 1691–1696, 1964.

[40] Y. Xu, X. Xie, Y. Duan, L. Wang, Z. Cheng, and J. Cheng, “A review of impedance measurements of whole cells,” 3 2016.

[41] T. Sun and H. Morgan, “Single-cell microfluidic Impedance cytometry: A review,” 4 2010.

[42] H. Shintaku, T. Okitsu, S. Kawano, S. Matsumoto, T. Suzuki, I. Kanno, and H. Kotera, “Effects of fluid dynamic stress on fracturing of cell-aggregated tissue during purification for islets of Langerhans transplantation,” *Journal of Physics D: Applied Physics*, vol. 41, no. 11, 2008.

[43] M. Ramamirez-Dominguez, *Pancreatic Islet Isolation*, vol. 938. 2016.

APPENDIX **A**

Figures and plots

A.1 Pancreatic islet identification

A.1.1 Optical absorption spectroscopy

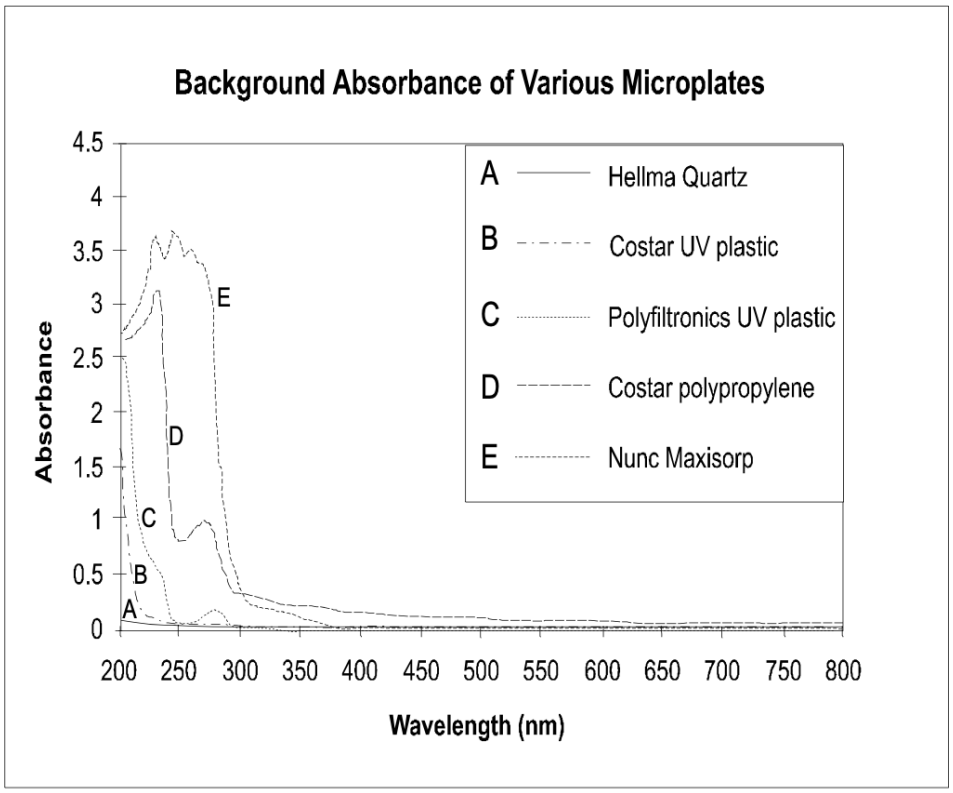

Figure A.1: Optical absorption spectrum of the Nunc Maxisorp culture plates. The plate absorbs light waves below 290nm [35].

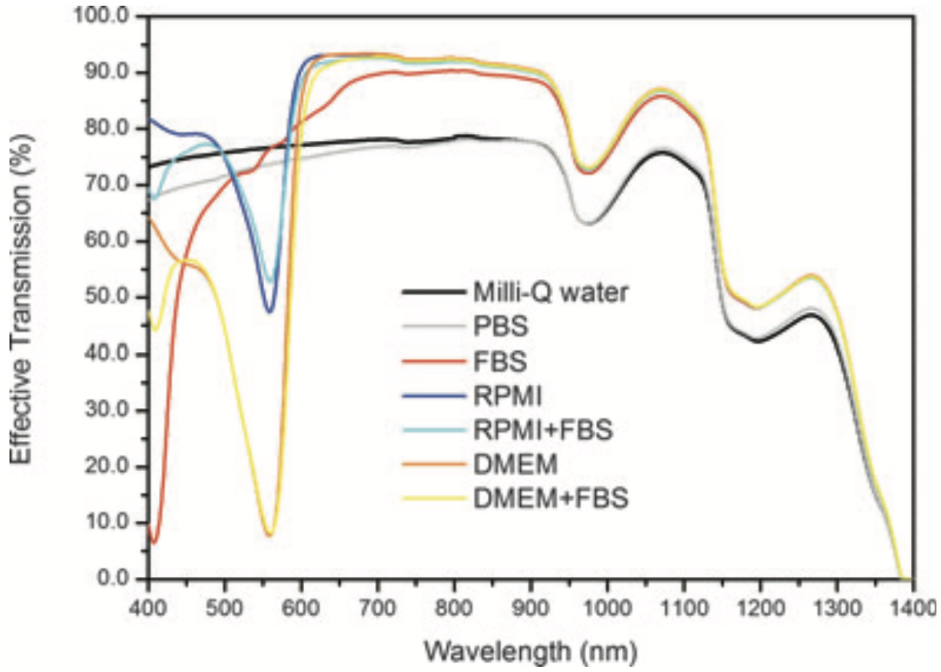

Figure A.2: Optical transmission spectrum of various fluids and culture media [36]. The addition of bovine serum alters the optical response of the medium.

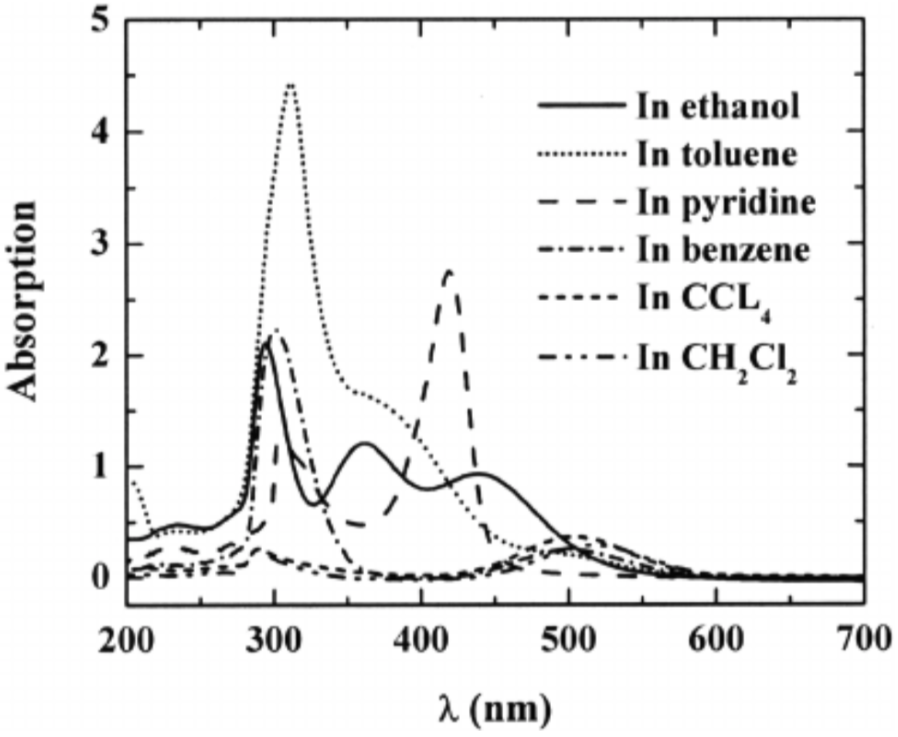

Figure A.3: Optical absorption spectrum of iodine in various fluids [37].

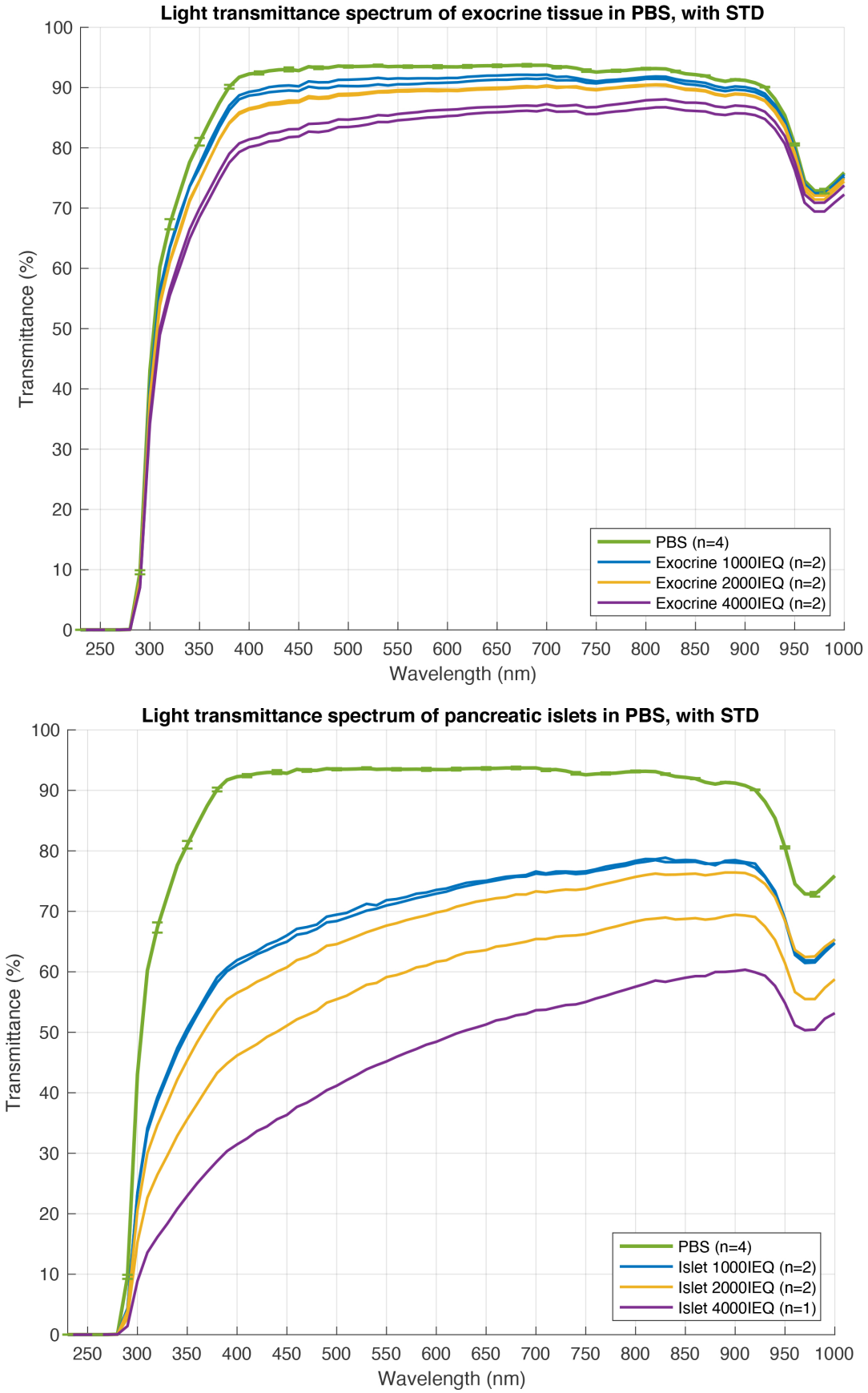

Figure A.4: Experiment 1: The transmission spectrum of exocrine tissue (top) and pancreatic islets (bottom) suspended in PBS. The error bars represent the standard deviation of the performed measurements.

A.2 Process validation and optimization

A.2.1 Exploring sequential and simultaneous density gradients

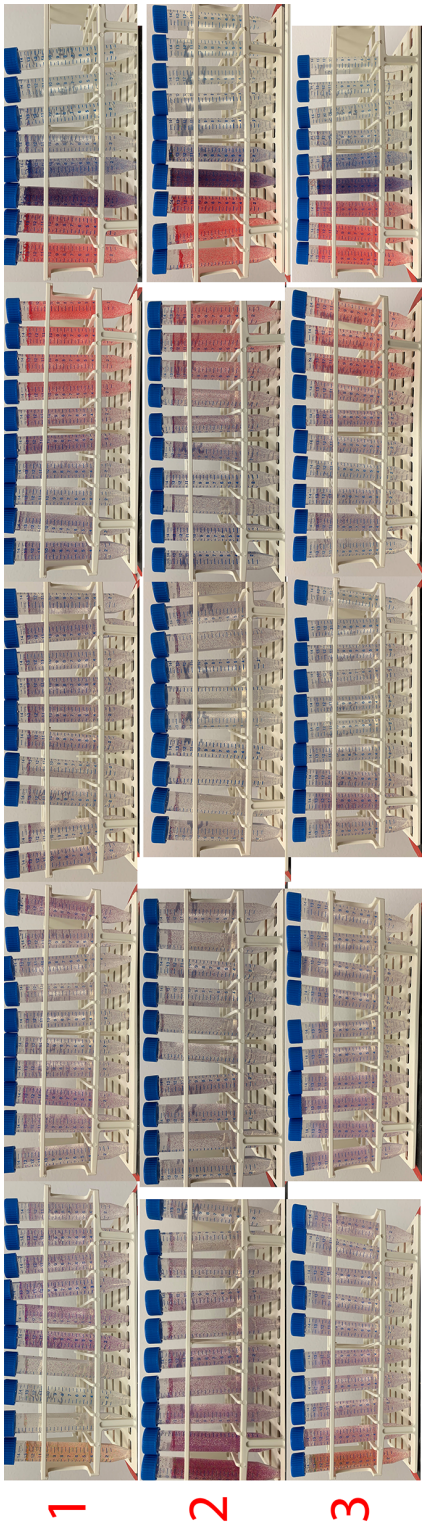

Figure A.5: Density bead separation in 3 sequential density gradients, showing tubes containing 13ml of fluids with increasing density matching the measurements (with number 1 on the left) of figure 3.11. Density beads of various density represent different types of tissue, with purple representing pancreatic islets and red representing exocrine tissue.

APPENDIX B

Additional notes

B.1 Culture Medium

The culture medium, CMRL1066 500 mL, for pancreatic islets contains the following list of additives:

- Ciproxin (2mg/ml) 5 mL
- Gentamicin (50mg/ml) 0,5 mL
- L-Glutamin (200mM) 5 mL
- Hepes (1M) 5 mL
- Nicotinamide (300mg/ml) 2 mL
- Human Serum 52 mL

APPENDIX C

Additional performed work

C.1 Risk analysis

C.1.1 HFMEA and FMEA risk analyses

To make sure the development is going in the right direction and nothing has been forgotten, two types of risk analyses have been performed. Both of these analyses were aimed at increasing safety by taking a close look at the process steps and the hardware. One of these analyses was the Healthcare Failure Mode and Effect Analysis (HFMEA), in which the processes are evaluated on what can go wrong. In this risk analysis, as shown in figure C.1, scores are given based on possible damage and expected frequency, eventually indicating in how important it is to take action for the specific topic. This ultimately led to a number of risks which were to be accepted, and some others which can either be controlled or require redesigns or validation studies to avoid, an overview of which is shown in table C.1.

Scenario	Accept	Control	Critical
Allogenous	25	37	6
Autologous	23	35	13

Table C.1: The results of the HFMEA risk analysis performed on both the allogenous and autologous situations. The critical results have led to redesigns of the specific relevant components.

The other risk analysis that has been performed is the Failure Mode and Effects Analysis (FMEA), which is aimed at minimizing the risk that a patient can suffer after failures occur with PRISM 2.0. This method, which is shown in figure C.2, combines the effects for the patient, with the frequency of occurrence and the risk of not being able to detect the error. The outcome of the FMEA risk analysis led to 14 situations requiring a technical solution, 7 that required a validation study and 3 situations that need to be added to the user manual.

Examples of processes that required a verification study, to ensure the technical solution is correct, are: a measurement of the amount of tissue in the Latham bowl, a validation of the cooling capacity of the water chiller and a corrosion test on the proposed materials.

S1.25	Temperatuursensor warm deel heeft afwijking	3	2	6	Beheersen	Verificatie van hardware van thermokoppler (afhankelijk van verwachte drift), jaarlijkse testen of hardware goed werkt.	x	x	x	Toevoegen PvE, Software Eisen, handleiding
S1.26	Foutconditie in sturingsalgoritme	3	5	15	Beheersen	Verificatie van control-algorithme infuuszakverwarmer		x		Toevoegen Software Eisen
S1.27	Zie boven: 1.5									
S1.28	Digest-analyser geeft verstoorde data	4	1	4	Beheersen	In handleiding: Sample-port is leidend			x	Toevoegen Handleiding
S1.29	Onbedoeld opengaan van klep V5	4	2	8	Beheersen	Opvangen in GUI. LEDs op kleppen.		x		Toevoegen Software Eisen
S1.30	Niet werken klep V5	2	3	6	Beheersen	Initiatie-test kleppen. LEDs op kleppen.	x	x		Toevoegen PvE en Software Eisen
S1.31	Onbedoeld dichtgaan van klep V5	2	2	4	Beheersen	Opvangen in GUI. LEDs op kleppen.	x	x		Toevoegen PvE en Software Eisen
S1.32	Kleppen verkeerd aangestuurd	3	1	3	Accepteren	Verificaties kleppen		x		Toevoegen Software Eisen
S1.33	Kleppen verkeerd aangestuurd	4	1	4	Accepteren	Verificaties kleppen		x		Toevoegen Software Eisen
S1.34	Falen rollerpompen	4	1	4	Accepteren	Initiatie-test rollerpompen		x		Toevoegen Software Eisen
S1.35	Rollerpompen te snel/langzaam	2	1	2	Accepteren	Initiatie-test rollerpompen. Verificatie rollerpompen.		x		Toevoegen Software Eisen
S1.36	Kleppen verkeerd aangestuurd	2	1	2	Accepteren	Verificaties kleppen		x		Toevoegen Software Eisen
S1.37	Koelwaterbad verwarmt ipv koelt	4	1	4	Beheersen	Temperatuursensor in kast + warning/error message		x		Toevoegen Software Eisen
S1.38	Koelwaterbad staat niet aan	3	3	9	Beheersen	Temperatuursensor in kast + warning/error message, RS232 communicatie		x		Toevoegen Software Eisen

Figure C.1: Example of the performed Healthcare Failure Mode and Effect Analysis (HFMEA), which indicates the need to accept, control or prevent possible failures.

Gevaar	Mogelijke faalwijze	Mogelijk gevolg	Mogelijke oorzaak	G (gevolg)	R (realisatie)	D (non-detectie)	RPG (risico)	Beheers-maatregel	Actie
Pressure	Blow-out van de vloeistoffen	Disposable moet vervangen worden, en	Verkeerd aansturen van de vloeistofstromen/ slang komt klem te	3	7	1	21	Gebruik door getrainde gebruiker	Toevoegen aan Handleiding.
Pressure	Blow-out van de vloeistoffen (autologous)	Disposable moet vervangen worden, en ander weefsel gebruikt worden.	Verkeerd aansturen van de vloeistofstromen/ slang komt klem te zitten	9	7	1	63	Gebruik door getrainde gebruiker	Toevoegen aan Handleiding.
Vibration	Loszittende componenten	Falen van mechatronica	Centrifuges / transport	2	5	2	20	Gebruiken van schroeven met rubber ring (trilllingdampers)	Toevoegen aan PvE.
Vibration	Loszittende componenten (autologous)	Falen van mechatronica	Centrifuges / transport	7	5	2	70	Gebruiken van schroeven met rubber ring (trilllingdampers)	Toevoegen aan PvE.
Magnetic fields	Motoren worden beinvloed door extern magnetisch veld.	Isolatieproces is beinvloed, met als gevolg lagere kwaliteit isolatie	Externe apparatuur (bijv. MRI)	3	1	10	30	Niet in buurt van sterk magnetisch veld gebruiken (voldoet overigens ook niet aan richtlijnen voor MRI-ruimte).	Toevoegen aan handleiding.
Biological									
Bio-	Biofilm formatie in	Besmetting van orgaan	Ventilator is niet goed schoon te	9	2	1	18	Ventilator is goed reinigbaar	Toevoegen aan PvE.
Bio-contaminati on	Donor orgaan besmet (allogeen)	Gebruiker raakt besmet	Blow-out tijdens proces	9	2	9	162	Handleiding: allogeen donororgaan zijn voorgeselecteerd aan de hand van specfieke uitsluitingscriteria, waaronder	Toevoegen aan handleiding.
Bio-	Orgaan besmet	Gebruiker raakt besmet	Blow-out tijdens proces	9	4	9	324	Handleiding: gebruik van handschoenen.	Toevoegen aan

Figure C.2: The Failure Mode and Effects Analysis (FMEA), is aimed at protecting a patient from possible failures of the equipment. By creating a score based on the possible consequences, frequency of the failure and the non-detection of the failure, areas have been found which require a technical solution.

C.1.2 Tissue volume measurement

The risk analyses have shown that during an autologous pancreatic islet isolation, there is a high need to know the total volume of tissue that resides in the Latham bowl during the digestion phase. This is needed because the amount of tissue volume dictates, during the isolation process, what steps to take next. Therefore, an exploratory study has been initiated to see if, with the use of camera's, the total volume of tissue in the Latham bowl can be measured. To simulate the conditions during the digestion phase, at which time the measurement is needed, the bowl was filled with Ringer Acetate, and during the test exocrine tissue was inserted into the bowl with 2 ml at a time. Between every measurement step the tissue was shaken loose and allowed to resettle when the centrifuge picked up speed again. With the use of a telephone camera, photos were taken at approximately the same distance and evaluated on segmentation with the use of Image Pro Premier, an example of this can be seen in figure C.3. The output of the segmentation software was the total area of pixels that it deemed to be part of the pre-set conditions.

These results, shown in figure C.4, have been plotted against the amount of tissue entered in the bowl and show to have a fairly linear increase with the amount of tissue in the bowl. The measurement for 10 ml is off, due to this image being taken from further away. This plot also shows that 2 ml of tissue is too little to be measured properly, this is because of how the bowl is connected to the rotating holder, blocking part of the field of vision. However, these results indicate that there is a possibility for a visual examination of the amount of tissue present in the bowl. Therefore, the development of a fixed camera system has been initiated, which, with some calibration, should be able to measure the amount of tissue through image segmentation.

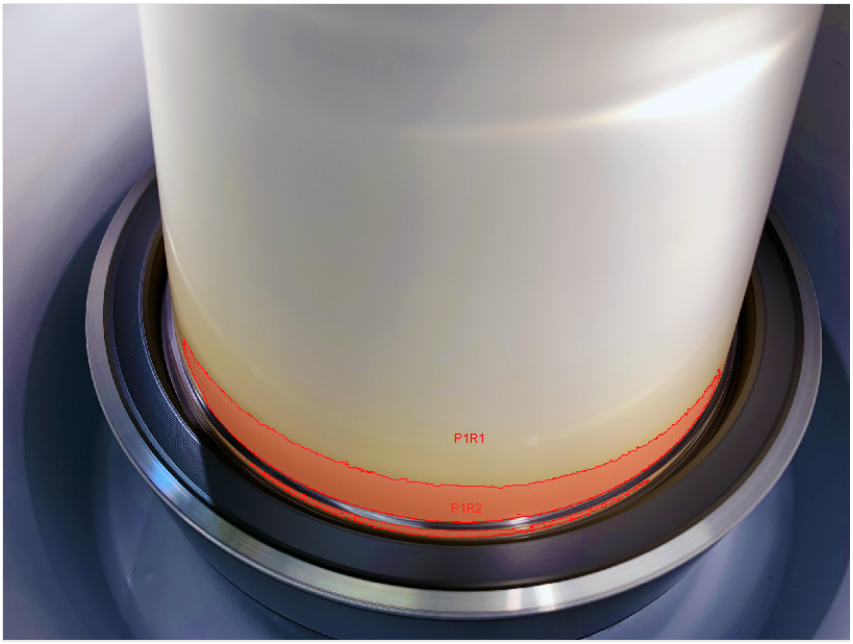

Figure C.3: Image segmentation using Image Pro Premier have been performed on a Latham bowl with 6 ml of tissue. The output of this segmentation is the area of pixels which have been identified to be a part of the tissue.

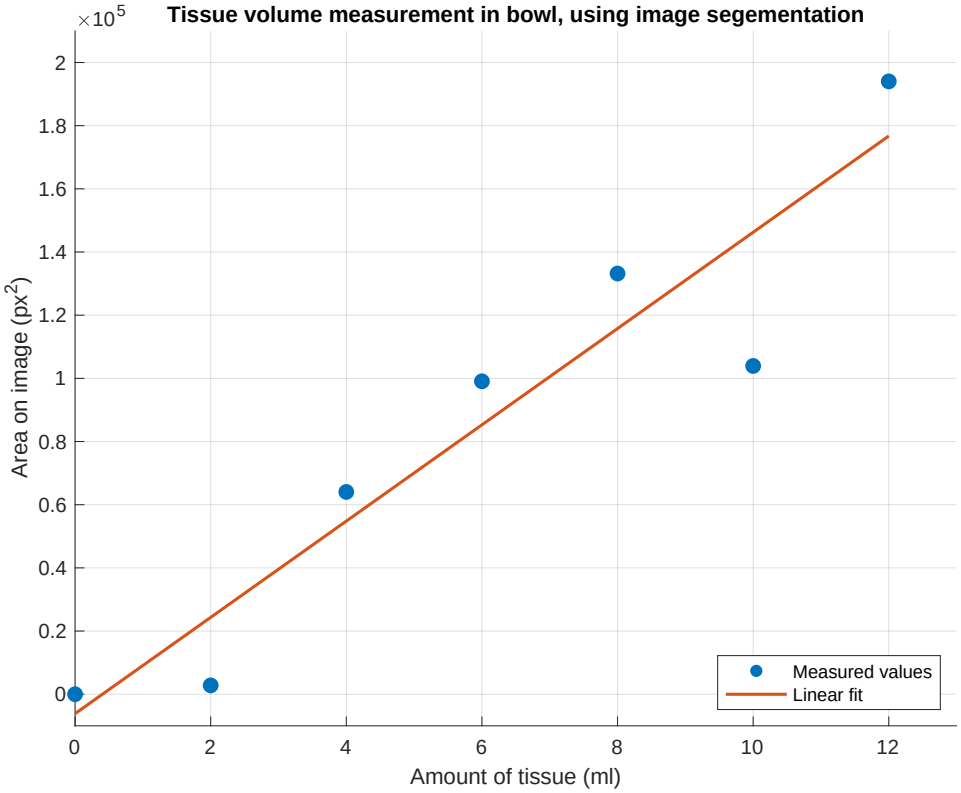

Figure C.4: With the output in square pixels from the Image Pro Premier software, a graph has been created in which this output is plotted against the volume in the bowl. The results show an increase in area with an increase in tissue.

C.1.3 Water chiller validation

During the digest phase of pancreatic islet isolations, the tissue is being broken down with the use of enzymes, which cut the collagen strands holding the tissue together [27]. Once the tissue is properly digested, the enzymes need to be switched off, which is achieved by the addition of human serum, and cooling the enzymes to reduce their activity. The risk analysis has shown that the proper cooling (to a temperature below 7 °C) of this fluid mixture is an important step to take, which otherwise can have consequences for the end product.

Therefore a validation study of the cooling capacity of the water chiller has been performed, in which the outflow temperature of the digest fluid mixture was measured at various pump speeds and water chiller settings. The setup of this experiment is shown in figure C.5, and shows the variables and the goals that need to be achieved. The equipment used in this study is: Julabo FC1600S water chiller, a Medtronic BIOtherm heat exchanger, a Thermaltake Pacific radiator, Masterflex Variable-Speed Drive with an Easyload 2 pump head, and an Ebro TFN 520 temperature sensor using Type T thermocouples.

The results of this study are shown in the top graph of figure C.6, and show that at a flow speed of 250 and 300 ml/min the capacity of the heat exchanger and coolant flow is not sufficient to cool the liquids below 7 °C. The flow speeds of 200 ml/min and below show that for most temperature settings of the water chiller the outflow temperature of the digest flow remains below a temperature of 7°C. Because lower flow speeds add more time to the pancreatic islet isolation procedure, the digest flow of 200 ml/min is preferable above the lower flow speeds. Resulting in the water chiller needing to cool the coolant to a temperature of 3°C and lower.

After leaving the heat exchanger, the coolant then travels to the radiator, which in turn cools the internal spaces of PRISM 2.0. Therefore, the bottom graph of figure C.6 shows the temperature of the coolant liquid at the radiator, after passing through the heat exchanger. The results show that at a temperature of 2°C the temperature in the radiator remains below 7°C with a digest flow speed of 200 ml/min.

These results combined lead to the conclusion that the waterchiller is suitable for the task. With the digest flow of 200 ml/min and the water chiller set on 1°C or 2°C, the cooling is sufficient to avoid any difficulties during the isolation process.

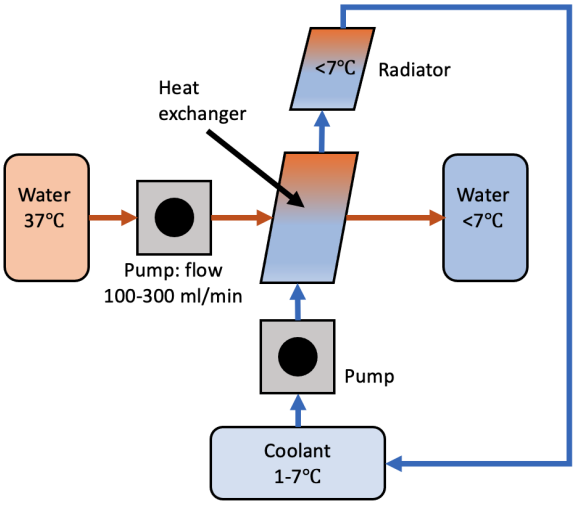

Figure C.5: Schematic set up of the water chiller validation study.

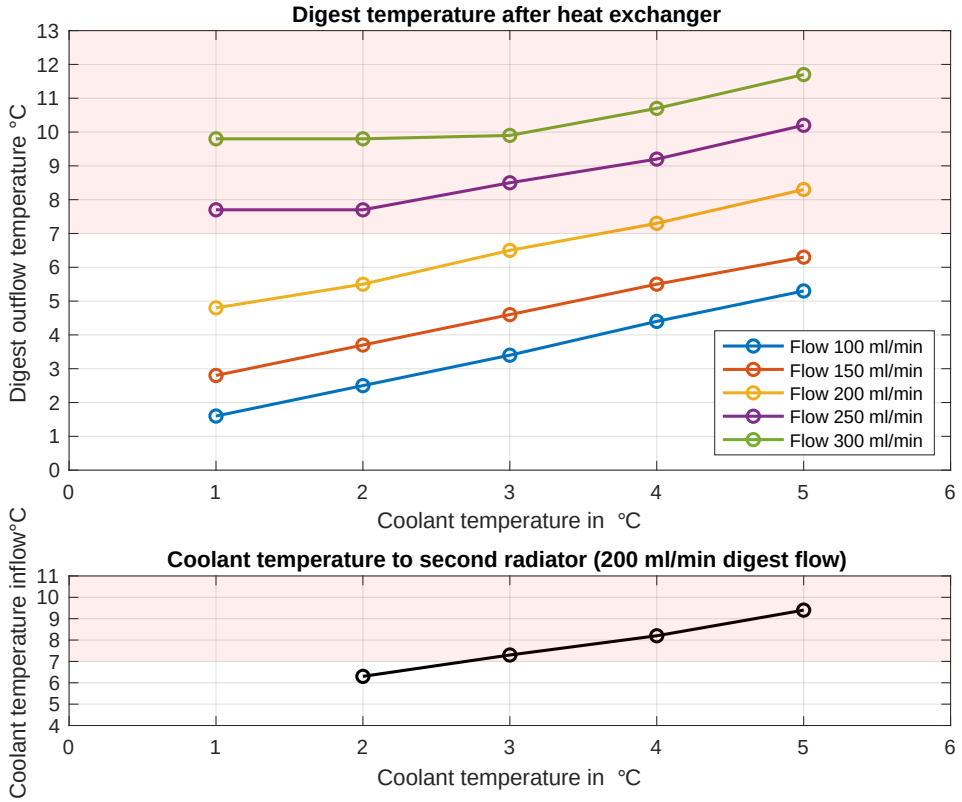

Figure C.6: Results of the validation study of the water chiller. Top graph shows the outflow temperature of the digest flow at various speeds and coolant temperatures. The bottom graph shows the temperature of the coolant to the radiator, with a 200 ml/min digest flow speed.

C.1.4 Material corrosion tests

The risk analysis indicated that, due to the use of the device in a Good Manufacturing Practices (GMP) cleanroom facility, corrosion should be prevented, as this is difficult to clean and could affect the lifespan of the component. Therefore, the proposed materials for PRISM 2.0 were tested by exposing them to the two more aggressive cleaning agents that are used in the GMP facilities, virkon and RBS solution. The materials tested materials were steel 304 and steel 316, and were tested in accordance with table C.2. By exposing the steel to a heavy dose of chemicals for a long period of time, an indication can be gathered on how well the steel performs when exposed to multiple cleaning sessions. The results, which are shown in figure C.7, show that steel 304 (number 2 in the figure) corroded and steel 316 (number 1 in the figure) did not. Therefore, despite the higher cost, a decision has been made to use steel 316 as a building material for PRISM 2.0.

Duration (days)	**Condition**	**Cleaning agent**
2	Submerged	Virkon 20g/L
1	50/50 submerged/air	Virkon 20g/L
4	Submerged	2% RBS
3	50/50 submerged/air	2% RBS
2	Submerged	Virkon 20g/L
2	50/50 submerged/air	Virkon 20g/L

Table C.2: Corrosion testing conditions to which steel 304 and steel 316 have been exposed.

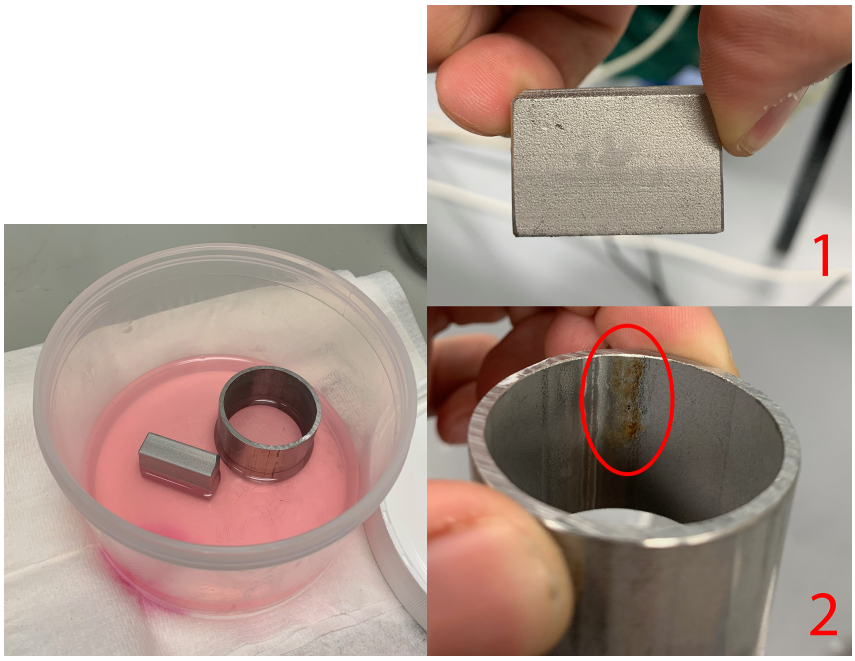

Figure C.7: Left: Example of the steel being tested in a 50/50 condition using Virkon. Right: The end result of the corrosion test, showing that material 1 (steel 316) did not corrode, and material 2 (steel 304) did show signs of corrosion.

C.2 Design

C.2.1 Mockup and solidworks

Once the decision was made, after the validation studies of the previous sections, to use a process including two simultaneous density gradients, the development process could be taken further. This meant that, using all the lessons learned so far, PRISM 2.0 could start to take shape. The starting point of this process was to take a good look at the first version of the machine, PRISM 1.0, which is shown in figure C.8, and identify parts of the device that work as intended and parts that need improvement.

The first mockup that was created using cardboard and duct tape, and is shown in figure C.9, and shows the layout of a device that incorporates the idea's for PRISM 2.0, but yet lacks the definitive measurements of the final version. The first mockup has proven to be a very useful tool in the interaction with the LUMC technical development department, because this visualization of the design idea's opened good discussions on what paths to take for further development.

Through iterations of various designs, mockups and solidwork files were created that include definitive dimensions for PRISM 2.0. These versions are shown in figures C.10 and C.11 and come close to what PRISM 2.0 will look like. With most of the basic elements completed, leaving mainly the smaller details to be completed.

The next step in this process is to get hands on experience with the design through validation studies. To this end, the second version of the mockup has been equipped with some of the equipment, and is shown in figure C.12. These validation studies combined with the user experience, will open up the design for further iterative steps.

Figure C.8: PRISM 1.0

Figure C.9: Mockup 1

Figure C.10: Mockup 2

Figure C.11: Solidworks

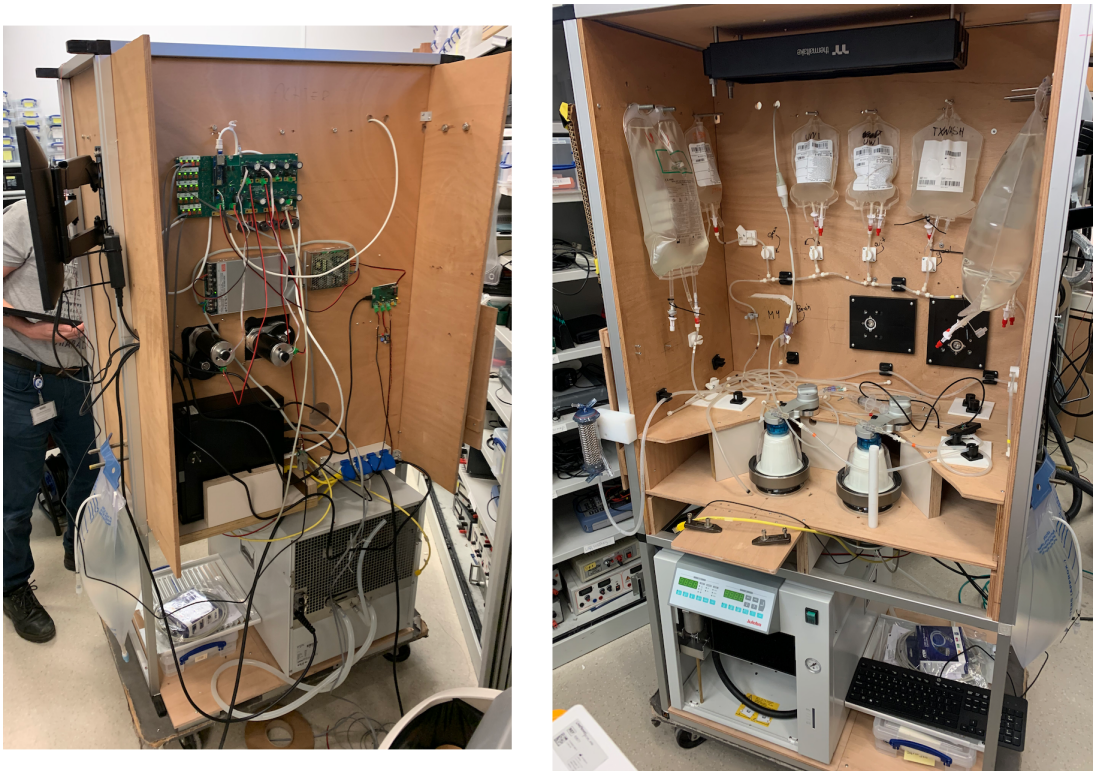

Figure C.12: Mockup version 2, partly equipped with equipment and machinery for further validation studies.

C.2.2 Schematics

Together with the overall design of PRISM 2.0, schematics had to be created which represent various processes that take place in PRISM 2.0, such as the tubing sets for isolation procedures and overviews of all electrical connections. An example of one of these schematics is shown in figure C.13, and shows the tubing and flow directions for an autologous pancreatic islet isolation process.

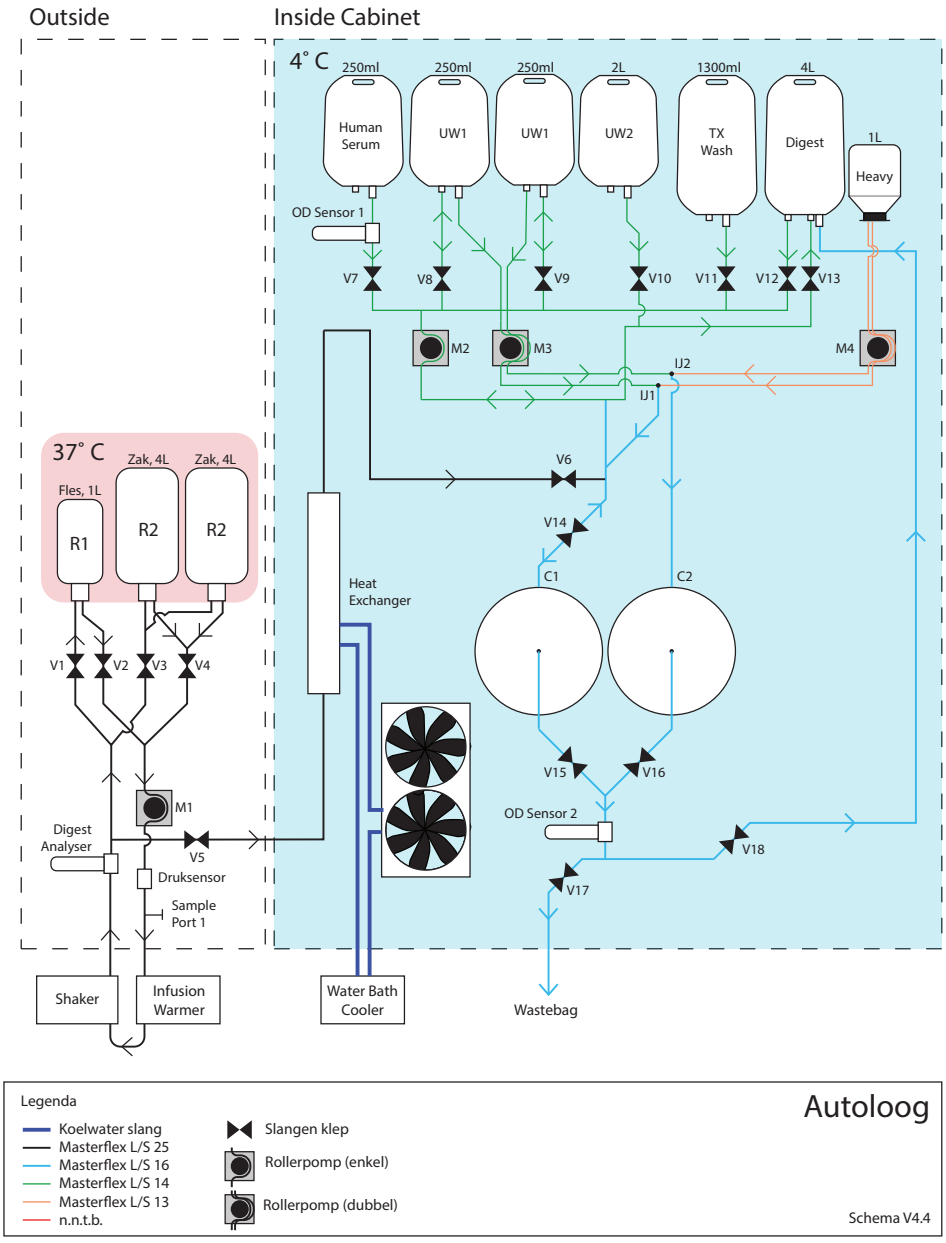

Figure C.13: Schematic